

Phylogeny of iguanodontian dinosaurs and the evolution of quadrupedality

Karen E. Poole

ABSTRACT

Iguanodontians are a large and biogeographically widespread group of dinosaurs, known from every modern continent, with a temporal range from the Late Jurassic through the Late Cretaceous. While the nested hadrosauroids have been studied extensively, the phylogeny of non-hadrosauroid iguanodontians remains less clear. This study presents a character matrix with 323 characters, and both parsimony and time-calibrated Bayesian analyses. While these result in different topologies, they both recover a Thescelosauridae outside of Iguanodontia. Within Iguanodontia, they both recover *Muttaborrasaurus* and *Tenontosaurus* as sister taxa to Rhabdodontidae, with a larger group of Gondwanan Rhabdodontoidea (*nomen cladi novum*) in the Bayesian analysis. A small Dryosauridae forms the sister group to Ankylopollexia, which has *Uteodon* and *Camptosaurus* as the most basally branching taxa. Within Styrcosterna two distinct clades are recovered: Iguanodontidae, and a group of taxa with robust forelimbs. The holotype of *Mantellisaurus* is sister to “*Dollodon*”, supporting the hypothesis that these taxa are synonymous.

The “hatchet-shaped” sternal thought to be a synapomorphy of Styrcosterna occurs in two taxa recovered outside that group: *Macrogyphosaurus* and the unnamed taxon from the Kirkwood Formation of South Africa. Characters associated with quadrupedality are mapped on the phylogeny, indicating a transition from bipedality to quadrupedality occurred in a stepwise manner at the base of Ankylopollexia. Based on synapomorphies of the groups, the major innovations in Ankylopollexia were postcranial, while those of hadrosauroids were centered on dentition and the dentaries. There is a clear faunal succession from the Late Jurassic to Early Cretaceous non-hadrosauroid ankylopollexians to the Late Cretaceous hadrosauroids.

Karen Poole. Department of Basic Sciences, New York Institute of Technology College of Osteopathic Medicine at Arkansas State University, Wilson Hall, 2405 Aggie Rd., Jonesboro Arkansas 72401, USA. kpoole@nyit.edu

Keywords: Iguanodontia; Ornithopoda; Ornithischia; phylogeny; parsimony; Bayesian

Submission: 18 July 2016. Acceptance: 25 October 2022.

Final citation: Poole, Karen E. 2022. Phylogeny of iguanodontian dinosaurs and the evolution of quadrupedality. *Palaeontologia Electronica*, 25(3):a30. <https://doi.org/10.26879/702>
palaeo-electronica.org/content/2022/3707-iguanodontian-phylogeny

Copyright: November 2022 Society of Vertebrate Paleontology.

This is an open access article distributed under the terms of the Creative Commons Attribution License, which permits unrestricted use, distribution, and reproduction in any medium, provided the original author and source are credited.
creativecommons.org/licenses/by/4.0

INTRODUCTION

Iguanodontians are a clade of herbivorous dinosaurs within the diverse Ornithischia; more specifically, they are derived ornithopods (Figure 1). The first genus named in the group was *Iguanodon* Mantell 1825, which long served as a wastebasket taxon; as such, the genus and the clades to which it belongs have a complex taxonomic history. Currently, the generally accepted phylogeny has Iguanodontia nested within Ornithopoda and Hadrosauridae nested within Iguanodontia. This phylogeny creates paraphyletic groupings of non-hadrosaurid iguanodontians (hereafter iguanodontians) and non-iguanodontian ornithopods. There are several major changes in morphology between the more basal taxa and hadrosaurids that make this group ideal for studying character evolution. The premaxillary teeth are lost while maxillary and dentary teeth become more numerous, higher crowned, and closely packed into dental batteries. Additionally, there is a general trend toward increased size in iguanodontians, which shift from bipedality to quadrupedality. The most notable morphological change associated with this is seen in the carpal elements of iguanodontians, which become massive and fused together, while those of hadrosaurids are diminutive or lost entirely.

Iguanodontians are known from all modern continents and have a temporal span of roughly 100 million years from the Late Jurassic through the end of the Cretaceous Period. During this time, the supercontinent of Pangaea was rifting into smaller landmasses; by the end of the Cretaceous, these were recognizable as the modern continents.

This study reviews the taxonomic history of Iguanodontia and uses parsimony and time-calibrated Bayesian methods to produce phylogenetic hypotheses and map the geographic distribution of taxa.

Taxonomic History

Early work. The term Iguanodontia is often attributed to Dollo (1888), but Norman (2015) observed that Dollo never used this term. In fact, he offered new definitions of Iguanodontidae and Camptonotidae.

The name Iguanodontia was first used by Baur in 1891 and by his definition included the families Iguanodontidae, Hypsilophodontidae, Hadrosauridae, Scelidosauridae, Stegosauridae, Agathaumidae, and possibly Ornithomimidae. This grouping (excluding the saurischian clade Ornithomimidae) is equivalent to Ornithischia (Seeley, 1887), though Baur gave no explanation for why the latter name would not suffice. Following Seeley, he did not consider Dinosauria to be a natural

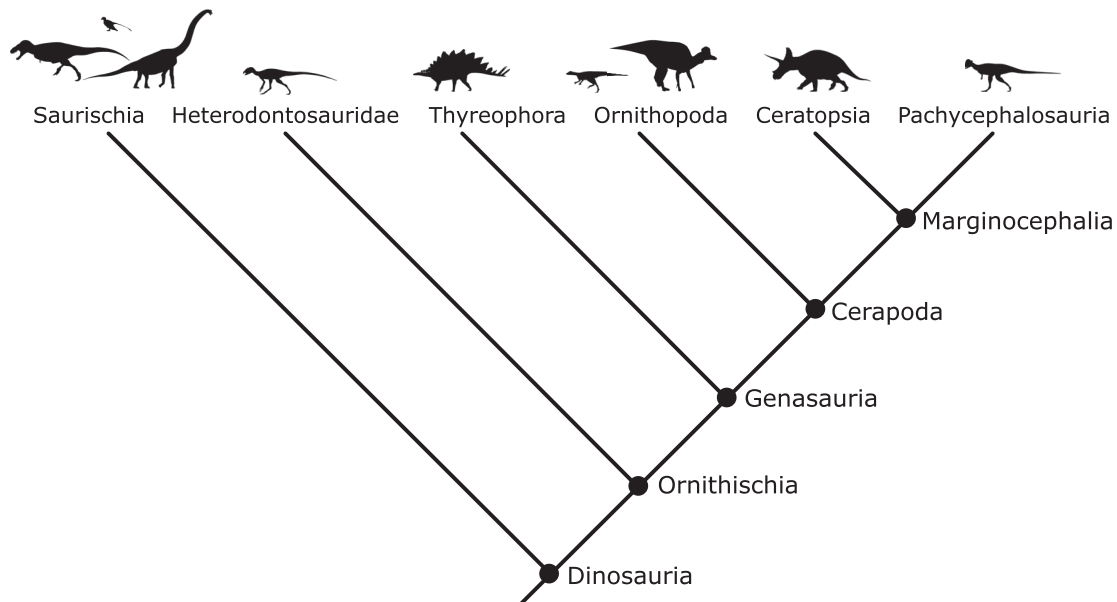


FIGURE 1. Simplified phylogeny showing the current understanding of ornithischian relationships, based on Butler et al. (2008). Silhouettes from Phylopic.org. *Daspletosaurus* by Tasman Dixon, *Brachiosaurus* by Michael P. Taylor, *Lambeosaurus* by Craig Dylke (all public domain). *Triceratops* by Raven Amos, *Heterodontosaurus* by Jaime Headden, *Stegosaurus* by Andrew A. Farke, *Hypsilophodon* by Mathew Wedel (<https://creativecommons.org/licenses/by/3.0/>), *Stegoceras* by Caleb M. Brown (<http://creativecommons.org/licenses/by-sa/3.0/>).

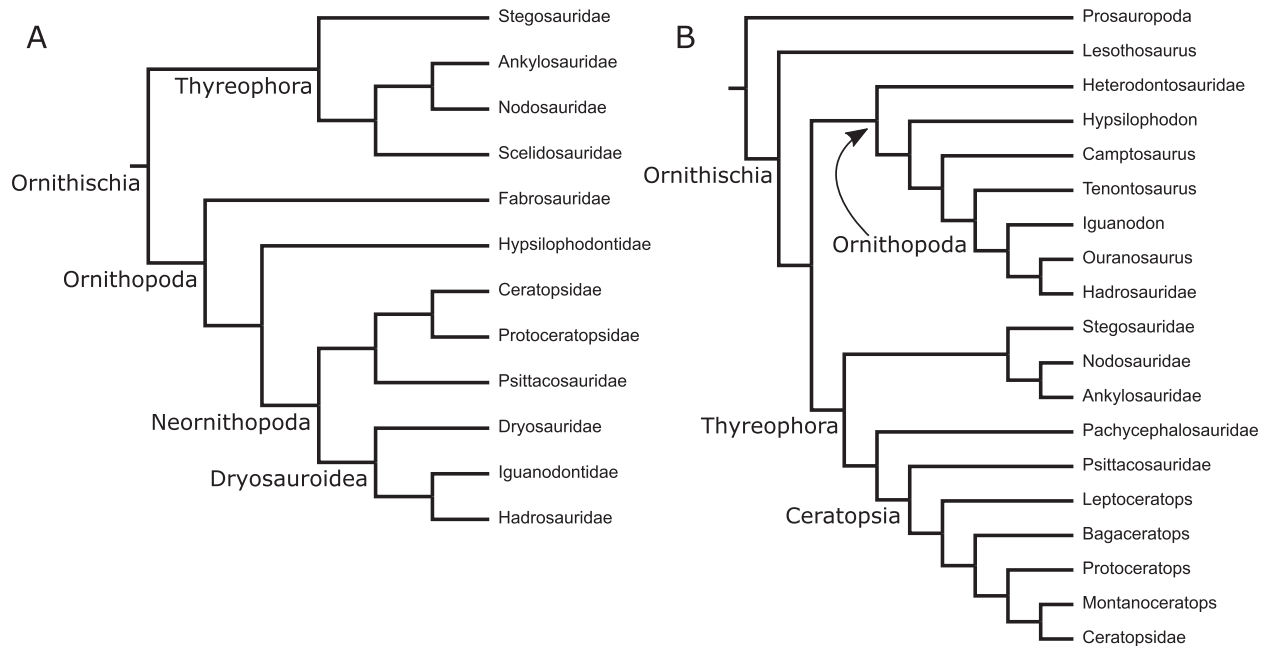


FIGURE 2. Early cladistic analyses of ornithischian phylogeny found by (A) Norman, 1984, and (B) Sereno, 1984. H1 and H2 indicate alternate positions for Heterodontosauridae, and P1 and P2 indicate alternate positions for Pachycephalosauridae.

group and intended the name Iguanodontia to be an order or suborder, at an equivalent level to Crocodylia. The term Iguanodontia appeared in the literature through the early 20th century (e.g., Lull, 1908), though Williston (1905) drew a distinction between iguanodontians and other “pre dentate” dinosaurs such as *Stegosaurus* and *Scelidosaurus*, and Osborn (1906) distinguished between iguanodontians and ceratopsians. Already, the term had a more restricted meaning than Baur’s original definition. In 1911, Lull described three groups belonging to the Ornithopoda: Iguanodontia, Ceratopsia, and Stegosauria. He equated the name Ornithopoda with Pre dentata (Marsh, 1896). Lull (1911) defined iguanodontians as those ornithopods that were unarmored and without horns.

The family-level name Iguanodontidae was first used by Gervais (1853), though no definition of the group was given. Huxley (1870) described Iguanodontidae as one of three groups within Dinosauria, the others being Scelidosauridae and Megalosauridae. He assigned to this family *Cetiosaurus*, *Iguanodon*, *Hypsilophodon*, *Hadrosaurus*, and possibly *Stenopelix*. This grouping is more equivalent to later conceptions of Ornithopoda, with the obvious exception of the sauropod *Cetiosaurus*.

Through the middle of the twentieth century, the term Iguanodontia fell out of use, while Iguanodontidae remained a commonly used family name.

The more ambiguous ‘iguanodonts’ was also commonly used (e.g., Gilmore, 1909; Osborn, 1912). Romer’s (1956) classification included Iguanodontidae as a family within suborder Ornithopoda including the genera *Iguanodon*, *Camptosaurus*, and *Rhabdodon* (though excluding *Dryosaurus* and *Dysalotosaurus*, which he placed in Hypsilophodontidae).

The Cladistic Era. With the advent of cladistics, nomenclature changed rapidly. In 1984, Norman and Sereno each presented a phylogeny of Ornithischia at the Third Symposium on Mesozoic Terrestrial Ecosystems (Figure 2). Norman’s phylogeny used only families as operational taxonomic units (OTUs), and found Iguanodontidae as sister to Hadrosauridae, with Dryosauridae just outside this node. He recovered Hypsilophodontidae outside of a clade containing Dryosauridae, Iguanodontidae, Hadrosauridae, and Ceratopsia. While this hypothesis was not supported for many years, it is interesting to note that some recent analyses have found at least some taxa considered to be “basal ornithopods” outside of Ceratopsia (Butler et al., 2008; Boyd, 2012, 2015; Spencer, 2013). Sereno (1984) used a mix of family and genus level OTUs, and found Hadrosauridae to be nested within ‘iguanodonts’, thus making the traditional grouping of Iguanodontidae paraphyletic. Sereno (1986) renewed the term Iguanodontia for this larger clade, while also naming the less inclusive clades

TABLE 1. A summary of the most recent phylogenetic definitions for higher order taxa given by Sereno and Norman.

Clade	Definition	
	Sereno 2005	Norman 2014b
Ornithopoda	The least inclusive clade containing <i>Heterodontosaurus tucki</i> Crompton and Charig, 1962 and <i>Parasaurolophus walkeri</i> Parks, 1922 but excluding <i>Pachycephalosaurus wyomingensis</i> (Gilmore, 1931), <i>Triceratops horridus</i> Marsh, 1889, <i>Ankylosaurus magniventris</i> Brown, 1908.	Stem-based: all cerapodans closer to <i>Edmontosaurus</i> than to <i>Triceratops</i> (Norman et al., 2004).
Euornithopoda	The most inclusive clade containing <i>Parasaurolophus walkeri</i> Parks 1922, but not <i>Heterodontosaurus tucki</i> Crompton and Charig, 1962, <i>Pachycephalosaurus wyomingensis</i> (Gilmore, 1931), <i>Triceratops horridus</i> Marsh, 1889, <i>Ankylosaurus magniventris</i> Brown, 1908.	
Iguanodontia	The most inclusive clade containing <i>Parasaurolophus walkeri</i> Parks, 1922 but not <i>Hypsilophodon foxii</i> Huxley, 1869, or <i>Thescelosaurus neglectus</i> Gilmore, 1913.	Stem-based: <i>Edmontosaurus regalis</i> and all taxa more closely related to <i>E. regalis</i> than to the taxa subtended to the clade (Hypsilophodontia) that includes <i>Hypsilophodon foxii</i> and <i>Tenontosaurus tilletti</i> .
Dryomorpha	The most inclusive clade containing <i>Dryosaurus altus</i> (Marsh, 1878) and <i>Parasaurolophus walkeri</i> Parks, 1922	
Ankylopollexia	The least inclusive clade containing <i>Camptosaurus dispar</i> (Marsh, 1879) and <i>Parasaurolophus walkeri</i> Parks, 1922.	Stem-based: <i>Edmontosaurus regalis</i> and all taxa more closely related to <i>E. regalis</i> than to <i>Dryosaurus altus</i> .
Styracosterna	The most inclusive clade containing <i>Parasaurolophus walkeri</i> Parks, 1922 but not <i>Camptosaurus dispar</i> (Marsh, 1879).	Node-based: <i>Batyrosaurus rozhdetsvenskyi</i> , <i>Edmontosaurus regalis</i> , their common ancestor, and all of its descendants.
Hadrosauroidae	The most inclusive taxon containing <i>Parasaurolophus walkeri</i> Parks, 1922 but not <i>Iguanodon bernissartensis</i> Boulenger, 1881.	
Hadrosauridae	The least inclusive taxon containing <i>Saurolophus osborni</i> Brown, 1912 and <i>Parasaurolophus walkeri</i> Parks, 1922 and including <i>Hadrosaurus foulkii</i> Leidy, 1858.	Euhadrosauria Node-based: <i>Parasaurolophus</i> , <i>Saurolophus</i> , <i>Edmontosaurus</i> , their most recent common ancestor, and all of its descendants.

Dryomorpha, Ankylopollexia, and Styracosterna (see Table 1). He diagnosed Iguanodontia based on the following characters: “the absence of premaxillary teeth, the presence of leaf-shaped denticles in the cheek teeth, and the loss of one phalanx from manus digit III”. In his phylogeny, Iguanodontia included *Tenontosaurus*, *Dryosaurus*, *Camptosaurus*, *Probactrosaurus*, *Iguanodon*, and *Ouranosaurus*, as well as Hadrosauridae. His analysis recovered Hypsilophodontidae as a monophyletic group, sister to Iguanodontia, which together comprise Euornithopoda. The most basal ornithopods in the analysis are the Heterodontosauridae. The subsequent phylogenetic analyses of Forster (1990), Weishampel and Heinrich (1992), and Sereno (1998) found similar results.

Sereno (1998) defined Iguanodontia based on phylogenetic relationships rather than a suite of characters as all euornithopods closer to *Parasau-*

rolophus than to *Hypsilophodon*. He defined Ornithopoda as the least inclusive clade containing *Heterodontosaurus* and *Parasaurolophus*, but excluding *Pachycephalosaurus*, *Triceratops*, and *Ankylosaurus*. He defined the clade Euornithopoda as further excluding *Heterodontosaurus* (Sereno, 1999, 2005).

Subsequent studies at the genus level failed to recover Hypsilophodontidae as a monophyletic group (Scheetz, 1999; Winkler et al., 1997; Weishampel et al., 2003). Treating these genera as separate OTUs recovered largely pectinate topologies with ‘hypsilophodonts’ as a paraphyletic group with respect to Iguanodontia. Due to inconsistent relationships among hypsilophodontids, Sereno (2005) emended the definition of Iguanodontia to the most inclusive clade containing *Parasaurolophus walkeri* but not *Hypsilophodon foxii* or *Thescelosaurus neglectus*.

In a paper describing the new genus of Patagonian dinosaur *Gasparinisaura*, Coria and Salgado (1996) named the clade Euiguanodontia, and defined it as *Gasparinisaura* and Dryomorpha, excluding *Tenontosaurus* and hypsilophodontids. However, subsequent analyses (e.g., Weishampel et al., 2003; Butler et al., 2008; this study) find *Gasparinisaura* arising from a more inclusive node than *Tenontosaurus*. In this topology, Euiguanodontia is nonsensical, and the name has not been adopted.

In the second edition of *The Dinosauria*, phylogenies of basal ornithopods and basal iguanodontians were analyzed separately, thus little can be concluded about higher-level relationships (Norman, 2004; Norman et al., 2004). However, phylogenetic definitions were given for these groups: Ornithopoda was defined as a stem-based taxon composed of all cerapodans closer to *Edmontosaurus* than to *Triceratops*—this included *Heterodontosaurus* (Norman et al., 2004). Iguanodontia was defined as all euornithopods closer to *Edmontosaurus* than to *Thescelosaurus* (Norman, 2004).

The explosion of iguanodontian taxa. The number of iguanodontian genera increased quickly beginning in the 1990s, as new fossils were described for the first time (Rich and Rich, 1989; Coria and Salgado, 1996; Head, 1998; Kirkland, 1998; Taquet and Russell, 1999; DiCroce and Carpenter, 2001; Wang and Xu, 2001; Coria and Calvo, 2002; Kobayashi and Azuma, 2003; You et al., 2003; Novas et al., 2004; You et al., 2005; Gilpin et al., 2006; Calvo et al., 2007; Sues and Averianov, 2009; Dalla Vecchia 2010; McDonald et al., 2010b; McDonald et al., 2010c; Wu et al., 2010; You et al., 2011; Godefroit et al., 2012; McDonald et al., 2012; Coria et al., 2013), and previously known specimens were reanalyzed (Weishampel et al., 2003; Paul, 2007; Paul, 2008; Carpenter and Ishida, 2010; Norman 2010; McDonald et al., 2010a; McDonald, 2011; Paul, 2012). There remains disagreement about some of these taxon assignments; this study predominantly follows the taxonomy laid out by Norman (2013).

McDonald et al. (2010c) and McDonald (2012a) made the first attempts at analyzing the phylogenetic relationships of the plethora of new taxa, including as many as 66 ornithopod genera in the analyses (Figure 3). However, these studies had a small number of characters (135) relative to the number of taxa, and the consensus tree was resolved poorly, with a largely pectinate topology.

Norman (2015) restricted his analysis to well-preserved taxa (27) and used just over a hundred characters (105). As in McDonald's analyses, Nor-

man included *Hypsilophodon* as the only representative basal ornithopod, although he also included the basal ornithischian *Lesothosaurus*, on which the tree was rooted (Figure 4). His analysis recovered a monophyletic group of 'iguanodontoids', including, in addition to *Iguanodon*, the recently discovered *Proa*, *Jinzhouosaurus*, and *Bolong*, as well as genera created recently for species formerly assigned to *Iguanodon*: *Barilium dawsoni* and *Mantellisaurus atherfieldensis*. He assigned the name Clypeodonta to "*Hypsilophodon foxii*, *Edmontosaurus regalis*, their most recent common ancestor, and all of its descendants." However, *Hypsilophodon* was the only basal ornithopod present in this analysis, so it is unclear how Clypeodonta relates to Ornithopoda sensu Norman et al. (2004).

The work of Butler et al. (2008) examined the phylogeny of Ornithischia. It did not include many iguanodontians; however, it informed the selection of the more basal taxa included in the current analysis. Butler et al. did not offer a definition of Iguanodontia, but defined ornithopods as "All genasaurians more closely related to *Parasaurolophus walkeri* Parks, 1922, than to *Triceratops horridus* Marsh, 1889", closely following the definition of Norman et al. (2004) rather than the definition given by Sereno (1998). Most importantly, this analysis found Heterodontosauridae as a basally branching member of Ornithischia, making Sereno's definition of Ornithopoda (1998) nearly equivalent to Ornithischia (though it is node-based, rather than stem-based). They also recovered several genera previously considered to be basally branching ornithopods (e.g., Norman et al., 2004) outside of Cerapoda, as basally branching neornithischians. These include *Agilisaurus*, *Hexinlusaurus*, and *Othnielia*.

Although it does not have precedence, the stem-based definition of Ornithopoda used by Butler et al. (2008) has already been used widely (Buchholz, 2002; Wagner, 2004; Norman et al., 2004). As there is a need for a term to describe the sister group of Marginocephalia within Cerapoda, and Ornithopoda is already recognized as such, this usage is adopted here, despite the lack of priority for the definition.

Finally, Boyd (2012, 2015) recovered many putative basally branching ornithopods outside of Cerapoda (Figure 5), leaving *Hypsilophodon* as the sole non-iguanodontian ornithopod. As there are no marginocephalians in the current analysis, it is impossible to say whether certain taxa are basally branching ornithopods or basally branching neor-

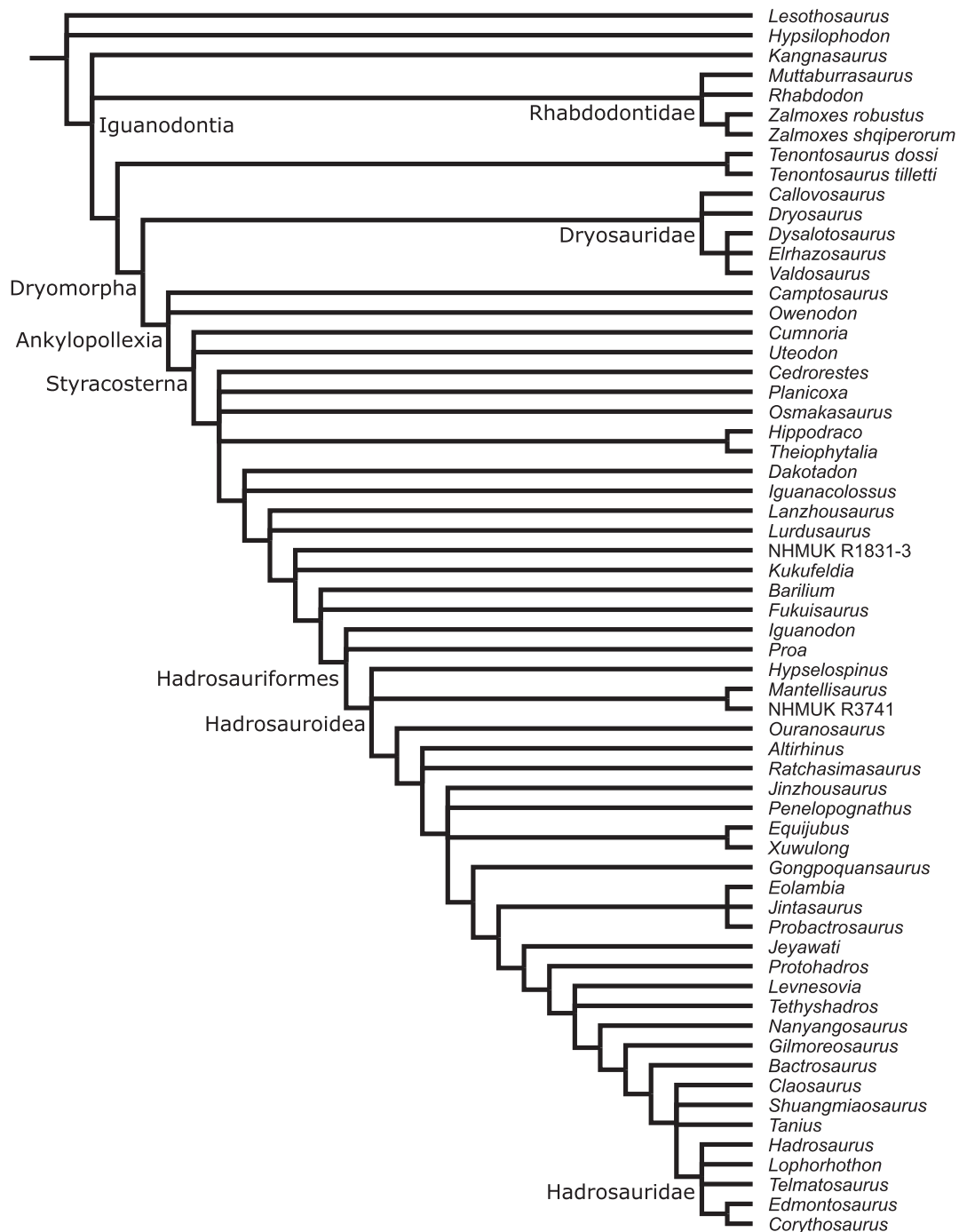


FIGURE 3. Iguanodontian phylogeny as presented by McDonald (2012a). This is an Adam's consensus tree of 24,460 MPTs, with terminology for higher taxa following Sereno (2005).

nithischians. Therefore, the more inclusive term “basal neornithischian” is preferred here—a future analysis including marginocephalians will help to clarify this ambiguity.

By using a larger character matrix than those of previous studies, and including many basal neornithischians as outgroups, this analysis seeks

to test which taxa belong within Iguanodontia, and to define this and any subclades both phylogenetically and via character-based diagnoses.

Biogeography

As basal neornithischians were diversifying in the Early Jurassic, Pangaea was still contiguous,

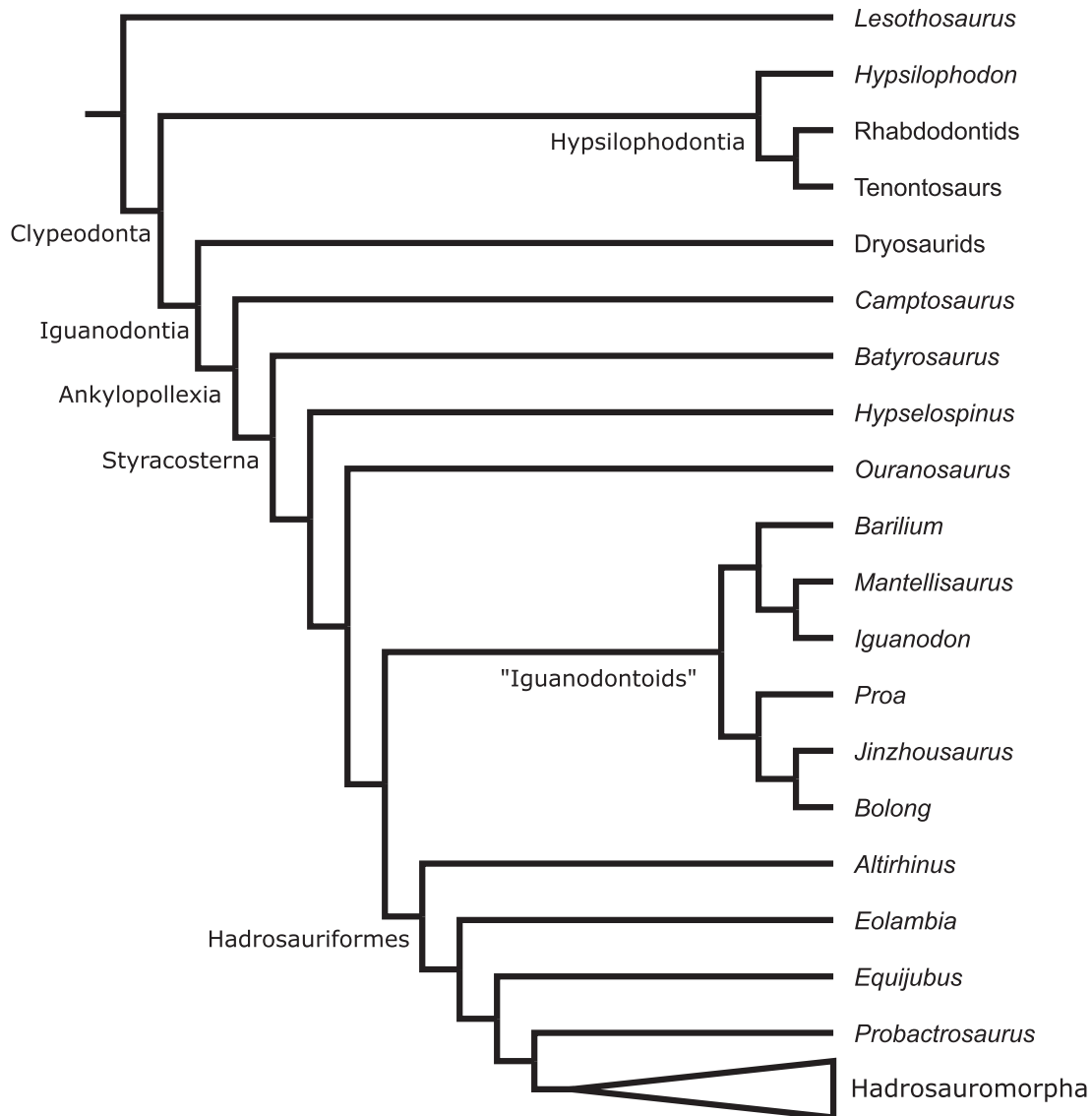


FIGURE 4. Iguanodontian phylogeny presented by Norman (2015). Consensus of three MPTs.

with the Tethys Ocean lying between Asia and Eastern Gondwana (Blakey, 2008). Gondwana and Laurasia were united via northern Africa. Rifting between Africa and North America began in the Triassic, but the formation of oceanic crust (and therefore continental separation) did not occur until the Early Jurassic, approximately 190-180 Ma (Bartolini and Larson, 2001; Veevers, 2004). Through the Cretaceous, the Laurasian continents maintained intermittent contact, although epeiric seas divided North America in two large landmasses, and Europe into a series of smaller landmasses (Esmerode et al., 2007; Miall et al., 2008; Scotese, 2014). Meanwhile, rifting continued in Gondwana, producing the southern continents we are familiar with today. Given these physical con-

straints, one would expect that endemism within neornithischians would increase from the Triassic through the Cretaceous, and any late appearing clade would have more restricted ranges.

Biogeography of iguanodontians has been analyzed quantitatively by several researchers (Milner and Norman, 1984; Upchurch et al. 2002; Ezcurra and Angolín, 2012; Boyd, 2015). Upchurch et al. (2002) used tree reconciliation analysis (TRA) to examine biogeographical patterns across Dinosauria. This approach was important in reconstructing overall patterns of vicariance through the Mesozoic. Ezcurra and Agnolín (2012) also used TRA across a wide range of taxa and found frequent links between European and Gondwanan taxa. Boyd (2015) used both parsimony and likeli-

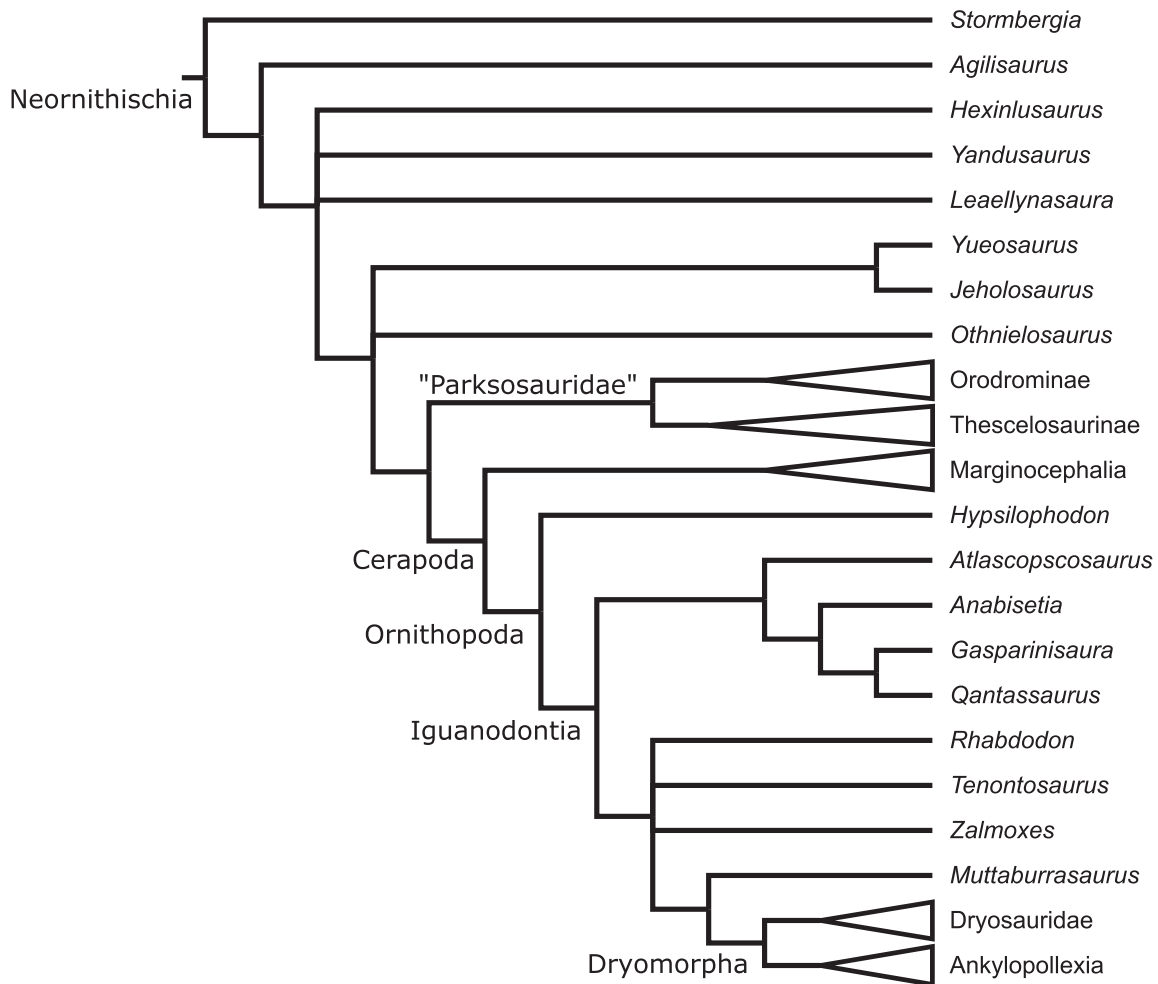


FIGURE 5. Phylogeny of Boyd (2012), cropped to relevant portion with collapsed clades. Note that Thescelosauridae, composed of many taxa previously regarded as basally branching ornithopods, lies outside of both Ornithopoda and Cerapoda. Strict consensus of 36 MPTs.

hood models to infer ancestral areas of nodes within Ornithischia, finding diversification of Neornithischia within Africa in the Early Jurassic, dispersing to Asia by the Late Jurassic. The ancestral area reconstruction for Iguanodontia is resolved more poorly, with different models finding this in Europe or in Asia, and differing dispersal within the group. This study employs model-based approaches such as Dispersal-Extinction-Cladogenesis (DEC) (Ree and Smith, 2008; Matzke 2012, 2013b) for ancestral area reconstruction (AAR).

Institutional Abbreviations

AM, Albany Museum, Grahamstown, South Africa; **AMNH**, American Museum of Natural History, New York City, New York, USA; **IMM**, Inner Mongolia Museum, Hohhot, China; **MC**, Museum Crúzy,

Crúzy, France; **MNHN**, Museum National d'Histoire Naturelle, Paris, France; **MPT**, Museo Provincial de Teruel, Spain; **MUCPv**, Museo de Geología y Paleontología de la Universidad Nacional del Comahue, Neuquén, Argentina; **NHMUK**, Natural History Museum, London, United Kingdom; **NMV**, National Museum of Victoria, Melbourne, Australia; **NRRU**, Nakhon Ratchasima Rajabhat University, Thailand; **PRC**, Palaeontological Collection, Palaeontological Research and Education Centre, Mahasarakham University, Thailand; **RBINS** (formerly IRSNB), Royal Belgian Institute of Natural Sciences, Brussels, Belgium; **SDSM**, Museum of Geology, South Dakota School of Mines and Technology, Rapid City, South Dakota, USA; **USNM**, National Museum of Natural History, Smithsonian Institution, Washington, D.C., USA; **YPM**, Yale Peabody Museum, New Haven, Connecticut, USA.

METHODS

Character Selection

A matrix of 323 characters was compiled, with 171 (53%) from the postcranial skeleton. The character list is given in Appendix 1, and the character matrix in Appendix 2. The matrix was constructed in Mesquite (version 2.72; Maddison and Maddison, 2009) and combines characters drawn from Norman (2002), Weishampel et al. (2003), Butler et al. (2008), Boyd et al. (2009), Prieto-Márquez and Salinas (2010), and McDonald (2012a).

After the characters and character states from all these studies were combined, duplicate characters were eliminated, and those that were uninformative to the analysis were deleted. Characters were reworded, where necessary, to follow a standardized format (Serenó, 2007). Characters that were inapplicable to some taxa were revised to use reductive coding (Strong and Lipscomb, 1999). This approach produced 184 characters, with 104 from the cranial and dental regions. Then 139 new characters were added (48 cranial, 91 postcranial), noted as “new” in Appendix 1. The measured values for states of all ratio-based characters were graphed, and states were determined based on gaps present in those values.

Taxon Selection

All putative genera of iguanodontians were considered in the analysis, including many non-iguanodontian neornithischians and a few basally branching ornithischians as outgroups. Of the 73 selected OTUs, specimens of 45 were examined directly (62%), while the others were coded from literature descriptions (Appendix 3). Taxa with large amounts of missing data were not excluded *a priori* (Kearney and Clark, 2003; Wiens and Moen, 2008; Wiens and Morrill, 2011). Some named taxa were excluded from the analysis *a priori*, either because they do not possess apomorphies or a unique suite of character states, or because they are junior synonyms of other taxa. These taxa and the rationale for their exclusion is provided in Appendix 4.

Naming conventions follow the rules and recommendations of the International Code of Phylogenetic Nomenclature, version 4c (Cantino and deQueiroz, 2010).

Phylogenetic Analysis

Both parsimony and time-calibrated Bayesian analyses were performed. Despite the potential for conflict between parsimony and model-based methods (Felsenstein, 1978; Farris, 1983; Swof-

ford et al., 2001; Wright and Hillis, 2014), comparison of the resulting trees shows which areas of the topology are robust and supported by both methods, addressing concerns that Bayesian analyses with missing data will recover nodes with erroneously high support values (Simmons, 2012, 2014; Xu and Pol, 2013) by allowing comparison between results of the parsimony and Bayesian analyses. Matching nodes found under both methods indicate which areas of the tree are well supported by the data, while differences in topologies or relative support show which areas remain less certain.

The introduction of relaxed-clock Bayesian methods that create time-calibrated phylogenies is useful particularly within paleontology (Drummond et al., 2006; Pyron, 2011; Ronquist et al., 2012). While developed with combined data sets of extant and extinct taxa using molecular and morphological data, these methods have also been used for analysis of entirely extinct groups known only from morphological data (Gorscak and O'Connor, 2016).

Ultimately, both parsimony and Bayesian methods are useful, though the results must be interpreted differently. Parsimony provides the simplest representation of the data, with no added parameters. Clades in these analyses tend to be supported by a higher number of characters, but those characters are more labile (Lee and Worthy, 2012). It does not take temporal data into account and allows long ghost lineages.

Bayesian analyses allow us to model evolutionary processes more explicitly and to account for time as a factor in the phylogeny. This tends to disfavor long ghost lineages. It is also important to note that the Bayesian tree presented here is not a consensus, but a Maximum Clade Credibility tree: of the trees sampled, it is the single tree with the highest overall posterior probability.

Parsimony analysis. A parsimony analysis was conducted in TNT 1.1 (Goloboff et al., 2008). A New Technology Search was conducted using a driven search set to find the best score 500 times using default settings of sectorial searches, ratchet, drift, and tree fusing. Pruned consensus (reduced consensus of Wilkinson [2003]) was used to determine which taxa acted as wild cards for removal *post hoc* from the consensus tree, resulting in removal of six taxa: *Oryctodromeus*, *Atlascopscosaurus*, *Planicoxa*, *Cumnoria*, *Cedrorestes*, and NHMUK R28860 (“*Kukufeldia*”). After pruning, a strict consensus tree was calculated. Jackknife supports were calculated using 10,000 replicates in a traditional search. Initially, the default value of

0.33 was used for the chance of dropping a character from the matrix. As this resulted in overall low values, the analysis was redone using a 0.1 probability of dropping characters. This results in overall higher values but allows for a better assessment of the relative support of the nodes present in the tree. Bremer supports were calculated by performing a traditional search with 5,000 RAS and tree bisection reconnection (TBR), while keeping trees suboptimal up to seven steps. The trees were rooted on the basal ornithischian *Eocursor* (Butler et al., 2007).

To assess the impact of adding many new postcranial characters to the matrix, an additional parsimony analysis was run in which the 80 new postcranial characters added to this matrix were excluded.

Tip-dated Bayesian analysis. A time-calibrated analysis was carried out in BEAST 2.0 (Bouckaert et al., 2014) with an xml file created in BEASTmaster (Matzke, 2014). Ages of tips were determined based on temporal data given in descriptions, or from studies dating relevant beds (Appendix 4). The entire possible age range, including error, was used in this analysis (O'Reilly et al., 2014). For taxa constrained to a particular stage or substage, numerical dates were assigned according to Gradstein et al. (2012). However, note that error estimates are not given for substage boundaries. Uniform priors were assigned to age ranges. Two tips known from well-dated localities were assigned fixed ages: *Tenontosaurus dossi* at 113 ma (Jacobs et al., 1991) and *Protohadros* at 95 ma (Kennedy and Cobban, 1990). The root of the tree was constrained with a lognormal prior with both mean and standard deviation equal to 1. This creates a 95% probability of the root occurring between 215 and 228 ma, while allowing the possibility of older dates.

A relaxed clock model was implemented in which branch lengths were uncorrelated to adjacent branches (Drummond et al., 2006; Rannala and Yang, 2007; Lepage, et al., 2007), and drawn from a lognormal distribution with mean=0.001 and standard deviation=1. Characters used an Mk ordered or Mk unordered model, as appropriate (Lewis, 2001).

A Birth-Death Skyline (BDSKY) model with serial sampling was used as a tree model (Stadler et al., 2013). This is an extension of a birth-death model that allows those rates to change across time bins. Bins were assigned by geologic stages: Late Triassic, Early, Middle, and Late Jurassic, and Early and Late Cretaceous. Broad priors were

assigned to speciation rate (λ), extinction rate (μ), and sampling rate (ψ), with each allowed to vary between 0 and 10. The sampling rate is the rate at which a lineage is sampled and allows for taxa of different ages to be included in the analysis; this should not be confused with the sampling probability (ρ), which represents the probability of sampling a lineage within a particular time bin. Sampling probability was fixed at 0.1, as assigning broad priors to all tree model variables provides too little constraint to the model, which often fails to converge (Drummond and Bouckaert, 2015). Matzke (2014) suggested fixing $\rho=1$, but this would indicate perfect sampling. Given the incomplete nature of the fossil record, sampling probability is more likely (to an order of magnitude estimate) in the range of 1% to 10%. Analyses were conducted with $\rho=0.1$ and $\rho=0.01$ to determine the effect of different values of sampling probability. While, as expected, it altered the posterior distributions of λ , μ , and ψ , there was no effect on tree topology.

Both analyses were run for 50 million generations, saving trees every 10,000 generations, producing a total sample of 5,001 trees. Convergence was assessed based on Estimated Sample Size (ESS) of all posterior values: ESS>200 was considered the minimum threshold for convergence. In addition, the trace plots for variables were assessed visually to ensure that stationarity and sufficient mixing occurred. TreeAnnotator was used to find the Maximum Clade Credibility (MCC) tree, with a burn-in of 20%. Synapomorphies were identified on the MCC tree by importing the tree to the character matrix in Mesquite and mapping the characters.

Biogeographic Analysis

Ancestral areas were calculated for the consensus time-calibrated tree using the R package BioGeoBEARS (Matzke, 2013a), using DEC, DIVAlike, and BAYAREA models, without the J parameter allowing founder events. Given the wide geographic range of the taxa and the sparseness of the fossil record, including founder events in the model does not seem theoretically sound. While it does create a model better fitted to the data, this is more likely due to fossil lineages appearing suddenly in the record of an area due to changes in sedimentology regimes or access to outcrops.

Models were compared using the Akaike Information Criterion (AIC) to determine which model best fit the tree. A time stratified approach was used, in which switching areas was given equal weight through the Kimmeridgian, after

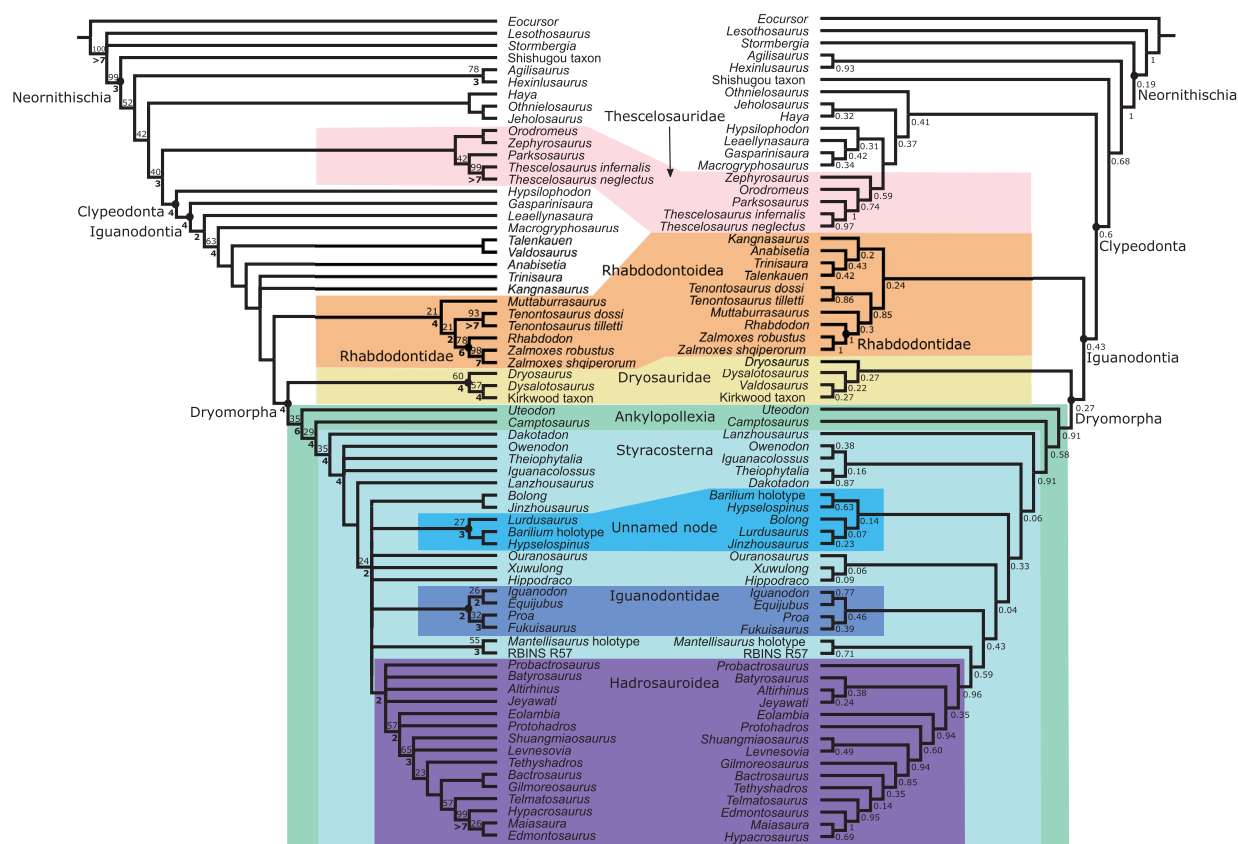


FIGURE 6. Parsimony (left) and Bayesian (right) trees plotted together. Strict consensus of 84 MPTs after pruning *Oryctodromeus*, *Atlascopcosaurus*, *Planicoxa*, *Cumnoria*, *Cedrorestes*, and NHMUK R28860. Jackknife values above 20 (with 10% chance of character removal) are shown above and to the left of their respective nodes, and bolded. CI=0.272, RI=0.634. Maximum clade credibility tree produced by Bayesian analysis showing posterior probabilities below and to the right of their respective node.

which switching areas between Laurasian and Gondwanan areas became less likely by a factor of 10.

RESULTS

The topology recovered in the parsimony (Figures 6, 7) and Bayesian analyses (Figures 6, 8) is similar within Dryosauridae and Ankylopollexia. However, there are substantial differences in the basal section of the tree. In the parsimony tree, this region is pectinate with long ghost lineages, though thescelosaurids and rhabdodontoids form small clades (Figure 7). In the Bayesian topology, most of the non-ankylopollexian iguanodontians are included within a large Hypsilophodontidae (which includes Thescelosauridae) and rhabdodontoids (which includes many more genera than in the parsimony topology). These topological differences occur because of differences in the models: the

birth-death model implemented in the Bayesian analysis favors a bifurcating topology without multiple long branches, whereas parsimony analyses tend towards a pectinate topology when there is not a strong phylogenetic signal. While the recovered topologies of each method will be discussed below, further work is needed to resolve the relationships in this area of the tree.

There are several shared features of the two topologies: (1) *Tenontosaurus* and *Muttaborrasaurus* are sister taxa to Rhabdodontidae, forming a more inclusive Rhabdodontoidea, (2) *Uteodon* is the most basal ankylopollexian, (3) the small clade Iguanodontidae includes *Iguanodon*, *Equijubus*, *Proa*, and *Fukuisaurus*, and (4) there is clear stratigraphic separation between non-hadrosauroid ankylopollexians and hadrosauroids. Unambiguous synapomorphies for both analyses listed in Appendix 5.

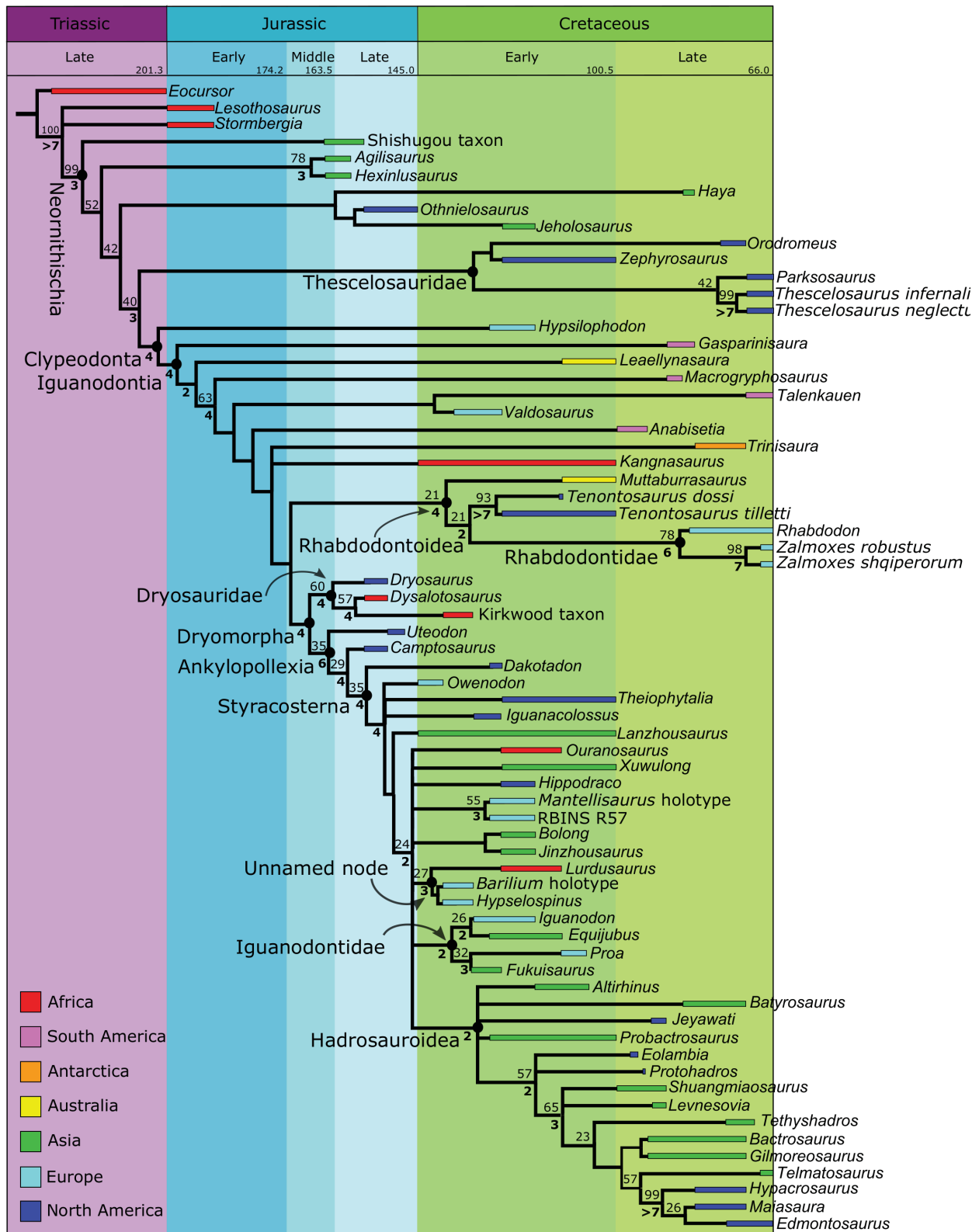


FIGURE 7. Time scaled parsimony tree, showing assigned age ranges and broad-scale geographic data. Jackknife values above 20 (with 10% chance of character removal) are shown above and to the left of their respective nodes. Bremer supports above one are shown below and to the left of their respective nodes, and bolded.

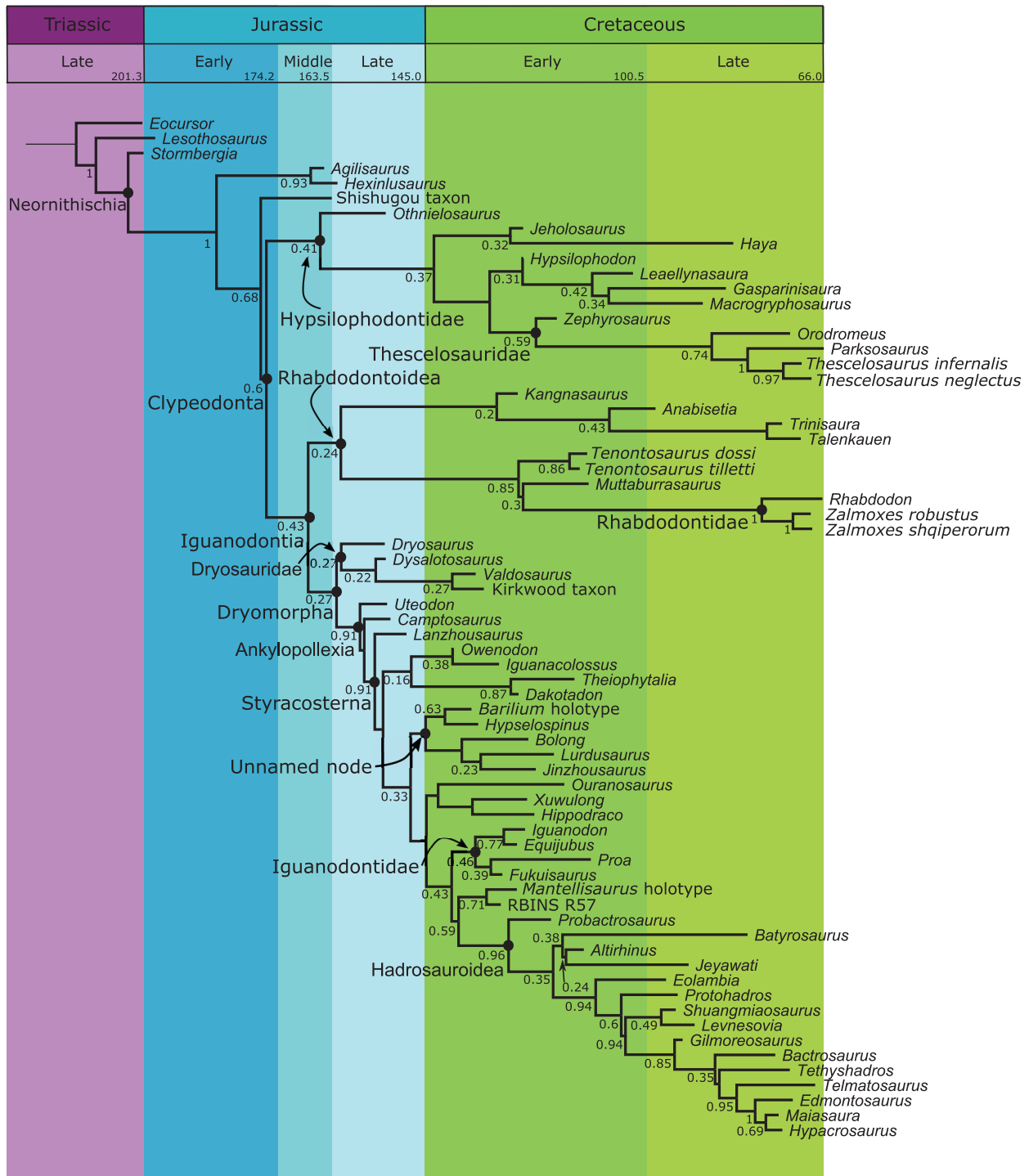


FIGURE 8. Maximum Clade Credibility tree produced by Bayesian analysis. Posterior probabilities are shown to the left of their nodes. The geologic timescale is shown across the top. Tips represent the average age found for each OTU across all sampled trees.

Parsimony Analysis

Initial parsimony analysis yielded 2843 MPTs with a tree length of 1394 steps. After running “pruned trees” in TNT, six ingroup taxa were

removed from the strict consensus: *Oryctodromeus*, *Atlascopscosaurus*, *Planicoxa*, *Cumno-ria*, *Cedrorestes*, and NHMUK R28860 (“*Kukufeldia*”). Rerunning the analysis without

TABLE 2. Phylogenetic definitions used in this analysis.

Clade	Definition	Original Author (Other Uses)
Neornithischia	All genasaurians more closely related to <i>Parasaurolophus walker</i> , Parks, 1922, than to <i>Ankylosaurus magniventris</i> Brown, 1908 or <i>Stegosaurus stenops</i> Marsh, 1877.	Butler et al., 2008
Ornithopoda	All genasaurians more closely related to <i>Parasaurolophus walker</i> , Parks, 1922, than to <i>Triceratops horridus</i> Marsh, 1889	Butler et al., 2008
Thescelosauridae	All neornithischians more closely related to <i>Thescelosaurus neglectus</i> Gilmore, 1913 than to <i>Hypsilophodon foxii</i> Huxley, 1869, <i>Dryosaurus altus</i> (Marsh, 1878), or <i>Parasaurolophus walkeri</i> Parks 1922.	New, after Thescelosauridae, Buchholz, 2002 (Boyd, 2015)
Clypeodonta	<i>Hypsilophodon foxii</i> , <i>Edmontosaurus regalis</i> , their most recent common ancestor, and all of its descendants.	Norman, 2014a
Iguanodontia	The most inclusive clade containing <i>Parasaurolophus walkeri</i> Parks 1922 but not <i>Hypsilophodon foxii</i> Huxley, 1869, or <i>Thescelosaurus neglectus</i> Gilmore, 1913.	Sereno, 2005, emended from Sereno 1998
Rhabdodontoidea	A stem-based taxon including all taxa more closely related to <i>Zalmoxes robustus</i> (Nopcsa 1902) and <i>Rhabdodon priscus</i> Matheron 1869 than to <i>Dryosaurus altus</i> (Marsh, 1878).	New clade name
Rhabdodontidae	A node-based taxon consisting of the most recent common ancestor of <i>Zalmoxes robustus</i> (Nopcsa 1902) and <i>Rhabdodon priscus</i> Matheron 1869 and all the descendants of this common ancestor.	Weishampel et al., 2003
Dryomorpha	The most inclusive clade containing <i>Dryosaurus altus</i> (Marsh, 1878) and <i>Parasaurolophus walker</i> , Parks 1922	Sereno, 2005, emended from Sereno, 1986
Dryosauridae	The most inclusive clade containing <i>Dryosaurus altus</i> (Marsh, 1878) but not <i>Parasaurolophus walkeri</i> Parks 1922.	Sereno, 2005, emended from Milner and Norman, 1984
Ankylopollexia	The least inclusive clade containing <i>Camptosaurus dispar</i> (Marsh, 1879), <i>Uteodon aphanocetes</i> (Carpenter and Wilson, 2008) and <i>Parasaurolophus walker</i> , Parks 1922.	This study, emended from Sereno, 1998
Styracosterna	The most inclusive clade containing <i>Parasaurolophus walker</i> Parks, 1922 but not <i>Camptosaurus dispar</i> (Marsh 1879) or <i>Uteodon aphanocetes</i> (Carpenter and Wilson 2008).	This study, emended from Sereno, 1998
Iguanodontidae	The most inclusive clade containing <i>Iguanodon bernissartensis</i> Boulenger, 1881 but not <i>Parasaurolophus walkeri</i> Parks, 1922.	Sereno, 2005, emended from Sereno 1998
Hadrosauroidea	The most inclusive taxon containing <i>Parasaurolophus walkeri</i> Parks, 1922 but not <i>Iguanodon bernissartensis</i> Boulenger 1881, or <i>Mantellisaurus atherfieldensis</i> (Hooley 1925).	Sereno, 2005, emended from Sereno, 1998

these taxa yielded 114 MPTs; the strict consensus of these is shown in Figure 6.

The strict consensus of 114 MPTs is shown along with the Bayesian tree in Figure 6. A time scaled tree showing known temporal ranges of taxa is shown in Figure 7. Jackknife values at most nodes are low, but Bremer supports show some areas of the tree to be well supported. The phylogenetic definitions used here are summarized in Table 2.

The most notable features of this topology are the inclusion of *Tenontosaurus* and *Muttaborrasaurus* in a clade with Rhabdodontidae. Additionally, there is a clade of styracosternans that includes *Barilium*, *Hypselospinus*, and *Lurdusaurus*. This group is characterized by robust forearm elements,

presence of a radial tuberosity for insertion of *m. biceps brachii* and enlarged pollex unguals (at least 25% of radial length). There is also a small clade that includes *Iguanodon* and is here referred to as Iguanodontidae, though this is a smaller, more closely related group of taxa than the historical conception of iguanodontids. While there is some overlap with the ‘iguanodontoids’ of Norman (2015), several taxa from that clade are recovered in other groups in this topology.

Also of note is that the holotype of *Mantellisaurus atherfieldensis* (NHMUK R5764) forms a clade with the holotype of “*Dollodon bampingi*” (RBINS R57). This supports the contention that *D. bampingi* is a junior subjective synonym of *M. atherfieldensis*, as discussed by McDonald (2012b)

TABLE 3. Distributions of modeled variables in Bayesian analysis.

Statistic	ESS	Mean	Standard Deviation
Posterior	365	-5592	13.90
Likelihood	343	-4919	11.89
Birth rate (λ)			
Late Cretaceous	979	0.371	0.106
Early Cretaceous	3950	0.316	0.155
Late Jurassic	1318	0.344	0.117
Middle Jurassic	3823	0.314	0.155
Early Jurassic	3832	0.315	0.158
Late Triassic	33	0.288	0.087
Death rate (μ)			
Late Cretaceous	995	0.359	0.109
Early Cretaceous	4001	0.305	0.154
Late Jurassic	3085	0.254	0.121
Middle Jurassic	3809	0.306	0.156
Early Jurassic	4001	0.307	0.154
Late Triassic	32	0.278	0.090
Sampling rate (ψ)			
Late Cretaceous	3836	1.22E-3	1.45E-3
Early Cretaceous	3323	2.52E-3	2.08E-3
Late Jurassic	4001	8.45E-4	9.15E-4
Middle Jurassic	291	6.61E-3	3.99E-3
Early Jurassic	99	7.59E-3	2.90E-3
Late Triassic	138	1.03E-2	3.72E-3
Sampling proportion (ρ)	-	0.1	-

and Norman (2013, 2015). This *Mantellisaurus* clade is the sister to hadrosauroids.

It is also worth noting that based on previous definitions, Ornithopoda cannot be delineated easily on this phylogeny, as there are no marginocephalians included. Following the topology of Butler et al. (2008), Ornithopoda here would lie at the node basal to Thescelosauridae and Clypeodonta, but this is contradicted by the phylogeny of Boyd (2012), in which Thescelosauridae lies outside of Cerapoda (Ornithopoda + Marginocephalia). Further analysis with a wider sampling of basal ornithischians, and especially marginocephalians, is necessary to determine whether Thescelosauridae is included in Ornithopoda.

Bayesian Analysis

The MCC tree with posterior probabilities is shown along with the parsimony tree in Figure 6, and the time-calibrated tree is Figure 8. The value of ESS was well over 200 for most variables except the birth, death, and sampling rates for time bins 5

and 6 (Early Jurassic and Late Triassic). Given that only three taxa are present across both these bins, this is unsurprising. As determining birth and death rates near the root of the tree is not the goal of this study, and there are no differences in topology with the parsimony tree or Bayesian analyses without a skyline component, the smaller ESS for these parameters is not a cause for concern. The ESS and posterior distributions for key variables are given in Table 3.

Notable features of the topology of the Bayesian tree are a clade of hypsilophodontids that form the sister group to Iguanodontia. This hypsilophodontid clade includes thescelosaurids. Within Iguanodontia, there are two clades: Dryomorpha and Rhabdodontoidea, which includes Rhabdodontidae, *Tenontosaurus*, *Muttaborrasaurus*, *Talenkauen*, *Trinisaura*, *Anabisetia*, and *Kangnasaurus*. Within Dryomorpha, the topology of the Bayesian tree is similar to that of the parsimony tree, with *Uteodon* and *Camptosaurus* as the only non-styracosternan ankylopollexians, a small Iguanodonti-

dae, and a clade of taxa with robust forelimbs. *Mantellisaurus* groups with RBINS R57, and these are sister to Hadrosauroidae. Within Hadrosauroidae, the topology is consistent with the parsimony analysis (though polytomies in the parsimony tree are resolved into bifurcating branches in the Bayesian results) with one exception. *Tethyshadros* is recovered branching from a node basal to *Bactrosaurus* and *Gilmoresaurus* in the parsimony tree, but at a less inclusive node in the Bayesian tree. The genera found in Ankylopollexia, Styrcosterna, Iguanodontidae, and Hadrosauroidae are all identical in the parsimony and Bayesian topologies. This overall consistency indicates that the topology is supported by the data, regardless of the model.

SYSTEMATIC PALEONTOLOGY

Thescelosauridae Sternberg, 1937

Phylogenetic definition. All neornithischians more closely related to *Thescelosaurus neglectus* Gilmore, 1913 than to *Hypsilophodon foxii* Huxley, 1869, *Dryosaurus altus* (Marsh, 1878), or *Parasaurolophus walkeri* Parks, 1922.

Unambiguous synapomorphies. In the parsimony analysis (Figure 7), thescelosaurids are characterized by three unambiguous synapomorphies: dentary tooth row straight in dorsal view (98.0), 10-12 ridges on the maxillary teeth (136.3), and acromion process of scapula does not extend beyond the edge of the coracoid (196.0).

In the Bayesian analysis (Figure 8), a more extensive Thescelosauridae is characterized by two unambiguous synapomorphies: 10-12 ridges on the maxillary teeth (136.3) and 9-11 ridges on the dentary teeth (137.3).

Topology. Thescelosauridae is recovered in the parsimony analysis (Figures 6, 7) containing *Thescelosaurus*, *Parksosaurus*, *Orodromeus*, and *Zephyrosaurus*, though the group has poor support (Jackknife value=7). Unlike in Boyd (2012), *Haya* is recovered at a node basal to thescelosaurids, rather than within the Thescelosaurinae. *Macrogryphosaurus* and *Talenkauen*, which Boyd also found within Thescelosaurinae, are recovered within Iguanodontia, based on the presence of opisthocoele cervical vertebrae, and a postacetabular process that is less than 30% of total ilium length.

In the Bayesian analysis (Figures 6, 8), Thescelosauridae is nested within a larger Hypsilophodontidae. Though it only has moderate support (PP=0.59), the internal nodes have higher posterior probabilities. The genera included in this group match those recovered in the parsimony analysis;

the one difference in topology is that *Orodromeus* and *Zephyrosaurus* form successive outgroups to *Thescelosaurus* + *Parksosaurus* instead of forming a distinct Orodrominae (as found by Boyd 2012). Though *Haya* and *Macrogryphosaurus* are recovered as closely related hypsilophodontids, they are not found within Thescelosauridae as proposed in Boyd (2012).

Clypeodonta Norman, 2015

Phylogenetic definition. *Hypsilophodon foxii*, *Edmontosaurus regalis*, their most recent common ancestor, and all of its descendants (Norman, 2015).

Unambiguous synapomorphies. For the topology recovered by parsimony, Clypeodonta has nine unambiguous synapomorphies: presence of a quadrate buttress or "hamular process" (63.1), quadrate with a lateral condyle that is larger than the medial condyle (69.2), mandibular articulation that is horizontal to dorsomedially inclined in caudal view (70.0/1), maxillary and dentary teeth with crowns that taper toward the root (127.1, 128.1), with the base of the crown defined by an everted lip which makes the crown slightly inset from the root (146.1, 147.1), presence of a primary ridge on labial side of maxillary teeth (139.1), and elongate centra of postaxial cervical vertebrae, with cranio-caudal length more than twice the dorsoventral height (159.1).

Within the Bayesian topology, Clypeodonta is characterized primarily by features of the teeth and jaws: presence of a diastema in the maxilla (16.1), equal lengths in the oral margin of the premaxilla and prementary (84.1), a coronoid process that extends more than one crown height dorsal to the tooth row (101.1), surangular with a small fenestra positioned dorsally on or near the dentary joint (111.1), surangular foramen rostral to the lateral lip of the glenoid (114.1), cheek teeth with asymmetrically distributed enamel (134.1), ridges running the full length of the crown on the labial side of maxillary teeth and the lingual side of dentary teeth (135.1), and a femoral head separated from the greater trochanter by a distinct constriction (292.1). **Topology.** In the parsimony tree (Figures 6, 7), Clypeodonta is the sister clade to Thescelosauridae. This node has a jackknife value of 15, but a relatively high Bremer support of 4. *Hypsilophodon* is recovered as the only non-iguanodontian clypeodontan.

In the Bayesian topology (Figures 6, 8), *Hypsilophodon* is recovered within a large Hypsilophodontidae. Consequently, Clypeodonta is a more inclusive clade than in the parsimony tree, includ-

ing Thescelosauridae, a clade with *Haya*, *Jeholosaurus*, and *Othnielosaurus*, and *Leaellynasaura*, *Gasparinisaura*, and *Macrogyphosaurus*. It excludes only a few basal neornithischians such as *Hexinlusaurus* and *Agilisaurus*. It is moderately supported, with a posterior probability (PP) of 0.60.

IGUANODONTIA Sereno, 1986

Phylogenetic definition. The most inclusive clade containing *Parasaurolophus walkeri* Parks, 1922 but not *Hypsilophodon foxii* Huxley, 1869, or *Thescelosaurus neglectus* Gilmore, 1913 (Sereno, 2005).

Unambiguous synapomorphies. In the parsimony analysis, Iguanodontia is characterized by a maxilla with a broad and triangular dorsal process of the maxilla (21.1), a quadrate extending ventrally such that the quadratojugal is well removed from the mandibular condyle (60.1), a single wear facet on each cheek tooth (131.1), opisthocoelus post-axial cervical vertebrae (157.1), a distinct indentation on the scapula superior to the glenoid, termed here the supraglenoid fossa (199.1), and a manual digit III with three or fewer phalanges (236.1).

Two other synapomorphies recovered for this clade are elongate prezygopophyses on the distal caudal vertebrae (185.1), and chevrons that are strongly and asymmetrically expanded distally (188.1). The former of these is found only in *Gasparinisaura* and *Leaellynasaura*, and the latter in these genera plus *Parksosaurus* and *Macrogyphosaurus*. While they are present at the base of the clade, these characters are not widespread, and therefore not useful in diagnosing the clade.

There is only one overlapping character here with the diagnosis of Sereno (1986); the reduction of phalanges in digit III. The presence of “leaf-shaped” or mamillated denticles is more restricted within Styracosterna, and while most iguanodontians lack premaxillary teeth, both *Talenkauen* and *Tenontosaurus dossi* have one premaxillary tooth. Iguanodontia is recovered with jackknife support of 19 and Bremer support of 4.

Within the Bayesian topology, Iguanodontia (PP=0.43) lacks the basal pectinate region found in the parsimony analysis and is instead composed of the sister groups of rhabdodontoids and Dryomorpha. *Gasparinisaura*, *Leaellynasaura*, and *Macrogyphosaurus* are excluded from Iguanodontia, and are recovered instead with the hypsilophodontids. This rearrangement of taxa leads to different synapomorphies for Iguanodontia between the parsimony and Bayesian analyses. Synapomorphies for the Bayesian topology include: premaxilla flaring

laterally to form a floor of the narial fossa (3.1), small antorbital fenestra (31.1), predentary with denticulate oral margin (87.1), ventral process of predentary deeply bifurcated (89.1), cheek teeth with crowns tapering toward the root (127.1, 128.1), cheek teeth that are closely packed without spaces between roots (126.1), cheek teeth with one wear facet on each tooth (131.1), cheek teeth lacking a basal ridge (“cingulum”) (148.1), caudal vertebrae with distal facets for chevrons much larger than proximal facets (183.0), humerus with an elongate deltopectoral crest (>43% humeral length) (214.1), manual digit III with three or fewer phalanges (236.1), first phalanx of manual digits II-IV more than twice the length of the second phalanx (239.1), ischium with an untwisted shaft (283.1), ischium with an expanded distal end (288.1), femur with a cranial intercondylar sulcus (300.1), and a caudal intercondylar sulcus partially roofed by the medial condyle (302.1).

Topology. In the parsimony analysis (Figures 6, 7), the basally branching portion of Iguanodontia forms a pectinate topology outside of Dryomorpha, which includes *Gasparinisaura*, *Leaellynasaura*, *Macrogyphosaurus*, *Talenkauen*, *Valdosaurus*, *Anabisetia*, *Trinisaura*, and *Kangnasaurus*. It is supported by a jackknife value of 19 and a Bremer support of 4.

In the Bayesian analysis (Figures 6, 8), Iguanodontia bifurcates into rhabdodontoids and dryomorphans. Iguanodontia is supported by a posterior probability of 0.43.

RHABDODONTOIDEA new clade name

Phylogenetic definition. A stem-based taxon including all taxa more closely related to *Zalmoxes robustus* and *Rhabdodon priscus* than to *Dryosaurus altus*.

Unambiguous synapomorphies. The smaller clade found in the parsimony analysis is characterized by four unambiguous synapomorphies: a sub-rectangular orbit (34.1), sinuous ventral edge of the jugal (56.1), caudodorsally extending postacetabular process of the ilium (265.1), and a femur that is straight in lateral view (290.0).

The larger Bayesian clade has two unambiguous synapomorphies: maxilla with a broad triangular dorsal process (21.1), and a straight maxillary tooththrow in ventral view (26.2).

Topology. The parsimony analysis (Figures 6, 7) recovers a clade containing rhabdodontids, *Tenontosaurus*, and *Muttaborrasaurus*; this is supported by a jackknife value of 23, and Bremer support of 4.

The Bayesian analysis (Figures 6, 8) also finds *Tenontosaurus* and *Muttaborrasaurus* as the sister taxa to Rhabdodontidae, but this is included within a larger clade with many Gondwanan taxa (*Kangnasaurus*, *Anabisetia*, *Trinisaura*, and *Talenkauen*). The basal node of the clade is poorly supported (PP=0.24), though the node supporting Rhabdodontidae, *Muttaborrasaurus*, and *Tenontosaurus* has stronger support (PP=0.85).

RHABDODONTIDAE

Weishampel, Jianu, Csiki, and Norman, 2003

Phylogenetic definition. A node-based taxon consisting of the most recent common ancestor of *Zalmoxes robustus* and *Rhabdodon priscus* and all the descendants of this common ancestor (Weishampel et al., 2003).

Unambiguous synapomorphies. Rhabdodontidae is characterized by the presence of apicobasally extending ridges on the cutting surfaces of unworn cheek teeth (lingual surface of maxillary teeth, labial surface of dentary teeth) (138.1), acromion process of scapula does not extend beyond the edge of the coracoid (196.0), medial condyle of the humerus transversely wider than the lateral (216.2), proximal flange present on the ulna (219.1), preacetabular process of the ilium twisted around its long axis (249.1), pubic peduncle of the ischium dorsoventrally compressed (280.1), and distal condyles of the femur expanded both cranially and caudally (304.1), metatarsal V absent (320.1).

Topology. This small clade contains two genera, *Zalmoxes* and *Rhabdodon*, both known from the Late Cretaceous of Europe. This clade is recovered in the parsimony analysis with a jackknife value of 81 and a Bremer support of 4, and in the Bayesian analysis with a posterior probability of 1. DRYOMORPHA Sereno, 1986

Phylogenetic definition. The most inclusive clade containing *Dryosaurus altus* (Marsh, 1878) and *Parasaurolophus walkeri* Parks, 1922 (Sereno, 2005).

Unambiguous synapomorphies. In both parsimony and Bayesian analyses, Dryomorpha is characterized by a premaxilla with a posterolateral process that contacts the lacrimal (6.1), a maxilla with a rostralateral process (18.1), a lacrimal that fits into a slot in the dorsal process of the maxilla (27.1), a quadratojugal that lacks a dorsal process (57.1), a coronoid process with subequal cranio-caudal widths of dentary and surangular (109.1), cheek teeth with secondary ridges that are thin and formed only from enamel (145.1), a radius that is triangular in distal view (224.1), and an ischium

with the obturator process within the proximal 25% of the ischium (287.1).

In the parsimony analysis, Dryomorpha is further supported by a maxillary tooth row that is medially bowed in ventral view (26.0), a jugal that is excluded from the antorbital fenestra by lacrimal-maxilla contact (47.0), a quadratojugal that lacks a foramen through the center of the element (58.0), and absent ossified hypaxial tendons on the caudal vertebrae (322.0).

In the Bayesian analysis, Dryomorpha is also supported by the presence of a quadrate buttress or "hamular process" (63.1), presence of a quadrate (or paraquadrate) foramen or notch on the boundary between the quadrate and quadratojugal (65.1), and presence of a short midline process of the prementary dorsal to the dentary symphysis (90.1)

Topology. In both parsimony and Bayesian analyses (Figure 6), Dryomorpha contains two sister clades: Dryosauridae and Ankylopollexia. Support for this node is moderate (jackknife=19, Bremer support=4, PP=0.27).

DRYOSAURIDAE Milner and Norman, 1984

Phylogenetic definition. The most inclusive clade containing *Dryosaurus altus* (Marsh, 1878) but not *Parasaurolophus walkeri* Parks, 1922 (Sereno, 2005).

Unambiguous synapomorphies. Dryosauridae is characterized by nine unambiguous synapomorphies: premaxilla with a medial dorsal (nasal) process that does not contact the nasal (9.1), palpebrals that traverse the entire width of orbit (42.1), a dentary with dorsal and ventral margins (under the tooth row) that converge anteriorly (97.0), maxillary teeth with primary ridges that are centered mesio-distally (143.0), 15 or fewer dorsal vertebrae (161.0), posterior dorsal vertebrae with transverse processes longer than the dorsoventral height of the centrum (167.1), scapula with a weakly developed acromion process (195.0), prepubic process with a horizontal ridge on medial side (273.1) and a pubis with an obturator foramen completely enclosed by bone (275.0)

Topology. In addition to *Dryosaurus* and *Dysalotosaurus*, which have been found previously to form a clade (McDonald et al., 2010b), this analysis finds the unnamed Kirkwood taxon from South Africa within the group, as sister to *Dysalotosaurus*. The clade is well supported, with a jackknife value of 60, and Bremer support of 4. In the Bayesian topology, Dryosauridae also contains *Valdosaurus* as sister to the Kirkwood taxon (PP=0.27).

ANKYLOPOLLEXIA Sereno, 1986

Phylogenetic definition. The least inclusive clade containing *Camptosaurus dispar* (Marsh, 1879), *Uteodon aphanoecetes* (Carpenter and Wilson 2008), and *Parasaurolophus walkeri* Parks, 1922 (emended from Sereno, 1986).

Unambiguous synapomorphies. Ankylopollexia is characterized by nine unambiguous synapomorphies: deltoid ridge of the scapula close to parallel to the long axis of the scapula (198.0), humerus with a well-developed deltopectoral crest (212.0), ulna with a flange on the proximal end that wraps around the lateral edge of the radius (219.1) some fusion of the carpals (227.1), manual digit I oriented at least 45 degrees from the antebrachial axis (232.1), metacarpal I short and block-like (233.1), ungual of manual digit I subconical (241.1), brevis fossa of ilium not well defined by a lateral lip (259.0), ossified epaxial and hypaxial tendons arranged in a double-layered lattice (323.1).

Topology. This is a well-supported clade, with a Jackknife value of 35 and Bremer support of 6 in the parsimony analysis (Figure 7), and a posterior probability of 0.91 in the Bayesian tree (Figure 8). In both topologies, the most basally branching taxon is *Uteodon*, and *Camptosaurus* is recovered as the sister to Styrcosterna. These two genera are the only non-styrcosternan ankylopollexians.

STYRCOSTERNA Sereno, 1986

Phylogenetic definition. The most inclusive clade containing *Parasaurolophus walkeri* Parks 1922 but not *Camptosaurus dispar* (Marsh, 1879) or *Uteodon aphanoecetes* (Carpenter and Wilson 2008).

Unambiguous synapomorphies. Styrcosterna is characterized by five unambiguous synapomorphies: presence of denticulation on the oral margin of the premaxilla (5.1), 18-28 maxillary tooth positions (123.2), dentary teeth with a maximum of two to four ridges extending from the base to the tip of the crown on lingual side of teeth (137.1), maxillary tooth crowns mesiodistally narrower than dentary crowns (149.1), mid to posterior dorsal vertebrae with length much shorter than height (164.1).

Topology. Styrcosterna has strong support in both topologies (JV=35, BS=4, PP=0.91), but within this group, relationships are resolved poorly. The parsimony tree (Figure 7) has several polytomies and the Bayesian tree (Figure 8) recovers several small clades within Styrcosterna, but most have low support.

UNNAMED NODE

Comments. No formal definition is given for this clade of styrcosternans with robust forelimbs.

Variations on it are recovered in both parsimony and Bayesian analyses, but the lack of strong support and variability in included taxa makes this grouping tentative.

Unambiguous synapomorphies. This group is characterized by seven unambiguous synapomorphies: neural spines of caudal vertebrae bowed (180.1), robust ulna with length less than nine times diameter at mid-shaft (217.0), olecranon process of the ulna greater than 17% of ulna length (218.2), robust radius with minimal radial width equal to or greater than 12% radial length (221.1), presence of tubercle near proximal end of radius for insertion of *M. biceps* (223.1) manual ungual I greater than 30% the length of the radius (242.1), and obturator foramen of the pubis circular (276.1).

Topology. The parsimony analysis (Figures 6, 7) recovers a small clade of styrcosternans that includes *Hypselospinus*, the holotype of *Barillum*, and *Lurdusaurus*. In the majority rule consensus, *Bolong* and *Jinzhouosaurus* are also included in this clade. This larger clade including *Bolong* and *Jinzhouosaurus* is also recovered in the Bayesian analysis (Figures 6, 8), supported with a posterior probability of 0.14. The clade can be diagnosed by several synapomorphies, and some genera share character states that are found nowhere else in the analysis: *Hypselospinus* and *Lurdusaurus* each have olecranon processes that compose more than 17% of the ulna length, and a radial tubercle for the insertion of *M. biceps*.

IGUANODONTIDAE Gervais, 1853

Phylogenetic definition. A stem-based taxon including all taxa more closely related to *Iguanodon bernissartensis* than to *Edmontosaurus regalis*.

Unambiguous synapomorphies. This clade is characterized by three unambiguous synapomorphies: palpebrals that traverse the entire width of orbit (42.1), postorbital with a bifurcated squamosal process (45.1) small fenestra near the suture of the dentary and surangular lies within the surangular (112.1). (Note that this fenestra is not present in *Iguanodon* or *Equijubus*.)

Topology. This is another small clade of styrcosternans that includes *Iguanodon*, along with *Equijubus*, *Proa*, and *Fukuisaurus*. As such, the name Iguanodontidae is appropriate, although the taxa included within it are far more closely related to each other than those within the historical conception of Iguanodontidae (e.g., Huxley (1870) included *Hypsilophodon* and hadrosaurs within Iguanodontidae). The support for the group is not high, with a jackknife value=12 and a Bremer sup-

port of 2, but the same topology is recovered in the Bayesian analysis (with a posterior probability of 0.46).

MANTELLISAURUS + “*DOLLODON*”

Unambiguous synapomorphies. This grouping is supported by seven unambiguous synapomorphies: presence of a fossa or foramen just dorsal to the oral margin along the premaxilla-maxilla boundary (15.1), diastema of the maxilla one to two tooth widths long (17.0), strongly downturned rostral end of dentary ramus (95.1), subvertical coronoid process of dentary (105.1), mid to posterior dorsal vertebral centra with craniocaudal length subequal to or longer than dorsoventral height (164.0), humerus less than 62% of femoral length (211.0), metacarpal III long and slender with length more than 5.5 times minimum transverse width (230.1).

Topology. The holotype specimen of *Mantellisaurus* is recovered as the sister taxon to IRSNB 1551, referred to *Dollodon* by Paul (2008). The clade is supported with jackknife of 55 and a Bremer support of 3. This clade is also recovered in the Bayesian analysis (PP=0.71).

HADROSAUROIDEA Sereno, 1986

Phylogenetic definition. The most inclusive taxon containing *Parasaurolophus walkeri* Parks, 1922 but not *Iguanodon bernissartensis* Boulenger, 1881 (Sereno, 2005).

Unambiguous synapomorphies. Hadrosauroids are characterized largely by features related to the “dental battery”, which become even more exaggerated in the hadrosaurids. The clade has 18 unambiguous synapomorphies: antorbital fenestra absent (29.1), left and right squamosals separated by only a narrow band of the parietal (73.1), long diastema of the dentary, the width of three or more teeth (93.1), dentary, rostral extent of Meckel's groove meets the dentary symphysis: absent, ends more caudally (94.1), caudal extent of dentary tooth row is in line with or caudal to the apex of the coronoid process (103.2), coronoid process of the dentary oriented near vertically (105.1), coronoid process of the dentary with a rostrocaudally expanded apex (107.1), maxillary teeth with a primary ridge only (136.0), dentary tooth row with one functional tooth rostrally and caudally, and up to two teeth at and approaching the middle of the dental battery (150.1), maximum of two replacement dentary teeth (151.1), dentary without discrete alveoli, but parallel grooves lining a continuous dental battery (152.1), most proximal chevron placed at distal end of third caudal verte-

bra or more distally (186.2), coracoid, length of the scapular articulation less than 1.25 times the length of the lateral margin of the glenoid (207.1), radius length greater than 70% of humeral length (220.1), metacarpal III long and slender, length greater than 5.5 times the transverse width at mid-shaft (230.1), preacetabular process of the ilium is parallel-sided or slightly tapering at its distal end (251.0), base of the preacetabular process of the ilium is not transversely thickened ventrally (252.0), ischium shaft straight in lateral view (281.0), distal condyles of femur with rounded articular surfaces (305.1).

Topology. Support in the parsimony tree is low (jackknife=7, Bremer support=2), but there is strong support in the Bayesian tree (posterior probability=0.96). It includes *Probactrosaurus*, *Batyrosaurus*, *Altirhinus*, *Jeyawati*, *Eolambia*, *Protohadros*, *Shuangmiaosaurus*, *Levnesovia*, *Gilmoresaurus*, *Bactrosaurus*, *Tethyshadros*, *Telmatosaurus*, *Edmontosaurus*, *Maiasaura*, and *Hypacrosaurus*. This topology agrees with the results of other recent studies (e.g., Gates and Scheetz, 2014; Prieto-Márquez, 2012).

Ancestral Area Reconstruction

Among the models used (DEC, DIVALIKE and BAYAREA), the DIVALIKE model had the lowest AICc score, and AAR from this model is shown in Figure 9. Few clades in this analysis form distinct geographic clusters. Ankylopollexians are found primarily in Laurasia, with the exception of *Ouranosaurus* and *Lurdusaurus* in northern Africa. Based on the maximum likelihoods found in the AAR, ankylopollexians are likely to have originated in North America, and hadrosauroids are likely to have evolved in Asia.

While the large rhabdodontoid group recovered in the Bayesian analysis is not well supported, if this clade existed it was geographically widespread, and the ancestral area is not clear. A small clade within the rhabdodontoids is restricted to Gondwana; this includes the genera *Kangnasaurus* from South Africa, *Anabisetia* and *Talenkauen* from Argentina, and *Trinisaura* from Antarctica. The estimated mean age of the node at which this clade branches from the rest of the rhabdodontoids is 145 ma, with a 95% confidence interval ranging from a minimum age of 126 ma to a maximum of 168 ma. The large range here is likely due to the poorly constrained age of *Kangnasaurus*. While this range overlaps with the opening of the North Atlantic Ocean and the separation of Laurasia from Gondwana (Blakey, 2008), the large range of

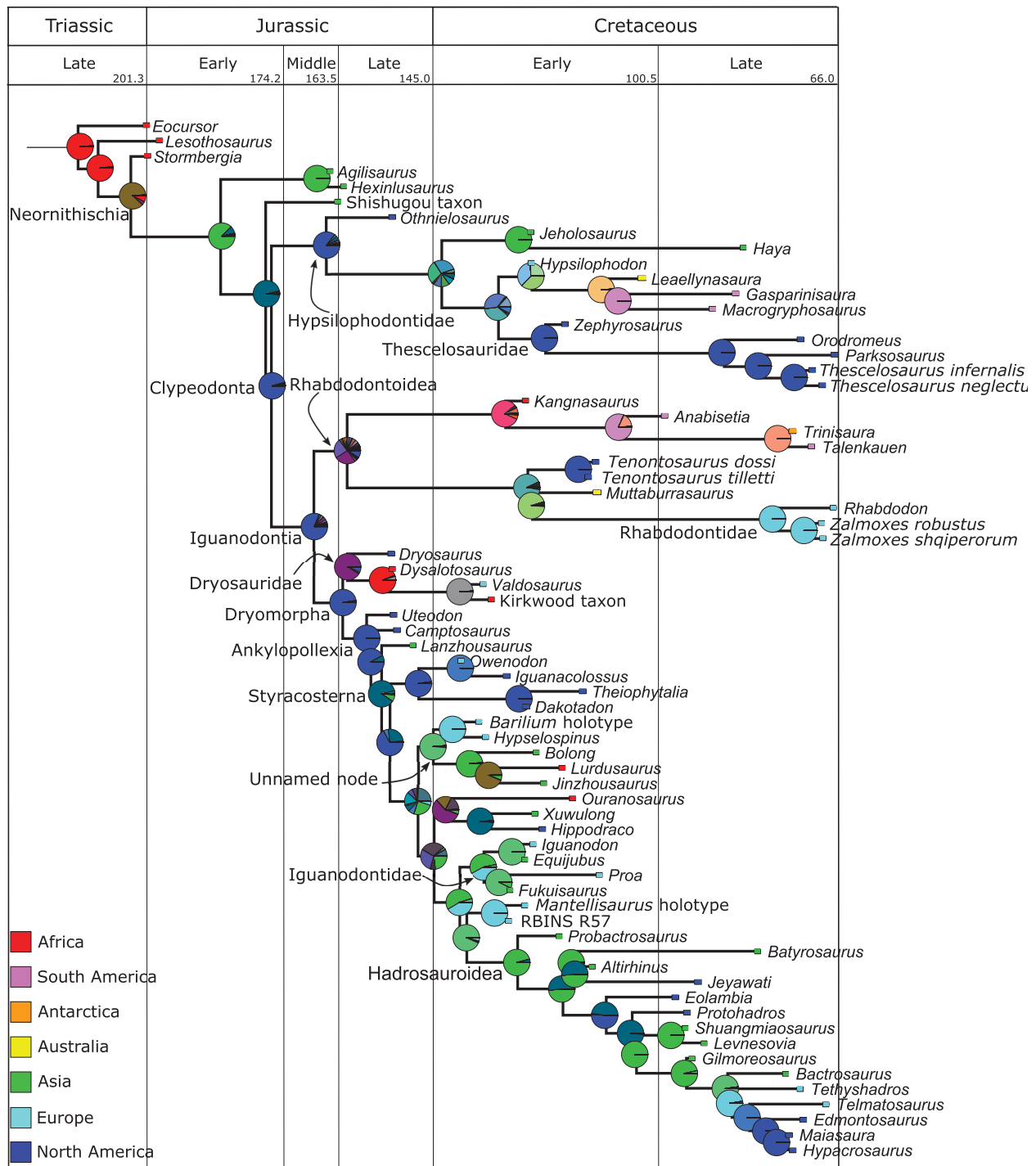


FIGURE 9. Ancestral Area Reconstruction on MCC tree from Bayesian analysis. Squares at tips show taxon ranges, pie charts at nodes show likelihoods of ancestral ranges. Key shows colors corresponding to modern continents; blended colors (e.g., the orange wedge in the node leading to *Leaellynasaura* and *Gasparinisaura*) indicate an ancestral range in both descendant ranges.

potential node ages makes it difficult to determine with any certainty whether this clade diverged due to vicariance.

The more basal Hypsilophodontidae are geographically wide-ranging, although they are best represented in the Late Cretaceous by Thescelosauridae from North America. The basal position of

Othnielosaurus also helps to increase the likelihood of the group originating in North America. The age of the nodes Clypeodonta and Iguanodontia indicate that late Early through Middle Jurassic aged deposits should be productive for finding fossils that elucidate the relationships at the base of Clypeodonta, and across basal Ornithischia.

Effect of Postcranial Characters

The parsimony analysis that excluded the 80 new postcranial characters produced 3,086 MPTs, with a strict consensus that is considerably less resolved than the primary analysis discussed here (Figure 10). Styrcosterna is recovered as a large polytomy including 18 terminals and two clades. Both Iguanodontidae and the unnamed styrcosterman clade collapse in this analysis. Thescelosauridae, rhabdodontoids, and Dryosauridae are recovered in this tree, and *Camptosaurus* and *Uteodon* are recovered as basal ankylopollexians outside of Styrcosterna, which is a slight improvement over the strict consensus found by McDonald (2012a), in which Ankylopollexia formed a large polytomy. The poor resolution of this tree indicates the improvement in resolution achieved with a concerted effort to include more postcranial characters.

DISCUSSION

Tree Topology and Nomenclature

In overall structure, this analysis agrees largely with previous work (Serenó, 1998; McDonald et al., 2010b; McDonald et al., 2012; Norman, 2015) in finding a series of nested clades within Iguanodontia: Dryomorpha, Ankylopollexia, Styrcosterna, and Hadrosauroidea. The sister group to Ankylopollexia is Dryosauridae; together these form the node-based Dryomorpha, and the sister group to this is the rhabdodontoids.

The topology found here agrees with that of Boyd (2012, 2015) in recovering a Thescelosauridae (=“Parksosauridae”) outside of Iguanodontia, although there are some differences in the taxa included. *Haya* is recovered at a node basal to thescelosaurids, rather than within the Thescelosaurinae. *Macrogryphosaurus* and *Talenkauen*, which Boyd also found within Thescelosaurinae, are recovered within Iguanodontia. Given that Thescelosauridae falls within Clypeodonta in the Bayesian topology, it is possible that the latter term may be equivalent or at least similar in taxonomic composition to Ornithopoda. To test this further,

several marginocephalians and relevant characters would need to be added to the analysis.

The Clypeodonta recovered in both the parsimony and Bayesian trees differs from that of Norman (2015), largely due to the inclusion of more non-iguanodontian neornithischians. Some of the characters cited by Norman to diagnose Clypeodonta (e.g., the presence of ridges on the labial surface of maxillary teeth) are more widespread, also occurring in Thescelosauridae.

As in the work of McDonald (2012a) and Dieudonné et al. (2016), and congruent with observations of Molnar (1996), this analysis recovers *Muttaburrasaurus* in a clade with Rhabdodontidae. Dieudonné et al. (2016) erected a node-based clade, Rhabdodontomorpha, for this group. In the parsimony analysis, rhabdodontomorphans also includes *Tenontosaurus*, while the Bayesian analysis finds *Tenontosaurus* as the sister to Rhabdodontomorpha. It also recovers a larger group of rhabdodontoids including more Gondwanan taxa. The taxa included in Rhabdodontoidea are likely to shift as new analyses are done, but the stem-based definition given here will create some stability. This grouping is congruent with biogeographic analyses linking European and Gondwanan taxa (Ezcurra and Agnólin, 2012). Rhabdodontoids are united primarily by dental features: teeth that are relatively wide mesiodistally, with a high number of secondary ridges that are thick, composed of both dentine and enamel (rather than being formed only of small crenulations in the enamel). While it is likely that these taxa form a clade, it is also possible that these character states are parallelisms, due to similar diets or chewing mechanisms.

When Ankylopollexia was named, *Uteodon aphanoeectes* had not yet been recognized and the specimens which now represent the taxon were referred to *Camptosaurus dispar*, which Sereno (1986) used to define Ankylopollexia. Considering these taxonomic changes, and Sereno’s original description of ankylopollexians as those iguanodontians that displayed fused carpals, it seems prudent to emend Sereno’s definition to include both *U. aphanoeectes* and *C. dispar* as reference taxa for Ankylopollexia. It should be noted that all nine of the unambiguous synapomorphies of this group are postcranial, with four associated with carpal fusion and modifications in the first manual digit. In addition to these, the presence of a flange on the ulna serves as an indicator of quadrupedality (Maidment and Barrett, 2014, and see below). Thus, the fundamental shift between non-

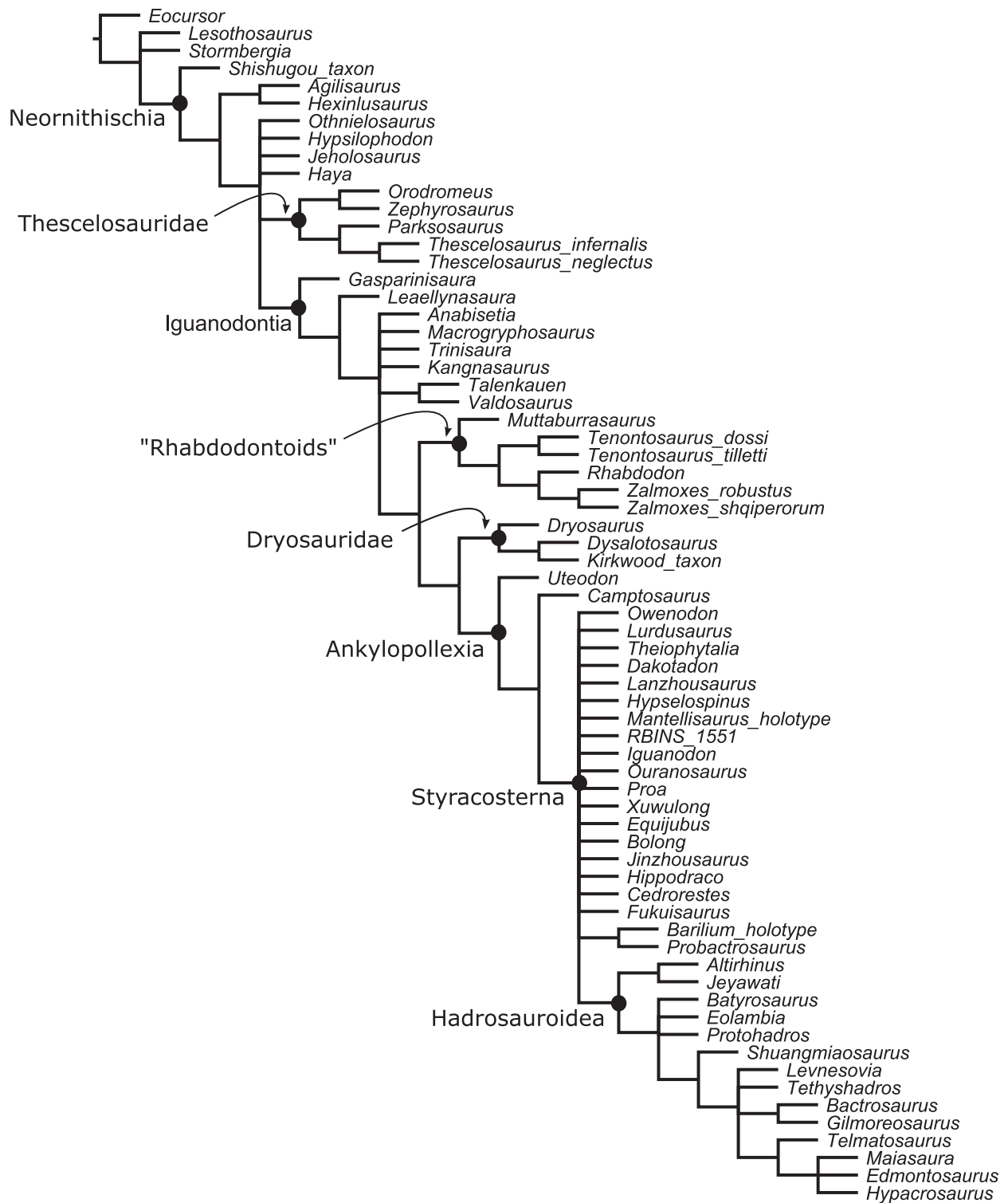


FIGURE 10. Strict consensus of 3,086 MPTs produced from a parsimony analysis excluding the 80 novel postcranial characters used in this analysis. Styrcosterna is composed of a large polytomy, and smaller polytomies are found outside Rhabdodontoidea and Thescelosauridae.

ankylopollexian iguanodontians and Ankylopollexia lies in the forelimbs, and in a shift to functional quadrupedality.

As with Ankylopollexia, the definition of Styrcosterna is emended to exclude both *Camptosaurus dispar* and *Uteodon aphanocetes*. It should also be noted that the eponymous feature of this group, the “hatchet-shaped” sternal, with a caudolateral process projecting from the main plate of the sternal, is more widespread than previously recognized, and found in at least two genera outside of Styrcosterna: the basal iguanodontian *Macrogyphosaurus*, and the unnamed dryosaurid from the Kirkwood Formation.

This analysis agrees partly with that of Norman (2015) in finding a clade within Styrcosterna including *Iguanodon* and *Proa*, but differs in placing *Batyrosaurus*, *Barilium*, *Bolong*, *Jinzhouosaurus*, and *Mantellisaurus* outside this clade. Aside from *Batyrosaurus* which is recovered as a basal hadrosauroid, these taxa are all found in the large polytomy of styrcosternans, just one node outside of iguanodontids. In that sense, this topology is not drastically different from that of Norman (2015), but the larger number of taxa included here may have caused the strict consensus to collapse.

The holotype of *Mantellisaurus* and RBINS R57 (“*Dollodon*”) being recovered as sister taxa within their own small clade lends support to the taxonomic conclusion of Norman (2013, 2015) and McDonald (2012b) that *Dollodon* should be considered a subjective junior synonym of *Mantellisaurus*.

There are two non-hadrosauroid clades within Styrcosterna, iguanodontoids and an unnamed clade with more robust forelimb elements and a larger ungual on the first digit (Figure 11). The lack of clear temporal succession or geographic separation between these two groups (Figure 9) indicates this was not due to faunal turnover or vicariance and could represent niche partitioning. As many of the synapomorphies are associated with heavier, more muscular forearms and a larger pollex ungual, it is also possible that these characters are linked functionally and represent parallelisms within Styrcosterna.

Morphological Patterns

One of the most surprising outcomes of this analysis in terms of character distribution is the homoplasy found in “hatchet shaped” sternals (those with a caudolateral process). This feature was thought to be diagnostic of Styrcosterna, even giving the name to the group (Serenó, 1986). However, it seems to have arisen at least three

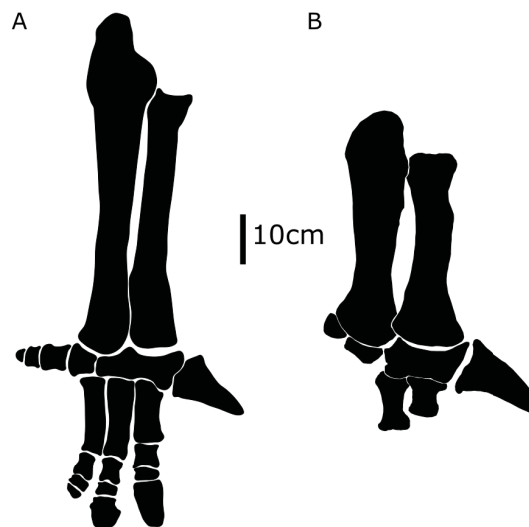


FIGURE 11. Silhouettes showing the radius, ulna and manus of A, *Iguanodon* (from RBINS 1534 and 1558) and B, *Lurdusaurus* (from MNHN.F.GDF 1700).

times within Iguanodontia: in *Macrogyphosaurus*, in the Kirkwood taxon (Dryosauridae), and in Styrcosterna (Figure 12). The position of *Macrogyphosaurus* is quite different between the parsimony and Bayesian analyses, but in both cases it is well outside of Styrcosterna. A similar morphology also occurs in Pachycephalosauridae (Maryańska and Osmólska, 1974; Perle et al., 1982).

The rugose caudal end of the process indicates it served as an attachment point for costal cartilage. This relationship appears to be present in non-styrcosternan neornithischians such as *Hypsilophodon* (Galton, 1974; Butler and Galton, 2008) and *Thescelosaurus* (NCSM 15728), which both show the sternal articulated with ossified segments of costal cartilage. While this may explain the function of the caudolateral process of the sternal, it fails to indicate any functional reason for the difference in morphology. Previous studies of comparative myology (e.g., Dilkes, 2000) have not discussed the sternal in detail. While it would have served as the origin of *M. pectoralis*, it remains unclear what changes to the myology might occur with the presence of a caudolateral process of the sternal.

There are some clear trends among dental characters that are helpful in distinguishing ankylopollexians, rhabdodontoids, and thescelosaurids.

Thescelosauridae retain the most plesiomorphic teeth, with five to six premaxillary teeth, cheek teeth with a distinct angle between crown and root,

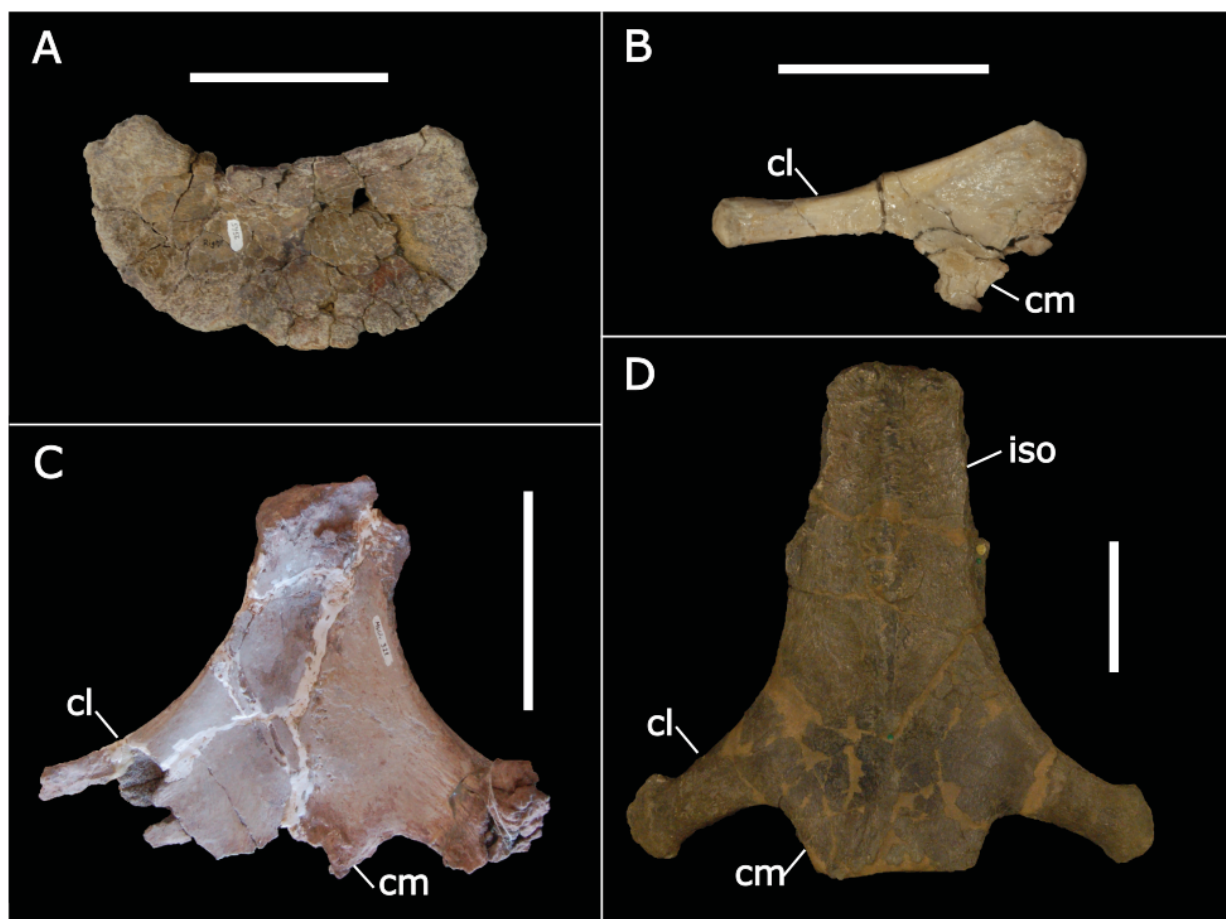


FIGURE 12. Sternals of A, *Tenontosaurus* (YPM 5456); B, the Kirkwood taxon (AM 6067); C, *Macrogyrophosaurus* (MUCPv 321); D, *Hypselospinus* (NHMUK R1885). A and B are right sternals in ventrolateral view, C and D are coossified left and right sternals, C in caudodorsal view and D in cranioventral view, including the midline interstitial ossification. Abbreviations: cl, caudolateral process; cm, caudomedial process; iso, interstitial ossification. Scale bar equals 10 cm in A, C, and D, and 1 cm in B.

spaces between roots, and a basal ridge (=cingulum) (Figure 13A). Rhabdodontoidea, Dryosauridae, and Ankylopollexia all have a reduction or complete loss of premaxillary teeth, cheek teeth that are closely packed with crowns that taper toward the root, and no basal ridge. While rhabdodontoids trend toward fewer but wider teeth with many ridges (Figure 13B), the teeth of ankylopollexians become more numerous and narrower (especially in the maxilla), with fewer ridges. The morphology of the dental ridges also differs: rhabdodontoids display thick, regularly spaced secondary ridges (Figure 13B), while ankylopollexians have thin, often irregular secondary ridges that merge or split with each other (Figure 13D). In this respect, *Tenontosaurus* is similar to ankylopollexians (Figure 13C). Within hadrosauroids, the secondary ridges are lost as the tooth crowns become even narrower and more numerous.

Locomotor Changes

Maidment and Barrett (2014) surveyed ornithischians to determine osteological correlates for quadrupedality using taxa that were either clearly bipedal or clearly quadrupedal. They found five characters that consistently correlated with quadrupedality, four of which are examined here (their “transversely broadened ilium” does not clearly correlate to any of the characters in this analysis). Changes in these character states are mapped onto the Bayesian phylogeny (Figure 14).

The four characters that Maidment and Barrett found to be correlates of quadrupedality that are present in this analysis are:

- 219.1** Ulna, flange on proximal end that wraps around the lateral edge of the radius: present.

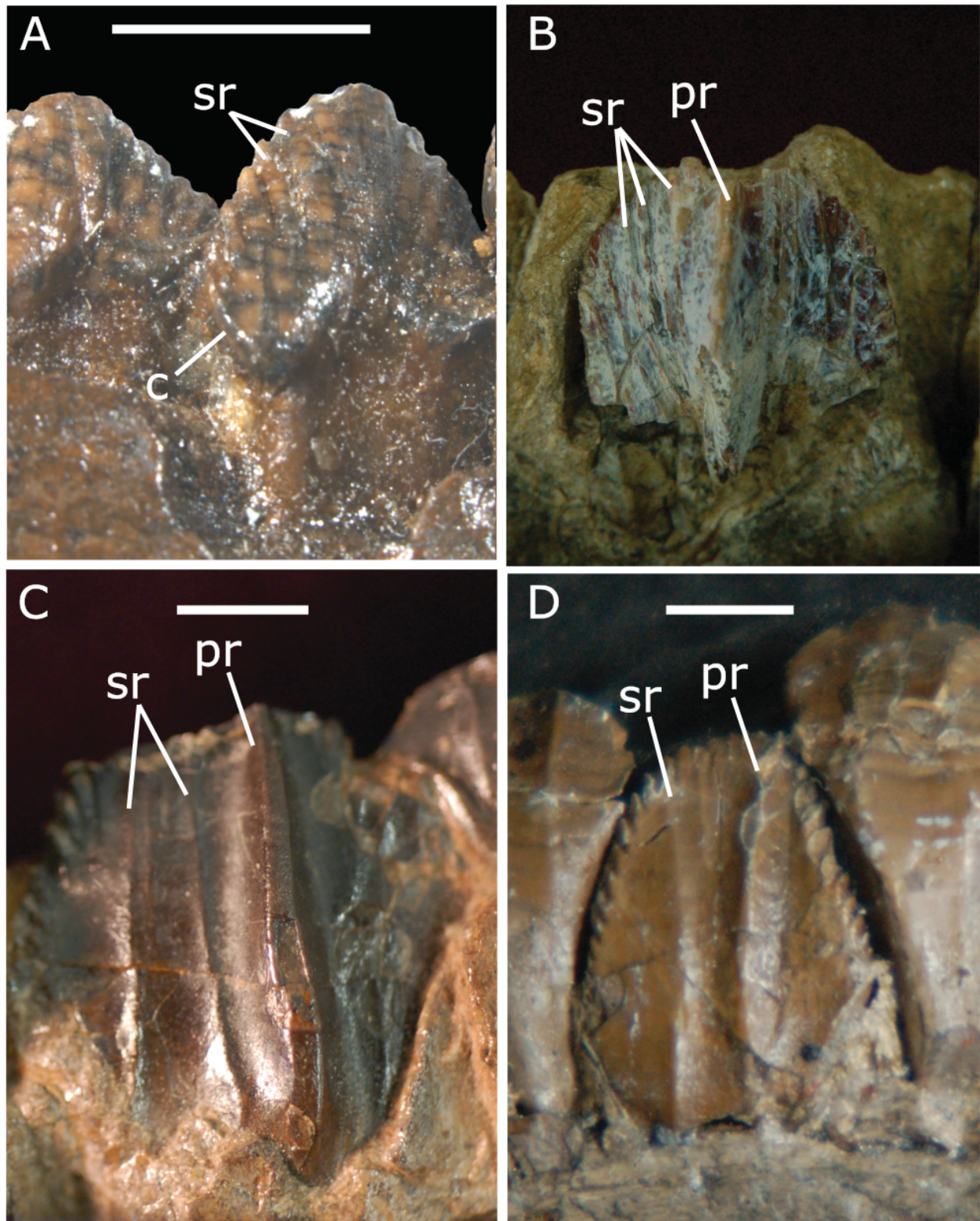


FIGURE 13. Dentary teeth in labial view of A, *Thescelosaurus infernalis* (SDSM 7210); B, *Rhabdodon* (MC.CY.QR1); C, *Tenontosaurus tilletti* (AMNH 3034); and D, *Owenodon* (NHMUK R2998). Abbreviations: c, cingulum; pr, primary ridge; sr, secondary ridge. Scale bars equal 5 mm.

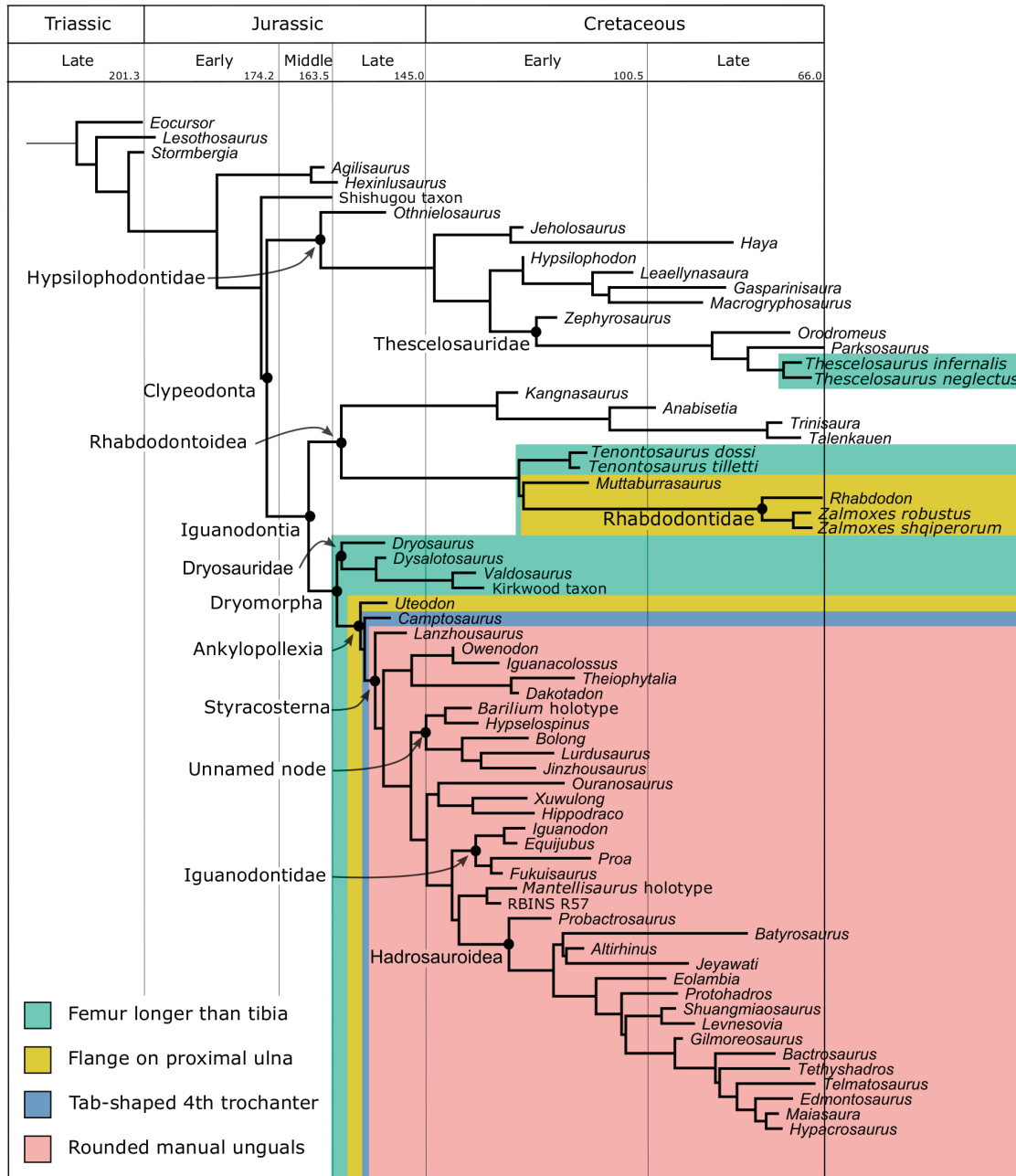


FIGURE 14. Time-calibrated Bayesian MCC tree, showing character state changes for osteological correlates of quadrupedality. Light red, femur longer than tibia; yellow, proximal ulnar flange present; green, tab-shaped fourth trochanter; blue, rounded manual unguals. Note that some posterior probabilities and labels for Ankylopollexia and Styracosterna have been removed for clarity; the groups are still indicated by closed circles at their respective nodes.

243.1 Manus unguals II and III, shape: dorsoventrally compressed, with a rounded tip.

289.1 Femur, length relative to tibia: longer than the tibia.

296.1 Femur, fourth trochanter, shape: prominent ridge (not pendant).

These characters change in a stepwise manner near the base of Ankylopollexia, indicating that quadrupedality evolved near the base of this

group. The accumulation of traits associated with quadrupedality across several nodes indicates that the evolution of quadrupedality occurred in a step-wise manner, such that the basal ankylopollexians *Uteodon* and *Camptosaurus* were likely facultative quadrupeds, while styracosternans were more likely obligate quadrupeds. Other characters distinguish ankylopollexians from dryosaurids and may indicate anatomical changes associated with quadrupedality. One is the muscle scar for *M. caudofemoralis longus*, which is a large oblong depression on the medial side of the fourth trochanter in ankylopollexians, but a small depression on the shaft of the femur in dryosaurids (Character 299). Another is the more complex arrangement of the ossified tendons (Character 323). The synchondrosis in the carpals and metacarpals may also be adaptive for quadrupedality, but this hypothesis is confounded by the co-occurring enlargement of the pollex unguis. Two of these correlates of quadrupedality also occur within rhabdodontoids. While not as clear as the shift at the base of Ankylopollexia, there may have been some degree of quadrupedality in this group.

Future Work

The relationships within Styracosterna remain difficult to resolve, and some of this may be due to poor taxonomy. A specimen-level phylogeny could determine which specimens form natural groupings and can be considered part of the same species. This may alleviate problems arising from incorrect *a priori* assumptions about relationships between specimens and help to resolve the phylogeny.

More fossils are needed to determine the origins of Iguanodontia (both within and outside of the clade). These will be found, most likely, in Middle to Late Jurassic and Early Cretaceous strata. North America has a high likelihood as the ancestral area for these groups, though the data are skewed due

to the high number of fossils already recovered there. Given the uncertainty of the topology at the base of Iguanodontia, and the geographic arrangement of the continents at the time, these basally branching taxa are likely to be geographically widespread.

The long ghost lineages in the basal portion of the tree in both parsimony and Bayesian analyses indicate that sampling for these generally smaller taxa has been poorer than that for ankylopollexians. Only in scrutinizing the fossil record for these more diminutive species will we be able to understand the evolution of Iguanodontia.

ACKNOWLEDGMENTS

I am grateful to C. Forster for many comments on early drafts of this work, and discussions of morphological characters. Helpful comments were also provided by J. Clark, M. Carrano, and D. Weishampel. Thanks also to A. Pyron for advice on Bayesian analysis, and to N. Matzke for answering questions related to BeastMaster and BioGeoBEARS. For enlightening conversations about ornithischian morphology, thanks to P. Barrett and A. Nabavizadeh. Thanks as well to three anonymous reviewers whose comments greatly improved this manuscript.

I am thankful to the many people who provided access to collections: R. Allain, D. Brinkman, K. Carpenter, M. Carrano, I. Cerda, S. Chapman, J.-P. Chenet, R. Coria, B. de Klerk, A. Folie, P. Halvik, S. Kaal, J. Kirkland, C. Levitt, C. Mehling, D. Pagnac, D. Pickering, J. Porfiri, T. Rich, J. Scanella, R. Scheetz, T. Schossleitner, D. Schwarz-Wings, J. Sertich, K. Spring, T. Tortosa, D. Weishampel, and Xu Xing.

Finally, my thanks to everyone for their patience with this paper, which I have kept in the works far too long.

REFERENCES

- Barrett, P.M. and Han, F.L. 2009. Cranial anatomy of *Jeholosaurus shangyuanensis* (Dinosauria: Ornithischia) from the Early Cretaceous of China. *Zootaxa*, 2072:31-55. <https://doi.org/10.11646/zootaxa.2072.1.2>
- Barrett, P.M., Butler, R.J., and Knoll, F. 2005. Small-bodied ornithischian dinosaurs from the Middle Jurassic of Sichuan, China. *Journal of Vertebrate Paleontology*, 25:823-834. [https://doi.org/10.1671/0272-4634\(2005\)025\[0823:sodftm\]2.0.co;2](https://doi.org/10.1671/0272-4634(2005)025[0823:sodftm]2.0.co;2)
- Barrett, P.M., Butler, R.J., Xiao-Lin, W., and Xing, X. 2009. Cranial anatomy of the iguanodontoid ornithopod *Jinzhouosaurus yangi* from the Lower Cretaceous Yixian Formation of China. *Acta Palaeontologica Polonica*, 54:35-48. <https://doi.org/10.4202/app.2009.0105>

- Barrett, P.M., Butler, R.J., Twitchett, R.J., and Hutt, S. 2011. New material of *Valdosaurus canaliculatus* (Ornithischia: Ornithopoda) from the Lower Cretaceous of southern England. *Studies on Fossil Tetrapods*, 86:131-163. <https://doi.org/10.24199/j.mmv.2016.74.04>
- Bartolini, A. and Larson, R.L. 2001. Pacific microplate and the Pangea supercontinent in the Early to Middle Jurassic. *Geology*, 29:735-738. [https://doi.org/10.1130/0091-7613\(2001\)029%3C0735:pmatps%3E2.0.co;2](https://doi.org/10.1130/0091-7613(2001)029%3C0735:pmatps%3E2.0.co;2)
- Baur, G. 1891. Remarks on the reptiles generally called Dinosauria. *The American Naturalist*, 25:434-454. <https://doi.org/10.1086/275329>
- Blakey, R.C. 2008. Gondwana paleogeography from assembly to breakup—A 500 my odyssey. *Geological Society of America Special Papers*, 441:1-28. [https://doi.org/10.1130/2008.2441\(01\)](https://doi.org/10.1130/2008.2441(01))
- Bouckaert, R., Heled, J., Kühnert, D., Vaughan, T., Wu, C-H., Xie, D., Suchard, MA., Rambaut, A., and Drummond, A.J. 2014. BEAST 2: A software platform for Bayesian evolutionary analysis. *PLoS Computational Biology*, 10:e1003537. <https://doi.org/10.1371/journal.pcbi.1003537>
- Boulenger G.A. 1881. Sur l'arc pelvien chez les dinosauriens de Bernissart. *Bulletin de l'Académie royal de Belgique*, 1:3-11.
- Boyd, C.A. 2012. Taxonomic revision of latest Cretaceous North American basal neornithischian taxa and a phylogenetic analysis of basal ornithischian relationships. Ph.D. dissertation, The University of Texas at Austin, Austin, Texas.
- Boyd, C.A. 2015. The systematic relationships and biogeographic history of ornithischian dinosaurs. *PeerJ* 3:e1523. <https://doi.org/10.7717/peerj.1523>
- Boyd, C.A., Brown, C.M., Scheetz, R.D., and Clarke, J.A. 2009. Taxonomic revision of the basal neornithischian taxa *Thescelosaurus* and *Bugenasaura*. *Journal of Vertebrate Paleontology*, 29:758-770. <https://doi.org/10.1671/039.029.0328>
- Brill, K. and Carpenter, K. 2007. A description of a new ornithopod from the Lytle Member of the Purgatoire Formation (Lower Cretaceous) and a reassessment of the skull of *Camptosaurus*, p. 49-67. In Carpenter, K. (ed.), *Horns and Beaks: Ceratopsian and Ornithopod Dinosaurs*. Indiana University Press, Bloomington. <https://doi.org/10.2307/j.ctt1zxz1md.8>
- Brown, B. 1908. The Ankylosauridae, a new family of armored dinosaurs from the Upper Cretaceous. *Bulletin of the AMNH*, 24(12):187-201.
- Buchholz, P.W. 2002. Phylogeny and biogeography of basal Ornithischia, p. 18-34. In Brown, D.E. (ed.), *The Mesozoic in Wyoming*. Tate Geological Museum, Casper.
- Butler, R.J. 2005. The 'fabrosaurid' ornithischian dinosaurs of the upper Elliot Formation (Lower Jurassic) of South Africa and Lesotho. *Zoological Journal of the Linnean Society*, 145:175-218. <https://doi.org/10.1111/j.1096-3642.2005.00182.x>
- Butler, R.J. and Galton, P.M. 2008. The 'dermal armour' of the ornithopod dinosaur *Hypsilophodon* from the Wealden (Early Cretaceous: Barremian) of the Isle of Wight: a reappraisal. *Cretaceous Research*, 29:636-642. <https://doi.org/10.1016/j.cretres.2008.02.002>
- Butler, R.J., Smith, R.M., and Norman, D.B. 2007. A primitive ornithischian dinosaur from the Late Triassic of South Africa, and the early evolution and diversification of Ornithischia. *Proceedings of the Royal Society of London B: Biological Sciences*, 274:2041-2046. <https://doi.org/10.1098/rspb.2007.0367>
- Butler, R.J., Upchurch, P., and Norman, D.B. 2008. The phylogeny of the ornithischian dinosaurs. *Journal of Systematic Palaeontology*, 6:1-40. <https://doi.org/10.1017/s1477201907002271>
- Calvo, J.O., Porfiri, J.D., and Novas, F.E. 2007. Discovery of a new ornithopod dinosaur from the Portezuelo formation (Upper Cretaceous), Neuquen, Patagonia, Argentina. *Archivos do Museu Nacional*, 65:471-483.
- Cambiaso, A.V. 2007. Los ornitópodos e iguanodontes basales (Dinosauria, Ornithischia) del Cretácico de Argentina y Antártida. Ph.D. dissertation, Universidad de Buenos Aires, Buenos Aires.
- Campione, N.E. and Evans, D.C. 2011. Cranial growth and variation in *Edmontosaurus* (Dinosauria: Hadrosauridae): implications for latest Cretaceous megaherbivore diversity in North America. *PLOS ONE*, 6:e25186. <https://doi.org/10.1371/journal.pone.0025186>
- Cantino, P.D. and de Queiroz, K. 2010. PhyloCode: a phylogenetic code of biological nomenclature, version 4c. <https://doi.org/10.1201/9780429446320>
- Carpenter, K. and Ishida, Y. 2010. Early and "Middle" Cretaceous iguanodonts in time and space. *Journal of Iberian Geology*, 36:145-164. https://doi.org/10.5209/rev_jige.2010.v36.n2.3

- Carpenter, K. and Wilson, Y. 2008. A new species of *Camptosaurus* (Ornithopoda: Dinosauria) from the Morrison Formation (Upper Jurassic) of Dinosaur National Monument, Utah, and a biomechanical analysis of its forelimb. *Annals of Carnegie Museum*, 76:227-263.
[https://doi.org/10.2992/0097-4463\(2008\)76\[227:ansoco\]2.0.co;2](https://doi.org/10.2992/0097-4463(2008)76[227:ansoco]2.0.co;2)
- Chanthasit, P. 2010. The ornithopod dinosaur *Rhabdodon* from the Late Cretaceous of France: anatomy, systematics and paleobiology. Ph.D. dissertation, Université Claude Bernard-Lyon I, Lyon.
- Cooper, M.R. 1985. A revision of the ornithischian dinosaur *Kangnasaurus coetzeei* Houghton, with a classification of the Ornithischia. *Annals of the South African Museum*, 95:281-317.
- Coria, R.A. and Calvo, J.O. 2002. A new iguanodontian ornithopod from Neuquen Basin, Patagonia, Argentina. *Journal of Vertebrate Paleontology*, 22:503-509.
[https://doi.org/10.1671/0272-4634\(2002\)022\[0503:aniofn\]2.0.co;2](https://doi.org/10.1671/0272-4634(2002)022[0503:aniofn]2.0.co;2)
- Coria, R.A. and Salgado, L. 1996. A basal iguanodontian (Ornithischia: Ornithopoda) from the Late Cretaceous of South America. *Journal of Vertebrate Paleontology*, 16:445-457.
<https://doi.org/10.1080/02724634.1996.10011333>
- Coria, R.A., Moly, J.J., Reguero, M., Santillana, S., Marensi, S. 2013. A new ornithopod (Dinosauria; Ornithischia) from Antarctica. *Cretaceous Research*, 41:186-193.
<https://doi.org/10.1016/j.cretres.2012.12.004>
- Crompton, A.W. and Charig, A.J. 1962. A new ornithischian from the Upper Triassic of South Africa. *Nature*, 196:1074-1077. <https://doi.org/10.1038/1961074a0>
- Dalla Vecchia, F.M. 2009. *Tethyshadros insularis*, a new hadrosauroid dinosaur (Ornithischia) from the Upper Cretaceous of Italy. *Journal of Vertebrate Paleontology*, 29:1100-1116.
<https://doi.org/10.1671/039.029.0428>
- DiCroce, T. and Carpenter, K. 2001. New ornithopod from the Cedar Mountain Formation (Lower Cretaceous) of eastern Utah. p. 183-196. In Tanke, D.H. and Carpenter, K. (eds.), *Mesozoic Vertebrate Life*. Indiana University Press, Bloomington.
- Dieudonné, P.E., Tortosa, T., Fernández-Baldor, F.T., Canudo, J.I., and Díaz-Martínez, I. 2016. An unexpected early rhabdodontid from Europe (Lower Cretaceous of Salas de los Infantes, Burgos Province, Spain) and a re-examination of basal iguanodontian relationships. *PLOS ONE*, 11:e0156251. <https://doi.org/10.1371/journal.pone.0156251>
- Dilkes, D.W. 2000. Appendicular myology of the hadrosaurian dinosaur *Maiasaura peeblesorum* from the Late Cretaceous (Campanian) of Montana. *Transactions of the Royal Society of Edinburgh: Earth Sciences*, 90:87-125. <https://doi.org/10.1017/s0263593300007185>
- Dollo L. 1888. Iguanodontidae et Camptonotidae. *Comptes Rendus hebdomadaires des séances de l'Académie des Sciences Paris*, CVI(106):775-777.
- Drummond A.J. and Bouckaert R.R. 2015. *Bayesian evolutionary analysis with BEAST*. Cambridge University Press, Cambridge. <https://doi.org/10.1017/cbo9781139095112>
- Drummond, A.J., Ho, S.Y.W., Phillips, M.J., and Rambaut, A. 2006. Relaxed phylogenetics and dating with confidence. *PLOS Biology*, 4:e88. <https://doi.org/10.1371/journal.pbio.0040088>
- Esmerode, E.V., Lykke-Andersen, H., and Surlyk, F. 2007. Ridge and valley systems in the Upper Cretaceous chalk of the Danish Basin: contourites in an epeiric sea. *Geological Society, London, Special Publications*, 276:265-282.
<https://doi.org/10.1144/gsl.sp.2007.276.01.13>
- Ezcurra, M.D. and Angolín, F.L. 2012. A new global palaeobiogeographical model for the late Mesozoic and early Tertiary. *Systematic Biology*, 61:553-566.
<https://doi.org/10.1093/sysbio/syr115>
- Farris, J.S. 1983. The logical basis of phylogenetic analysis, p. 1-47. In Platnick, N.I. and Funk, V.A. (eds.), *Advances in Cladistics, Volume 2, Proceedings of the Second Meeting of the Willi Hennig Society*. Columbia University Press, New York.
- Felsenstein, J. 1978. Cases in which parsimony or compatibility methods will be positively misleading. *Systematic Biology*, 27:401-410. <https://doi.org/10.1093/sysbio/27.4.401>
- Forster, C.A. 1990. The postcranial skeleton of the ornithopod dinosaur *Tenontosaurus tilletti*. *Journal of Vertebrate Paleontology*, 10:273-294.
<https://doi.org/10.1080/02724634.1990.10011815>
- Galton, P.M. 1974. The ornithischian dinosaur *Hypsilophodon* from the Wealden of the Isle of Wight. *Bulletin of the British Museum (Natural History)*, 25(1):1-152.
<https://doi.org/10.5962/p.313819>

- Galton, P.M. 1981. *Dryosaurus*, a hypsilophodontid dinosaur from the Upper Jurassic of North America and Africa postcranial skeleton. *Paläontologische Zeitschrift*, 55:271-312. <https://doi.org/10.1007/bf02988144>
- Galton, P.M. 1983. The cranial anatomy of *Dryosaurus*, a hypsilophodontid dinosaur from the Upper Jurassic of North America and East Africa, with a review of hypsilophodontids from the Upper Jurassic of North America. *Geologica et Palaeontologica*, 17:207-243. <https://doi.org/10.1007/bf02988144>
- Galton, P.M. 2009. Notes on Neocomian (Lower Cretaceous) ornithopod dinosaurs from England—*Hypsilophodon*, *Valdosaurus*, “*Camptosaurus*”, “*Iguanodon*”—and referred specimens from Romania and elsewhere. *Revue de Paléobiologie*, 28:211-273.
- Galton, P.M. and Taquet, P. 1982. *Valdosaurus*, a hypsilophodontid dinosaur from the Lower Cretaceous of Europe and Africa. *Geobios*, 15:147-159.
- Gasca, J., Moreno-Azanza, M., Ruiz-Omeñaca, J., and Canudo, J. 2015. New material and phylogenetic position of the basal iguanodont dinosaur *Delapparentia turoleensis* from the Barremian (Early Cretaceous) of Spain. *Journal of Iberian Geology*, 41:57-70. https://doi.org/10.5209/rev_jige.2015.v41.n1.48655
- Gates, T.A. and Scheetz, R. 2014. A new saurolophine hadrosaurid (Dinosauria: Ornithopoda) from the Campanian of Utah, North America. *Journal of Systematic Palaeontology*, 13:711-725. <https://doi.org/10.1080/14772019.2014.950614>
- Gervais, P. 1853. Observations relatives aux reptiles fossils de France. *Comptes-rendus de l'Academie des Sciences de Paris*, 36:374-377.
- Gilmore, C.W. 1909. Osteology of the Jurassic reptile *Camptosaurus*: with a revision of the species of the genus, and description of two new species. *Proceedings of the United States National Museum*, 36:197-332. <https://doi.org/10.5479/si.00963801.36-1666.197>
- Gilmore, C.W. 1913. A new dinosaur from the Lance Formation of Wyoming. *Smithsonian Miscellaneous Collections*, 61(5):1-5.
- Gilmore, C.W. 1931. A new species of troödont dinosaur from the Lance Formation of Wyoming. *Proceedings of the United States National Museum*, 79(2875):1-6.
- Gilpin, D., DiCroce T., and Carpenter, K. 2007. A possible new basal hadrosaur from the Lower Cretaceous Cedar Mountain Formation of eastern Utah, p. 79-89. In Carpenter K. (ed.), *Horns and Beaks: Ceratopsian and Ornithopod Dinosaurs*. Indiana University Press, Bloomington. <https://doi.org/10.2307/j.ctt1zxz1md.10>
- Godefroit, P., Dong, Z.M., Bultynck, P., Li, H., and Feng, L. 1998. New *Bactrosaurus* (Dinosauria: Hadrosauroida) material from Iren Dabasu (Inner Mongolia, PR China). *Bulletin de l'Institut Royal des Sciences Naturelles de Belgique, Sciences de la Terra*, 68 (Supplement):3-70.
- Godefroit, P., Li, H., and Shang, C.Y. 2005. A new primitive hadrosauroid dinosaur from the Early Cretaceous of Inner Mongolia (PR China). *Comptes Rendus Palevol*, 4:697-705.
- Godefroit, P., Escuillié, F., Bolotsky, Y.L., and Lauters, P. 2012. A new basal hadrosauroid dinosaur from the Upper Cretaceous of Kazakhstan, p. 335-358. In Godefroit, P. (ed.), *Bernissart Dinosaurs and Early Cretaceous Terrestrial Ecosystems*. Indiana University Press, Bloomington.
- Goloboff, P.A., Farris, J.S., and Nixon, K.C. 2008. TNT, a free program for phylogenetic analysis. *Cladistics*, 24:774-786. <https://doi.org/10.1111/j.1096-0031.2008.00217.x>
- Gorscak, E. and O'Connor, P.M. 2016. Time-calibrated models support congruency between Cretaceous continental rifting and titanosaurian evolutionary history. *Biology Letters*, 12:20151047. <https://doi.org/10.1098/rsbl.2015.1047>
- Gradstein, F.M., Ogg, J., Schmitz, M.A., and Ogg, G. 2012. *A geologic time scale*. Elsevier Publishing Company, Amsterdam.
- Han, F.L., Barrett, P.M., Butler, R.J., and Xu, X. 2012. Postcranial anatomy of *Jeholosaurus shangyuanensis* (Dinosauria, Ornithischia) from the Lower Cretaceous Yixian Formation of China. *Journal of Vertebrate Paleontology*, 32:1370-1395. <https://doi.org/10.1080/02724634.2012.694385>
- Head, J.J. 1998. A new species of basal hadrosaurid (Dinosauria, Ornithischia) from the Cenomanian of Texas. *Journal of Vertebrate Paleontology*, 18:718-738. <https://doi.org/10.1080/02724634.1998.10011101>
- Hooley RW. 1925. On the skeleton of *Iguanodon atherfieldensis* sp. nov., from the Wealden shales of Atherfield (Isle of Wight). *Quarterly Journal of the Geological Society of London*, 81:1-61.

- Horner, J.R. 1983. Cranial osteology and morphology of the type specimen of *Maiasaura peeblesorum* (Ornithischia: Hadrosauridae), with a discussion of its phylogenetic position. *Journal of Vertebrate Paleontology*, 3:29-38.
<https://doi.org/10.1080/02724634.1983.10011954>
- Horner, J.R. and Currie, P.J. 1994. Embryonic and neonatal morphology and ontogeny of a new species of *Hypacrosaurus* (Ornithischia, Lambeosauridae) from Montana and Alberta, p. 312–336. In Carpenter, K., Hirsch, K.F., and Horner, J.R. (eds.), *Dinosaur Eggs and Babies*. Cambridge University Press, Cambridge.
- Horner, J.R., Weishampel, D.B., and Forster, C.A. 2004. Hadrosauridae, p. 438-463. In Weishampel, D.B., Dodson, P., and Osmólska, H. (eds.), *The Dinosauria: Second Edition*. University of California Press, Berkeley.
- Hübner, T.R. and Rauhut, O.W.M. 2010. A juvenile skull of *Dysalotosaurus lettowvorbecki* (Ornithischia: Iguanodontia), and implications for cranial ontogeny, phylogeny, and taxonomy in ornithomimid dinosaurs. *Zoological Journal of the Linnean Society*, 160:366-396.
<https://doi.org/10.1111/j.1096-3642.2010.00620.x>
- Huxley, T.H. 1869. On *Hypsilophodon*, a new genus of Dinosauria. *Abstracts of the Proceedings of the Geological Society (of London)*, 204:3-4.
- Huxley, T.H. 1870. On the classification of the Dinosauria, with observations on the Dinosauria of the Trias. *Quarterly Journal of the Geological Society*, 26:32-51.
<https://doi.org/10.1144/gsl.jgs.1870.026.01-02.09>
- Jacobs, L.L., Winkler, D.A., and P.A. Murry, P.A. 1991. On the age and correlation of Trinity mammals, Early Cretaceous of Texas, USA. *Newsletters on Stratigraphy*, 24:35-43.
<https://doi.org/10.1127/nos/24/1991/35>
- Janensch, W. 1955. Der Ornithopode *Dysalotosaurus* der Tendaguruschichten. *Palaeontographica-Supplementbände*, 7:105-176.
- Kearney, M. and Clark, J.M. 2003. Problems due to missing data in phylogenetic analyses including fossils: a critical review. *Journal of Vertebrate Paleontology*, 23:263-274.
[https://doi.org/10.1671/0272-4634\(2003\)023\[0263:pdtmdj\]2.0.co;2](https://doi.org/10.1671/0272-4634(2003)023[0263:pdtmdj]2.0.co;2)
- Kennedy, W.J. and Cobban, W.A. 1990. Cenomanian ammonite faunas from the Woodbine Formation and lower part of the Eagle-Ford Group, Texas. *Paleontology*, 33:75-154.
- Kirkland, J.I. 1998. A new hadrosaurid from the upper Cedar Mountain Formation (Albian-Cenomanian: Cretaceous) of eastern Utah – the oldest known hadrosaurid (lambeosaurine?). In: Lucas SG, Kirkland JI, Estep JW, (eds). *Lower and Middle Cretaceous Terrestrial Ecosystems*. New Mexico Museum of Natural History and Science Bulletin 14:283-295.
- Kobayashi, Y. and Azuma, Y. 2003. A new iguanodontian (Dinosauria: Ornithomimidae) from the Lower Cretaceous Kitadani Formation of Fukui Prefecture, Japan. *Journal of Vertebrate Paleontology*, 23:166-175. [https://doi.org/10.1671/0272-4634\(2003\)23\[166:anidof\]2.0.co;2](https://doi.org/10.1671/0272-4634(2003)23[166:anidof]2.0.co;2)
- Lambe, L.M. 1920. The hadrosaur *Edmontosaurus* from the Upper Cretaceous of Alberta. *Geological Survey of Canada, Memoir* 120:1-79. <https://doi.org/10.4095/101655>
- Lee, M.S. and Worthy, T.H. 2012. Likelihood reinstates *Archaeopteryx* as a primitive bird. *Biology Letters*, 8:299-303. <https://doi.org/10.1098/rsbl.2011.0884>
- Leidy, J. 1858. *Hadrosaurus foulkii*, a new saurian from the Cretaceous of New Jersey, related to Iguanodon. *Proceedings of the Academy of Natural Sciences of Philadelphia*, 10:213-218.
- Lepage, T., Bryant, D., Philippe, H., and Lartillot, N. 2007. A general comparison of relaxed molecular clock models. *Molecular Biology and Evolution*, 24:2669-2680.
<https://doi.org/10.1093/molbev/msm193>
- Lewis, P.O. 2001. A likelihood approach to estimating phylogeny from discrete morphological character data. *Systematic Biology*, 50:913-925.
<https://doi.org/10.1080/106351501753462876>
- Lull, R.S. 1908. The cranial musculature and the origin of the frill in the ceratopsian dinosaurs. *American Journal of Science*, 25:387-399. <https://doi.org/10.2475/ajs.s4-25.149.387>
- Lull, R.S. 1911. Cretaceous Dinosaurs. Ten years' progress in vertebrate paleontology. *Bulletin of the Geological Society of America*, 28:208-212.
- Lydekker R. 1889. Notes on new and other dinosaur remains. *Geological Magazine*, VI:352-356.
- Maddison, W.P. and Maddison, D.R. 2009. Mesquite: a modular system for evolutionary analysis. Version 2.72. <http://mesquiteproject.org>.

- Maidment, S.C. and Barrett, P.M. 2012. Osteological correlates for quadrupedality in ornithischian dinosaurs. *Acta Palaeontologica Polonica*, 59:53-70.
<https://doi.org/10.4202/app.2012.0065>
- Main, D.J. 2013. Appalachian delta plain paleoecology of the Cretaceous Woodbine Formation at the Arlington Archosaur Site north Texas. Ph.D. dissertation, The University of Texas at Austin, Austin, Texas.
- Makovicky, P.J., Kilbourne, B.M., Sadleir, R.W., and Norell, M.A. 2011. A new basal ornithopod (Dinosauria, Ornithischia) from the Late Cretaceous of Mongolia. *Journal of Vertebrate Paleontology*, 31:626-640. <https://doi.org/10.1080/02724634.2011.557114>
- Mantell, G.A. 1825. Notice on the Iguanodon, a newly discovered fossil reptile, from the sandstone of Tilgate forest, in Sussex. *Philosophical Transactions of the Royal Society*, 115:179–186. <https://doi.org/10.1098/rstl.1825.0010>
- Marsh, O.C. 1877. A new order of extinct Reptilia (Stegosauria) from the Jurassic of the Rocky Mountains. *American Journal of Science*, 3(84):513-514.
- Marsh, O.C. 1878. Principal characters of American Jurassic dinosaurs. *American Journal of Science*, s3-16(95):411-416.
- Marsh, O.C. 1879. Notice of new Jurassic reptiles. *American Journal of Science*, 3(108):501-505.
- Marsh, O.C. 1889. Notice of gigantic horned Dinosauria from the Cretaceous. *American Journal of Science*, 3(224):173-176.
- Marsh, O.C. 1896. The Dinosaurs of North America. USGS Survey, 16:133-415.
<https://doi.org/10.5962/bhl.title.60562>
- Maryńska, T. and Osmólska, H. 1974. Pachycephalosauria, a new suborder of ornithischian dinosaurs. *Palaeontologia Polonica*, 30:45-102.
- Matheron P. 1869. Notes sur les reptiles fossiles des dépôts fluvio-lacustres crétacés du bassin à lignite de Fuveau. *Bulletin de la Société Géologiques de France (ser. 2)*, 26:781-795.
- Matzke, N.J. 2012. Founder-event speciation in BioGeoBEARS package dramatically improves likelihoods and alters parameter inference in Dispersal-Extinction-Cladogenesis (DEC) analyses. *Frontiers of Biogeography*, 4(suppl. 1):210.
- Matzke, N.J. 2013a. BioGeoBEARS: BioGeography with Bayesian (and Likelihood) Evolutionary Analysis in R Scripts. <http://CRAN.Rproject.org/package=BioGeoBEARS>.
- Matzke, N.J. 2013b. Probabilistic historical biogeography: new models for founder-event speciation, imperfect detection, and fossils allow improved accuracy and model-testing. *Frontiers of Biogeography*, 5:242-248. <https://doi.org/10.21425/f55419694>
- Matzke, N.J. 2014. BEASTmaster: Automated conversion of NEXUS data to BEAST2 XML format, for fossil tip-dating and other uses. Online at PhyloWiki.
<http://phylo.wikidot.com/beastmaster>.
- McDonald, A.T. 2011. The taxonomy of species assigned to *Camptosaurus* (Dinosauria: Ornithopoda). *Zootaxa*, 2783:52-68. <https://doi.org/10.11646/zootaxa.2783.1.4>
- McDonald, A.T. 2012a. Phylogeny of basal iguanodonts (Dinosauria: Ornithischia): An update. *PLoS ONE* 7(5):e36745. <https://doi.org/10.1371/journal.pone.0036745>
- McDonald, A.T. 2012b. The status of *Dollodon* and other basal iguanodonts (Dinosauria: Ornithischia) from the Lower Cretaceous of Europe. *Cretaceous Research*, 33:1-6.
<https://doi.org/10.1016/j.cretres.2011.03.002>
- McDonald, A.T., Barrett, P.M., and Chapman, S.D. 2010a. A new basal iguanodont (Dinosauria: Ornithischia) from the Wealden (Lower Cretaceous) of England. *Zootaxa*, 2569:1-43.
<https://doi.org/10.11646/zootaxa.2569.1.1>
- McDonald, A.T., Kirkland, J.I., DeBlieux, D.D., Madsen, S.K., and Cavin, J. 2010b. New basal iguanodonts from the Cedar Mountain Formation of Utah and the evolution of thumb-spiked dinosaurs. *PLoS ONE*, 5:e14075. <https://doi.org/10.1371/journal.pone.0014075>
- McDonald, A.T., Wolfe, D.G., and Kirkland, J.I. 2010c. A new basal hadrosauroid (Dinosauria: Ornithopoda) from the Turonian of New Mexico. *Journal of Vertebrate Paleontology*, 30:799-812. <https://doi.org/10.1080/02724631003763516>
- McDonald, A.T., Espilez, E., Mampel, L., Kirkland, J.I., and Alcalá, L. 2012. An unusual new basal iguanodont (Dinosauria: Ornithopoda) from the Lower Cretaceous of Teruel, Spain. *Zootaxa*, 3595:61-76. <https://doi.org/10.11646/zootaxa.3595.1.3>
- Miall, A.D., Catuneanu, O., Vakarelov, B.K., and Post, R. 2008. The western interior basin. *Sedimentary Basins of the World*, 5:329-362.
[https://doi.org/10.1016/s1874-5997\(08\)00009-9](https://doi.org/10.1016/s1874-5997(08)00009-9)

- Milner, A.R. and Norman, D.B. 1984. The biogeography of advanced ornithopod dinosaurs (Archosauria: Ornithischia)—a cladistic-vicariance model, p. 145-150. In: Reif, W.-E. and Westphal, F. (eds.), Third Symposium on Mesozoic Terrestrial Ecosystems. Attempto Verlag, Tübingen.
- Molnar, R.E. 1996. Observations on the Australian ornithopod dinosaur, *Muttaborrasaurus*. *Memoirs-Queensland Museum*, 39:639-652.
- Nopcsa, F. 1902. Dinosaurierreste aus Siebenbürgen II. (Schädelreste von *Mochlodon*). Mit einem Anhang: zur Phylogenie der Ornithopodiden. *Denkschriften der königlichen Akademie der Wissenschaften, Mathematisch-Naturwissenschaftlichen Klasse*, 72:149-175.
- Norman, D.B. 1980. On the ornithischian dinosaur *Iguanodon bernissartensis* from the Lower Cretaceous of Bernissart (Belgium). *Institut Royal des Sciences Naturelles de Belgique Memoire*, 178:1-103.
- Norman, D.B. 1984. A systematic reappraisal of the reptile order Ornithischia, p. 157-162. In: Reif, W.-E. and Westphal, F. (eds.), Third Symposium on Mesozoic Terrestrial Ecosystems. Attempto Verlag, Tübingen.
- Norman, D.B. 1986. On the anatomy of *Iguanodon atherfieldensis* (Ornithischia: Ornithopoda). *Bulletin-Institut Royal des Sciences Naturelles de Belgique. Sciences de la Terre*, 56:281-372.
- Norman, D.B. 2002. On Asian ornithopods (Dinosauria: Ornithischia). 4. *Probactrosaurus* Rozhdestvensky, 1966. *Zoological Journal of the Linnean Society*, 136:113-144. <https://doi.org/10.1046/j.1096-3642.2002.00027.x>
- Norman, D.B. 2004. Basal Iguanodontia, p. 413-437. In Weishampel, D.B., Dodson, P., and Osmólska, H. (eds.), *The Dinosauria* (2nd ed.). University of California Press, Berkeley. <https://doi.org/10.1525/california/9780520242098.003.0022>
- Norman, D.B. 2010. A taxonomy of iguanodontians (Dinosauria: Ornithopoda) from the lower Wealden Group (Cretaceous: Valanginian) of southern England. *Zootaxa*, 2489:47-66. <https://doi.org/10.11646/zootaxa.2489.1.3>
- Norman, D.B. 2013. On the taxonomy and diversity of Wealden iguanodontian dinosaurs (Ornithischia: Ornithopoda). *Revue de Paléobiologie*, 32:385-404.
- Norman, D.B. 2015. On the history, osteology, and systematic position of the Wealden (Hastings group) dinosaur *Hypselospinus fittoni* (Iguanodontia: Styrcosterna). *Zoological Journal of the Linnean Society*, 173:92-189. <https://doi.org/10.1111/zoj.12193>
- Norman, D.B., Sues, H.D., Witmer, L.M., and Coria, R.A. 2004. Basal Ornithopoda, p. 393-412. In Weishampel, D.B., Dodson, P., and Osmólska, H. (eds.), *The Dinosauria* (2nd ed.). University of California Press, Berkeley. <https://doi.org/10.1525/california/9780520242098.003.0021>
- Novas, F.E., Cambiaso A.V., and Ambrosio A. 2004. A new basal iguanodontian (Dinosauria, Ornithischia) from the Upper Cretaceous of Patagonia. *Ameghiniana*, 41:75-82.
- O'Reilly, J., Donoghue, P., Dos Reis, M., and Yang, Z. 2014. Evaluating the performance of node versus tip based fossil calibration of the molecular clock. *Journal of Vertebrate Paleontology*, 34(supplement):199.
- Osborn, H.F. 1906. *Tyrannosaurus*, Upper Cretaceous carnivorous dinosaur: (second communication). *Bulletin of the American Museum of Natural History*, 22:281-296.
- Osborn, H.F. 1912. Integument of the iguanodont dinosaur *Trachodon*. *Memoirs of the American Museum of Natural History, New Series*, 1:33-54.
- Parks, W.A. 1922. *Parasaurolophus walkeri*: a new genus and species of crested trachodont dinosaur. *University of Toronto Studies, Geological Series*, 13:1-32.
- Parks, W.A. 1926. *Thescelosaurus warreni*, a new species of orthopodous dinosaur from the Edmonton Formation of Alberta. *University of Toronto Studies, Geological Series*, 21:1-42.
- Paul, G.S. 2007. Turning the old into the new: a separate genus for the gracile iguanodont from the Wealden of England, p. 69-77. In Carpenter, K. (ed.), *Horns and Beaks: Ceratopsian and Ornithopod Dinosaurs*. Indiana University Press, Bloomington. <https://doi.org/10.2307/j.ctt1zxz1md.9>
- Paul, G.S. 2008. A revised taxonomy of the iguanodont dinosaur genera and species. *Cretaceous Research*, 29(2):192-216. <https://doi.org/10.1016/j.cretres.2007.04.009>
- Paul, G. 2012. Notes on the rising diversity of iguanodont taxa, and iguanodonts named after Darwin, Huxley, and evolutionary science. *Actas V Jornadas Internacionales sobre Paleontología de Dinosaurios y su Entorno, Salas de los Infantes, Burgos*, 121-131.

- Perle, A., Maryńska, T., and Osmólska, H. 1982. *Goyocephale lattimorei* gen. et sp. n., a new flat-headed pachycephalosaur (Ornithischia, Dinosauria) from the Upper Cretaceous of Mongolia. *Acta Palaeontologica Polonica*, 27(1-4):115-127.
- Prieto-Márquez, A. 2012. The skull and appendicular skeleton of *Gryposaurus latidens*, a saurolophine hadrosaurid (Dinosauria: Ornithopoda) from the early Campanian (Cretaceous) of Montana, USA. *Canadian Journal of Earth Sciences*, 49:510-532.
<https://doi.org/10.1139/e11-069>
- Prieto-Márquez, A. and Norell, M.A. 2010. Anatomy and relationships of *Gilmoreosaurus mongoliensis* (Dinosauria: Hadrosauridae) from the Late Cretaceous of Central Asia. *American Museum Novitates*, 3694:1-49. <https://doi.org/10.1206/3694.2>
- Prieto-Márquez, A. and Salinas, G.C. 2010. A re-evaluation of *Secernosaurus koerneri* and *Kritosaurus australis* (Dinosauria, Hadrosauridae) from the Late Cretaceous of Argentina. *Journal of Vertebrate Paleontology*, 30:813-837.
<https://doi.org/10.1080/02724631003763508>
- Pyron, R.A. 2011. Divergence time estimation using fossils as terminal taxa and the origins of Lissamphibia. *Systematic Biology*, 60:1-16. <https://doi.org/10.1093/sysbio/syr047>
- Rannala, B. and Yang, Z. 2007. Inferring speciation times under an episodic molecular clock. *Systematic Biology*, 56:453-466. <https://doi.org/10.1080/10635150701420643>
- Ree, R.H. and Smith, S.A. 2008. Maximum likelihood inference of geographic range evolution by dispersal, local extinction, and cladogenesis. *Systematic Biology*, 57:4-14.
<https://doi.org/10.1080/10635150701883881>
- Rich, T.H. and Rich, P.V. 1988. A juvenile dinosaur brain from Australia. *National Geographic Research*, 4:148.
- Rich, T.H. and Rich, P.V. 1989. Polar dinosaurs and biotas of the Early Cretaceous of southeastern Australia. *National Geographic Research*, 5:15-53.
- Romer, A.S. 1956. *Osteology of the Reptiles*. University of Chicago Press, Chicago, Illinois.
- Ronquist, F., Klopfstein, S., Vilhelmsen, L., Schulmeister, S., Murray, D.L., and Rasnitsyn, A.P. 2012. A total-evidence approach to dating with fossils, applied to the early radiation of the Hymenoptera. *Systematic Biology*, 61:973-999. <https://doi.org/10.1093/sysbio/sys058>
- Ruiz-Omeñaca, J.I. 2011. *Delapparentia turolensis* nov. gen et sp., un nuevo dinosaurio iguanodontoideo (Ornithischia: Ornithopoda) en el Cretácico Inferior de Galve. *Estudios geológicos*, 67(1):83-110.
- Scheetz, R.D. 1999. *Osteology of Orodromeus makelai* and the phylogeny of basal ornithopod dinosaurs. Ph.D. dissertation, Montana State University, Bozeman.
- Scotese, C.R. 2014. *Atlas of Earth History, Volume 1, Paleogeography*. PALEOMAP Project, Arlington, Texas.
- Seeley, H.G. 1887. Classification of the Dinosauria. *Geological Magazine (Decade III)*, 5:45-46.
<https://doi.org/10.1017/s0016756800156006>
- Sereno, P.C. 1984. The phylogeny of the Ornithischia: a reappraisal, p. 219-226. In: Reif, W.-E. and Westphal, F. (eds.), *Third Symposium on Mesozoic Terrestrial Ecosystems*. Attempto Verlag, Tübingen.
- Sereno, P.C. 1986. Phylogeny of the bird-hipped dinosaurs (Order Ornithischia). *National Geographic Research*, 2:234-256.
- Sereno, P.C. 1991. *Lesothosaurus*, "fabrosaurids," and the early evolution of Ornithischia. *Journal of Vertebrate Paleontology*, 11:168-197.
<https://doi.org/10.1080/02724634.1991.10011386>
- Sereno, P.C. 1998. A rationale for phylogenetic definitions, with application to the higher level taxonomy of Dinosauria. *Neues Jahrbuch für Geologie und Paläontologie Abhandlungen*, 210:41-83. <https://doi.org/10.1127/njgpa/210/1998/41>
- Sereno, P.C. 1999. The evolution of dinosaurs. *Science*, 284:2137-2147. <https://doi.org/10.1126/science.284.5423.2137>
- Sereno, P. C. 2005. Stem Archosauria—TaxonSearch. <http://www.taxonsearch.org/Archive/stem-archosauria-1.0.php>
- Sereno, P.C. 2007. Logical basis for morphological characters in phylogenetics. *Cladistics*, 23:1-23. <https://doi.org/10.1111/j.1096-0031.2007.00161.x>
- Shibata, M., Jintasakul, P., and Azuma, Y. 2011. A new iguanodontian dinosaur from the Lower Cretaceous Khok Kruat Formation, Nakhon Ratchasima in northeastern Thailand. *Acta Geologica Sinica?English Edition*, 85:969-976.

- Simmons, M.P. 2012. Misleading results of likelihood-based phylogenetic analyses in the presence of missing data. *Cladistics*, 28:208-222. <https://doi.org/10.1111/j.1096-0031.2011.00375.x>
- Simmons, M.P. 2014. A confounding effect of missing data on character conflict in maximum likelihood and Bayesian MCMC phylogenetic analyses. *Molecular Phylogenetics and Evolution*, 80:267-280. <https://doi.org/10.1016/j.ympev.2014.08.021>
- Spencer, M.R. 2013. Phylogenetic and Biogeographic Assessment of Ornithischian Diversity Throughout the Mesozoic: A Species-Level Analysis from Origin to Extinction. Ph.D. dissertation, University of Iowa, Iowa City.
- Stadler, T., Kühnert, D., Bonhoeffer, S., and Drummond, A.J. 2013. Birth–death skyline plot reveals temporal changes of epidemic spread in HIV and Hepatitis C virus (HCV). *Proceedings of the National Academy of Sciences*, 110:228-233. <https://doi.org/10.1073/pnas.1207965110>
- Sternberg, C.M. 1937. A classification of *Thescelosaurus*, with a description of a new species. *Proceedings of the Geological Society of America*, 1936:375.
- Strong, E.E. and Lipscomb, D. 1999. Character coding and inapplicable data. *Cladistics*, 15:363-371. <https://doi.org/10.1111/j.1096-0031.1999.tb00272.x>
- Sues, H.D. 1980. Anatomy and relationships of a new hypsilophodontid dinosaur from the Lower Cretaceous of North America. *Palaeontographica, Abteilung A: Paläozoologie - Stratigraphie*, 169:51-72.
- Sues, H.D. and Averianov, A. 2009. A new basal hadrosauroid dinosaur from the Late Cretaceous of Uzbekistan and the early radiation of duck-billed dinosaurs. *Proceedings of the Royal Society B: Biological Sciences*, 276:2549-2555. <https://doi.org/10.1098/rspb.2009.0229>
- Swofford, D.L., Waddell, P.J., Huelsenbeck, J.P., Foster, P.G., Lewis, P.O., and Rogers, J.S. 2001. Bias in phylogenetic estimation and its relevance to the choice between parsimony and likelihood methods. *Systematic Biology*, 50:525-539. <https://doi.org/10.1080/106351501750435086>
- Taquet, P. and Russell, D.A. 1999. A massively constructed iguanodont from Gadoufaoua, Lower Cretaceous of Niger. *Annales de Paléontologie*, 85:85-96. [https://doi.org/10.1016/s0753-3969\(99\)80009-3](https://doi.org/10.1016/s0753-3969(99)80009-3)
- Upchurch, P., Huxford, C.A., and Norman, D. B. 2002. An analysis of dinosaurian biogeography: evidence for the existence of vicariance and dispersal patterns caused by geological events. *Proceedings of the Royal Society B*, 269:613-621. <https://doi.org/10.1098/rspb.2001.1921>
- Varricchio, D.J., Martin, A.J., and Katsura, Y. 2007. First trace and body fossil evidence of a burrowing, denning dinosaur. *Proceedings of the Royal Society of London B: Biological Sciences*, 274:1361-1368. <https://doi.org/10.1098/rspb.2006.0443>
- Veevers, J.J. 2004. Gondwanaland from 650–500 Ma assembly through 320 Ma merger in Pangea to 185-100 Ma breakup: Supercontinental tectonics via stratigraphy and radiometric dating. *Earth-Science Reviews*, 68(1):1-132. <https://doi.org/10.1016/j.earscirev.2004.05.002>
- Wagner, J.R. 2004. The phylogenetic nomenclature of ornithischian dinosaurs (Vertebrata: Reptilia) and a consideration of the difficulties in converting the names of extinct clades, p. 28. First International Phylogenetic Nomenclature Meeting, Paris.
- Wang, X. and Xu, X. 2001. A new iguanodontid (*Jinzhousaurus yangi* gen. et sp. nov.) from the Yixian Formation of western Liaoning, China. *Chinese Science Bulletin*, 46:1669-1672. <https://doi.org/10.1007/bf02900633>
- Wang, X., Pan, R., Butler, R.J., and Barrett, P.M. 2010. The postcranial skeleton of the iguanodontian ornithopod *Jinzhousaurus yangi* from the Lower Cretaceous Yixian Formation of western Liaoning, China. *Earth and Environmental Science Transactions of the Royal Society of Edinburgh*, 101:135-159. <https://doi.org/10.1017/s1755691010009266>
- Weishampel, D.B. and Heinrich, R.E. 1992. Systematics of Hypsilophodontidae and basal Iguanodontia (Dinosauria: Ornithopoda). *Historical Biology*, 6:159-184. <https://doi.org/10.1080/10292389209380426>
- Weishampel, D.B. and Horner, J.R. 1986. The hadrosaurid dinosaurs from the Iren Dabasu Fauna (People's Republic of China, Late Cretaceous). *Journal of Vertebrate Paleontology*, 6:38-45. <https://doi.org/10.1080/02724634.1986.10011597>
- Weishampel, D.B., Norman, D.B., and Grigorescu, D. 1993. *Telmatosaurus transsylvanicus* from the Late Cretaceous of Romania: the most basal hadrosaurid dinosaur. *Palaeontology*, 36:361-385.

- Weishampel, D.B., Jianu, C.-M., Csiki, Z., and Norman, D.B. 2003. Osteology and phylogeny of *Zalmoxes* (n.g.), an unusual euornithopod dinosaur from the Latest Cretaceous of Romania. *Journal of Systematic Palaeontology*, 1(2):65-123.
<https://doi.org/10.1017/s1477201903001032>
- Wiens, J.J. and Moen, D.S. 2008. Missing data and the accuracy of Bayesian phylogenetics. *Journal of Systematics and Evolution*, 46:307-314.
- Wiens, J.J. and Morrill, M.C. 2011. Missing data in phylogenetic analysis: reconciling results from simulations and empirical data. *Systematic Biology*, 60:719-731.
<https://doi.org/10.1093/sysbio/syr025>
- Wilkinson, M. 2003. Missing entries and multiple trees: instability, relationships, and support in parsimony analysis. *Journal of Vertebrate Paleontology*, 23:311-323.
[https://doi.org/10.1671/0272-4634\(2003\)023\[0311:meamtj\]2.0.co;2](https://doi.org/10.1671/0272-4634(2003)023[0311:meamtj]2.0.co;2)
- Williston, S.W. 1905. The *Hallopus*, *Baptanodon*, and *Atlantosaurus* Beds of Marsh. *The Journal of Geology*, 13:338-350. <https://doi.org/10.1086/621233>
- Winkler, D.A., Murry, P.A., and Jacobs, L.L. 1997. A new species of *Tenontosaurus* (Dinosauria: Ornithopoda) from the Early Cretaceous of Texas. *Journal of Vertebrate Paleontology*, 17:330-348. <https://doi.org/10.1080/02724634.1997.10010978>
- Wright, A.M. and Hillis, D.M. 2014. Bayesian analysis using a simple likelihood model outperforms parsimony for estimation of phylogeny from discrete morphological data. *PLoS ONE* 9: e109210. <https://doi.org/10.1371/journal.pone.0109210>
- Wu, W.H. and Godefroit, P. 2012. Anatomy and relationships of *Bolong yixianensis*, an Early Cretaceous iguanodontid dinosaur from western Liaoning, China, p. 293-333 In Godefroit, P. (ed.), *Bernissart dinosaurs and Early Cretaceous terrestrial ecosystems*. Indiana University Press, Bloomington.
- Wu, W.H., Godefroit, P., and Hu, D.Y. 2010. *Bolong yixianensis* gen. et sp. nov.: a new iguanodontoid dinosaur from the Yixian Formation of western Liaoning, China. *Geology and Resources*, 19:127-133.
- Xu, X. and Pol, D. 2014. *Archaeopteryx*, paravian phylogenetic analyses, and the use of probability-based methods for palaeontological datasets. *Journal of Systematic Palaeontology*, 12:323-334. <https://doi.org/10.1080/14772019.2013.764357>
- You, H., Ji, Q., Li, J., and Li, Y. 2003. A new hadrosauroid dinosaur from the mid-Cretaceous of Liaoning, China. *Acta Geologica Sinica (English Edition)*, 77:148-154.
<https://doi.org/10.1111/j.1755-6724.2003.tb00557.x>
- You, H., Ji, Q., and Li, D. 2005. *Lanzhousaurus magnidens* gen. et sp. nov. from Gansu Province, China: the largest-toothed herbivorous dinosaur in the world. *Geological Bulletin of China*, 24:785-794.
- You, H., Li, D., and Liu, W. 2011. A new hadrosauriform dinosaur from the Early Cretaceous of Gansu Province, China. *Acta Geologica Sinica (English Edition)*, 85(1):51-57.
<https://doi.org/10.1111/j.1755-6724.2011.00377.x>

APPENDICES

APPENDIX 1.

List of characters and character state used in the phylogenetic analyses. Format follows Sereno (2007). Characters with no citation following are new in this analysis. * Indicates an ontogenetically sensitive character, o indicates an ordered character.

1. *Preorbital skull length: less than or equal to 50% of the basal skull length (0); more than 55% of the basal skull length (1). (Modified from Weishampel et al., 2003)
2. Premaxilla, width of the oral margin in dorsal view: narrower than width across orbital region of skull roof (0), equals or exceeds width across orbital region of skull roof (1). (Modified from Norman, 2002)
3. *Premaxilla, shape of subnarial region: narial portion of the body of the premaxilla slopes steeply from the external naris to the oral margin (0); ventral premaxilla flares laterally to form a partial floor of the narial fossa (1). (Weishampel et al., 2003; Butler et al., 2008)
4. Premaxilla, oral margin reflected dorsally: absent (0); present (1). (Modified from Norman, 2002)
5. Premaxilla, oral margin denticulation: absent (0); present (1). (Weishampel et al., 2003; McDonald, 2012a)
6. *Premaxilla, posterolateral process contacts lacrimal: absent (0); present (1). (Modified from Weishampel et al., 2003, Milner and Norman, 1984, 1990; Sereno, 1984, 1986)
7. Premaxilla, posterolateral process, shape: tapers to a point (0); does not taper, caudal end is blunt (1). (modified from McDonald, 2012a, Prieto-Márquez and Salinas, 2010).
8. Premaxilla, position of the ventral (oral) margin: level with the maxillary tooth row (0); ventral to maxillary tooth row (1). (Norman, 2002; Butler et al., 2008)
9. Premaxilla, medial dorsal (nasal) process contacts the nasal: present (0); absent (1). (Butler et al., 2008)
10. Premaxilla, discrete rugose rostral margin, extending onto the medial dorsal (nasal) process: absent (0); present (1).
11. External naris, size: small, entirely overlies the premaxilla (0); enlarged, extends posteriorly to overlie both the premaxilla and maxilla (1). (Weishampel et al., 2003; Butler et al., 2008)
12. Nasals, deep elliptic fossa along midline: absent (0); present (1). (Butler et al., 2008)
13. *Nasals, placement of most dorsal point: caudally, at junction with frontals (0); more rostral, such that the nasal extends further dorsally than the frontals (1).
14. Nasals, thickened, paired domes on caudal portion: absent (0); present (1).
15. Premaxilla-maxilla boundary, fossa or foramen just dorsal to the oral margin: absent (0); present (1). (Butler et al., 2008)
16. Maxilla, diastema: absent, maxillary teeth begin directly caudal to the premaxilla (0); present, first maxillary tooth is at least one crown width away from the premaxilla (1). (Modified from Butler et al., 2008)

17. Maxilla, diastema length: one to two tooth widths (0); three tooth widths or more (1).
18. Maxilla, rostralateral process in addition to the premaxillary process: absent (0); present (1). (Weishampel et al., 2003; Butler et al., 2008)
19. Maxilla, rostralateral process of the maxilla, length: shorter than the premaxillary process (0); longer than the premaxillary process (1).
20. Maxilla, prominent rostralateral boss articulates with the lateral face of the premaxilla: absent (0); present (1). (Butler et al., 2008)
21. Maxilla, dorsal process, shape in lateral view: narrow, parallel-sided, (0); broad and triangular (1). (Modified from Norman, 2002)
22. o*Maxilla, dorsal process, position: rostral to the midpoint of the maxilla (0); at the midpoint (1); caudal to the midpoint (2).
23. Maxilla, emargination of the caudal end of the tooth row: absent (0); present (1). (new)
24. Maxilla, form of emargination: smooth curve (0); angular ridge (1).
25. Maxilla, horizontal ridge, caudal portion covered by a series of obliquely inclined ridges: absent (0); present (1). (Modified from Boyd et al., 2009)
26. Maxilla, shape of tooth row in ventral view: medially bowed, with rostral and caudal ends curving laterally (0); laterally bowed (1); straight (2). (McDonald, 2012a)
27. Maxilla, articulation with lacrimal: simple scarf or butt joint (0); lacrimal fits into slot between medial and lateral portions of the dorsal process of the maxilla (1). (Modified from Butler et al., 2008)
28. Maxilla, exclusion from the antorbital fenestra by rostral extension of the jugal: absent (0); present (1).
29. Antorbital fenestra: present (0); absent (1). (Butler et al., 2008)
30. Antorbital fenestra, shape: triangular (0); oval or circular (1). (Butler et al., 2008)
31. Antorbital fenestra, size: large (at least 15% basal skull length) (0); relatively small (10% basal skull length or less) (1); reduced to a small foramen (2). (Modified from Weishampel et al., 2003)
32. Antorbital fossa, additional fenestra(e) within fossa rostral to external antorbital fenestra: absent (0); present (1). (Butler et al., 2008)
33. Lacrimal-nasal contact: present (0); absent (1). (Norman, 2002)
34. Orbit shape: circular (0), subrectangular at least in its lower margin (1); dorsoventrally elongated, either oblong or subtriangular (2). (Modified from Winkler et al., 1997)
35. *Frontal, proportions: short and broad (length roughly equal to width) (0); narrow and elongate (length roughly 2 times the width) (1); very elongate (length roughly 3 times the width) (2). (Modified from Weishampel et al., 2003; Butler et al., 2008; state 2 based on Barrett and Han, 2009)
36. Frontal, shape in dorsal view: widest point is posterior to midorbit level (0); widest point is at midorbital level (1). (Modified from Boyd et al., 2009)

37. Frontal, participation in dorsal orbital rim: present (0); absent (1). (Norman, 2002; McDonald, 2012).
38. Frontal, participation in the border of the supratemporal fenestra: present (0); absent, excluded by contact between the postorbital and parietal (1).
39. Palpebral(s): free and separated from orbital rim, articulate only to the prefrontal (0); fused to orbit rim (1). (Modified from Butler et al., 2008)
40. Palpebral(s), shape in dorsal view: rod-shaped (0); platelike (1). (Butler et al., 2008)
41. Palpebral/supraorbital, number of ossified segments: one (0); two (1). (Butler et al., 2008)
42. *Palpebral(s), length relative to rostrocaudal width of orbit if unfused to orbital rim: does not traverse entire width of orbit (0); traverses entire width of orbit (1). (Butler et al. 2008)
43. Palpebral, dorsoventrally flattened and rugose along the medial and distal edges: absent (0); present (1). (Boyd et al., 2009)
44. *Postorbital, projection into orbital margin or rugose area for articulation of the palpebral: absent (0); present (1). (Modified from Butler et al., 2008)
45. Postorbital, shape of squamosal process: tapered (0); bifurcated (1). (modified from McDonald, 2012; Prieto-Márquez, 2010).
46. *Jugal, proportions: length of rostral process greater than or equal to caudal process (0); caudal process longer than rostral process (1).
47. Jugal, exclusion of the rostral process from the antorbital fenestra by lacrimal-maxilla contact: absent (0); present (1). (Weishampel et al., 2003; Butler et al., 2008)
48. o Jugal, shape of rostral end in lateral view: tapering (0); near parallel sided with a rounded or blunt rostral end (1) expanded dorsoventrally (2). (Modified from Norman, 2002)
49. o Jugal, type of suture with maxilla: scarf joint (0); 'finger-in-recess' joint, (1); butt-joint, (2). (Norman, 2002).
50. Jugal, boss extending laterally from suborbital portion: absent (0); present (1). (Butler et al., 2008)
51. Jugal, articulation with ectopterygoid: present (0); absent (1). (Head, 1998; Norman, 2002; McDonald, 2012)
52. Jugal, caudal ramus, bifurcated caudal end: absent (0); present (1). (Butler et al., 2008)
53. Jugal, participation in infratemporal fenestra: forms cranial and ventral margin (0); also forms part of caudal margin (1). (Weishampel et al., 2003; Butler et al., 2008)
54. Infratemporal fenestra: ventral end narrower than dorsal end: absent (0); present (1).
55. Jugal, form of articulation with quadratojugal: contact is relatively simple, consisting of a butt or high-angle scarf joint, jugal lies entirely lateral to the quadratojugal (0); tongue and-groove contact whereby the jugal lies lateral to the quadratojugal dorsally while ventrally the jugal lies medial to the quadratojugal (1). (Weishampel et al., 2003)

56. Jugal, shape of ventral edge: straight (0); sinuous (1).
57. Quadratojugal, shape: a central body with a dorsally projecting quadrate process that meets or nearly meets the squamosal (often on the medial side of the quadrate) (0); no dorsal process, element is small and blocky (1).
58. Quadratojugal, foramen through center of element: absent (0); present (1).
59. Quadratojugal foramen, position: located within quadratojugal (0); on jugal-quadratojugal boundary (1). (Modified from Butler et al., 2008)
60. Quadratojugal, position of ventral margin relative to mandibular condyle of the quadrate: approaches the mandibular condyle (0); well-removed from the mandibular condyle (1). (Butler et al., 2008)
61. *Quadrate, ventral portion of shaft: cranially convex (0); straight (1); caudally convex (2). (Modified from Butler et al., 2008)
62. Quadrate, caudally curved proximal portion: present (0); absent, straight (1). (Boyd et al., 2009)
63. Quadrate buttress ("hamular process"): absent (0); present (1).
64. Quadrate, prominent oval fossa on pterygoid ramus: absent (0); present (1). (Butler et al., 2008)
65. Quadrate (paraquadratic) foramen or notch on boundary between quadrate and quadratojugal: absent (0); present (1). (Butler et al., 2008; Norman, 2002)
66. *Quadrate, paraquadratic foramen or notch, size: small, height less than 1/8th quadrate height (0); large, height more than 1/7th quadrate height (1). (Modified from Butler et al., 2008)
67. Quadrate, paraquadratic notch completely covered by quadratojugal: absent (0); present (1).
68. Quadrate, articular condyle shape: much wider transversely than craniocaudally (0); transverse width less than or equal to craniocaudal length (1). (Modified from Norman, 2002)
69. o Quadrate, mandibular condyle proportions: medial condyle is larger than lateral condyle (0); quadrate condyles subequal in size (1); lateral condyle is larger than medial (2). (Butler et al., 2008)
70. o Quadrate, mandibular condyles, orientation of distal margin relative to long axis of quadrate: dorsomedially sloped (0); horizontal (1); dorsolaterally sloped (2).
71. Squamosal, ventral (quadratic) process length: less than 25% length of the quadrate (0); greater than 30% (1). (Modified from Boyd et al., 2009)
72. Squamosal, relative lengths of pre- and post-quadratic processes: pre-quadratic process is longer than or subequal to the post-quadratic (0); pre-quadratic process is shorter (1).
73. o Squamosal, relationship of right and left squamosals on skull roof: widely separated by parietal (0); separated by only a narrow band of the parietal (1); in broad contact with each other (2) (Horner et al., 2004; McDonald, 2012)
74. Paroccipital processes, shape: extend laterally (0); pendant, distal end curves ventrally (1). (Modified from Weishampel et al., 2003; Butler et al., 2008)

75. Posttemporal foramen/fossa, position: totally enclosed with the paroccipital process (0); forms a notch in the dorsal margin of the paroccipital process, enclosed dorsally by the squamosal (1); enclosed entirely by the squamosal (2). (Modified from Butler et al., 2008)
76. Supraoccipital, participation in the dorsal margin of the foramen magnum: present (0); absent, excluded by exoccipitals, (1).
77. *Supraoccipital, sharp, well-defined median nuchal crest: absent (0); present (1).
78. Supraoccipital, inclination of caudal surface: rostr dorsally inclined (0); vertical (1) (McDonald, 2012; modified from Horner et al., 2004)
79. Basioccipital: participation in the ventral border of the foramen magnum: present (0); absent, excluded by the exoccipitals (1).
80. Basioccipital, ventral keel: absent (0); present (1). (Boyd et al., 2009)
81. o Basipterygoid processes, orientation: anteroventral (0); ventral (1); posteroventral (2). (Butler et al., 2008)
82. Premaxilla, contact with vomer: present (0); absent, excluded by maxillae (1). (Modified from Butler et al., 2008)
83. Pterygoid, contact with maxilla at posterior end of tooth row: absent (0); present (1). (Butler et al., 2008)
84. Prementary, size: short, caudal oral margin of the premaxilla opposes rostral dentary margin (or teeth) (0); subequal in length to the oral margin of the premaxilla (1). (Modified from Butler et al., 2008)
85. Prementary, rostral end in dorsal view: rounded (0); pointed (1); straight transverse margin (2). (Weishampel et al., 2003; Butler et al., 2008)
86. Prementary, sulci extending rostrally from the intersections of the lateral processes and the ventral process: absent (0); present (1). (Modified from McDonald, 2012a)
87. Prementary, denticulate oral margin: absent (0); present (1). (Weishampel et al., 2003; Butler et al., 2008)
88. Prementary, ventral process: single (0); bilobate (1). (Butler et al., 2008)
89. Prementary, ventral process, depth of bifurcation: restricted to distal end (0); deep bifurcation (1).
90. Prementary, short midline process dorsal to dentary symphysis: absent (0); present (1). (Modified from McDonald, 2012)
91. o Prementary, relative length of the dorsal and ventral processes: ventral process longer than dorsal (0); processes roughly equal in length (1); dorsal process longer than ventral (2).
92. Dentary, diastema between prementary and first tooth: absent (0); present (1).
93. Dentary, length of diastema: short, the width of one to two teeth (0); long, the width of three teeth or more (1). (Modified from Norman, 2002)

94. Dentary, rostral extent of Meckel's groove meets the dentary symphysis: present (0); absent, ends more caudally (1).
95. *Dentary ramus, shape of rostral end: straight (0); strongly downturned (1). (Norman, 2002)
96. o Dentary, position of rostral tip: dorsal to the ventral margin of the dentary ramus (0); level with the ventral border of the dentary ramus (1); well below the ventral border of the dentary ramus (2).
97. o*Dentary, relationship of dorsal and ventral margins (under the tooth row): converge anteriorly (0); sub-parallel (1); diverge anteriorly (2). (Modified from Butler et al., 2008; Norman, 2002; Weishampel et al., 2003; McDonald, 2012a)
98. Dentary, shape of tooth row in dorsal view: straight (0); bowed medially (1).
99. Dentary, position of apex of curve in medially bowed tooth row: at mid-length (0); in the caudal half of the dentary (1). (McDonald, 2012a, modified from Prieto-Márquez et al., 2006)
100. Dentary, caudoventral extension below angular: absent (0); present (1).
101. Dentary, coronoid process, height; short, extends no more than one tooth height above tooth row (0); distinctly higher (1). (Modified from Weishampel et al., 2003)
102. Dentary, medial edge of coronoid process, position: in line with dentition (0); lateral to dentition (1). (Modified from Butler et al., 2008)
103. o*Dentary: caudal extent of tooth row: terminates rostral to coronoid process (0); terminates between rostral margin and apex of coronoid process (1); terminates directly ventral to apex or more caudally (2). (Modified from Wu and Godefroit, 2012)
104. Dentary: if coronoid is lateral to dentition, trough present between toothrow and coronoid: absent (0) present (1).
105. o Dentary, coronoid process orientation: caudally inclined (0); subvertical (1); rostrally inclined (2). (modified from Prieto-Márquez et al., 2006; McDonald, 2012a)
106. Coronoid process, shape in lateral view: subtriangular, tapers dorsally (0); rectangular (rostral and caudal margins are nearly parallel (1).
107. Coronoid process, rostrocaudally expanded apex: absent (0); present (1). (Modified from McDonald, 2012a)
108. Coronoid process, surangular contribution: present (0); absent (1).
109. o Coronoid process, relative craniocaudal widths of dentary and surangular (at midpoint of coronoid process): surangular wider than dentary (0); subequal (1); surangular narrower than dentary (2).
110. External mandibular fenestra, situated on dentary-surangular-angular boundary: present (0); absent (1). (Butler et al., 2008)
111. Surangular, small fenestra positioned dorsally on or near the dentary joint: absent (0); present (1). (Modified from Butler et al., 2008)
112. Surangular, position of small rostral fenestra: lies on boundary of dentary and surangular (0); lies within

the surangular (1).

113. Surangular foramen near mandibular glenoid: present (0); absent (1). (Norman, 2002)

114. Surangular foramen, position relative to the lateral lip of the glenoid: foramen is directly ventral to process (0); foramen is placed more rostrally (1).

115. Surangular, lateral lip of the glenoid expanded dorsally into a distinct process: absent (0); present (1). (Modified from Butler et al., 2008; Boyd et al., 2009)

116. Angular position, visible on the lateral surface of the mandible: present (0); absent (1). (Norman 2002)

117. Jaw joint, position: weakly depressed ventral to toothrow (0); strongly depressed ventrally, more than 30% of the height of the quadrate is below the level of the maxilla (1). (Modified from Butler et al., 2008)

118. Articular, retroarticular process: elongate (0); rudimentary or absent (1). (Butler et al., 2008)

119. Premaxillary teeth: present (0); absent (1). (Butler et al., 2008)

120. o* Premaxillary teeth, number: six (0); five (1); two (2); one (3). (modified from Butler et al., 2008)

121. Premaxillary teeth, mesiodistal crown expansion above root: absent (0); present (1). (Butler et al., 2008)

122. Premaxillary teeth, spacing: closely spaced (0); gaps of about one crown width between teeth (1).

123. o*Maxillary teeth, number; 13 or fewer tooth positions (0); 14 to 16 positions (1); 18-28 positions (2); 30 or more positions (3). (Modified from Weishampel et al., 2002)

124. o*Dentary teeth, number. 13 or fewer tooth positions (0); 14 to 16 positions (1) 18 to 25 positions (2); 27 or more positions (3). (Modified from Weishampel et al., 2002)

125. Cheek teeth; dentary teeth extend farther rostrally than maxillary teeth: absent (0); present (1).

126. Cheek teeth, spaces between the roots: present (0); absent, teeth are closely packed (1).

127. o Maxillary teeth, morphology of roots: distinct neck between crown and root (0); crown tapers to root (1); crown not significantly wider than root (2). (Modified from Boyd et al., 2009).

128. Dentary teeth, morphology of roots: distinct neck between crown and root (0); crown tapers to root (1). (Modified from Boyd et al., 2009)

129. o*Maxillary teeth, ratio of crown height to width (for unworn teeth): less than 1.2 (0); 1.25 to 1.9 (1); greater than 2 (2).

130. o*Dentary teeth, ratio of crown height to width (for unworn teeth): less than 1.5 (0); 1.7 to 2.2 (1); greater than 2.5 (2).

131. Cheek teeth: number of wear facets on each tooth: two (0); one (1).

132. Cheek teeth, apicobasally extending thickening of crown along midline (not a primary ridge): absent (0); present (1).

133. Cheek teeth, form of marginal denticles: simple, arcuate (0); labiolingually expanded, with a mammillated edge (1); absent or reduced to small papillae (2). (Modified from Norman, 2002)
134. Cheek teeth, enamel distribution: symmetrical (0); asymmetrical: thicker on the labial side of maxillary teeth and on the lingual side of dentary teeth (1). (Weishampel et al. 2003; Butler et al., 2008)
135. Cheek teeth, apicobasally extending ridges on labial side of maxillary teeth and lingual side of dentary teeth: absent (0); present (1). (Butler et al., 2008)
136. o Maxillary teeth, maximum number of ridges extending from the base to the tip of the crown on labial side of teeth: primary ridge only (0); one primary and one secondary ridge (1); three to eight ridges (2); ten to twelve ridges (3); fourteen to seventeen ridges (4).
137. o Dentary teeth, maximum number of ridges extending from the base to the tip of the crown on lingual side of teeth: primary ridge only (0); two to four ridges (1); five to eight ridges (2); nine to eleven ridges (3); twelve to seventeen ridges (4).
138. Cheek teeth: apicobasally extending ridges on cutting surface of unworn teeth (lingual surface of maxillary teeth, labial surface of dentary teeth): absent (0); present (1).
139. Maxillary teeth, primary ridge on labial side of crown: absent (ridges may be present, but none is more prominent than others) (0); present (1). (Modified from Weishampel et al., 2003; Butler et al., 2008)
140. Maxillary teeth, primary ridge size: only slightly larger than secondary ridges (0); much larger than secondary ridges (1). (Modified from Weishampel et al., 2003 and Butler et al., 2008)
141. Dentary teeth, primary ridge on lingual side of crown: absent (ridges may be present, but none is more prominent than others) (0); present (1). (Modified from Weishampel et al. 2003; Butler et al., 2008)
142. Dentary teeth, primary ridge size: only slightly larger than secondary ridges (0); much larger than secondary ridges (1). (Modified from Weishampel et al., 2003 and Butler et al., 2008)
143. Maxillary teeth, primary ridge position: centered, although some teeth within the same dental battery may display a slight offset of the primary ridge (0); offset, giving crown asymmetrical appearance (1). (Modified from Butler et al., 2008 and Prieto-Márquez and Salinas., 2010)
144. Dentary teeth, primary ridge position: centered, although some teeth within the same dental battery may display a slight offset of the primary ridge (0); offset, giving crown asymmetrical appearance (1). (Modified from Butler et al., 2008; Prieto-Márquez and Salinas., 2010)
145. Cheek teeth, secondary ridges, shape in cross-section: thick and rounded, composed of both enamel and dentine (0); thin and sharp-edged, formed by crenulations in enamel (1).
146. Maxillary teeth, base of crown defined by an everted lip which makes the crown slightly inset from the root: absent (0); present (1).
147. Dentary teeth, base of crown defined by an everted lip which makes the crown slightly inset from the root: absent (0); present (1).
148. Cheek teeth, at least moderately developed labiolingual expansion at the base of the crown ("cingulum"): present (0); absent (1). (Butler et al., 2008)
149. Maxillary and dentary crowns, relative width: maxillary crowns approximately equal in width with dentary crowns (0); maxillary crowns narrower (1). (Norman, 2002)

150. o Dentary teeth, maximum number of functional teeth exposed on the occlusal plane: one (0); one functional tooth rostrally and caudally, and up to two teeth at and approaching the middle of the dental battery (1); three functional teeth throughout most of the dental battery, gradually decreasing to two near the rostral and caudal ends of the dentary (2). (Prieto-Márquez and Salinas, 2010)
151. o Dentary teeth, maximum number of replacement teeth: one (0); two (1); three or more (2). (Norman, 2002)
152. Dentary alveoli: distinct, separate alveoli (0); parallel grooves lining a continuous dental battery (1). (Modified from Wu and Godefroit, 2012)
153. o Cervical vertebrae, number: nine or fewer cervical vertebrae (0); 10 to 11 (1); 12 or more (2). (Modified from Butler et al., 2008, Weishampel et al., 2003 and Prieto-Márquez and Salinas., 2010)
154. Axis, neural spine, shape of dorsal margin in lateral view: concave to straight (0); convex (1); sinuous (convex in the cranial portion and concave in the caudal portion) (2). (last state adapted from Prieto-Márquez and Salinas., 2010)
155. Axis, postzygapophyses, position: below dorsal margin of the neural spine (0); at or above the dorsal margin of the neural spine (1).
156. Postaxial cervical vertebrae, epipophyses: present on anterior vertebrae (0); absent (1). (Butler et al., 2008)
157. *Postaxial cervical vertebrae, form of central surfaces: amphicoelous (0); at least slightly opisthocelous (1). (Butler et al., 2008)
158. Postaxial cervical vertebrae, degree of opisthocely: cranial surfaces slightly convex (0); cranial surfaces distinctly convex (1).
159. Postaxial cervical vertebrae, proportions of centra: craniocaudal length about equal to dorsoventral height (0); very elongate: craniocaudal length more than twice the dorsoventral height (1).
160. Cervical vertebrae, ventral keel on centra: absent (0); present (1).
161. Dorsal vertebrae, number: 15 or fewer dorsal vertebrae (0); 16 or more dorsals (1). (Weishampel et al., 2003; Butler et al., 2008)
162. o Dorsal vertebrae, length of mid-dorsal neural spines: short and rectangular, height and length roughly equal (0); height more than twice length (1); height more than four times length (2). (Norman, 2002)
163. Dorsal vertebrae, cranial and mid dorsals, ventral keel on centra: absent (0); present (1).
164. Dorsal vertebrae, proportions of mid to posterior centra: craniocaudal length is subequal to or longer than dorsoventral height (0); length is much shorter than height (1).
165. Dorsal vertebrae, shape of neural spines in posterior dorsals: straight (0); bowed caudally (1).
166. Dorsal vertebrae, prezygapophyses on posterior dorsals extend well past the cranial edge of the centrum: absent (0); present (1).
167. Dorsal vertebrae, posterior dorsals, length of transverse processes: less than or equal to centrum height (0); greater than centrum height (1).

168. Ossified intercostal plates: absent (0); present (1).
169. Sternal segments of the anterior dorsal ribs: not ossified (0); at least partially ossified (1). (Modified from Weishampel et al 2003)
170. Sacral vertebrae, number, including dorsosacrals and sacrocaudals: five or fewer (0); six or more (1). (Weishampel et al., 2003; Butler et al., 2008)
171. Sacral vertebrae, transverse thickening and increase in rugosity at tips of neural spines: present (0); absent (1).
172. o Sacral vertebrae, neural spines, extent of fusion: spines do not touch (0); some spines overlap, but are not fused (1); spines are fused into a single plate (2).
173. Sacral vertebrae, form of ventral surface of centra: rounded (0); keeled (1); grooved (2).
174. Sacral ribs, coalesce laterally to form a sacral yolk: absent (0); present (1).
175. Caudal vertebrae, proportions of proximal centra: craniocaudal length is subequal to or longer than dorsoventral height (0); length is much shorter than height (1).
176. Caudal vertebrae, ventral sulcus on centra: absent (0); present (1).
177. Caudal vertebrae, position of the most distal caudal rib (transverse process): 12th caudal vertebrae or more proximal (0); 13th or more distal (1).
178. Caudal vertebrae, height of neural spines on proximal caudals: height the same or up to 50% taller than the centrum (0); more than 50% taller than the centrum (1). (Weishampel et al., 2003; Butler et al., 2008)
179. Caudal vertebrae, orientation of neural spines on proximal caudals: project dorsally from centra (0); project caudodorsally from centra (1).
180. Caudal vertebrae, shape of neural spines on proximal caudals: straight (0); bowed caudally (1).
181. Caudal vertebrae, length of transverse processes on proximal caudals: longer than or subequal to neural spine height (0); shorter than neural spine (1). (Modified from Butler et al., 2008)
182. Caudal vertebrae, craniocaudal length of the distal facet for chevrons on proximal caudals: shorter than the ventral surface of the vertebrae (between the proximal and distal facets) (0); longer than the ventral surface (1).
183. Caudal vertebrae, proportions of articular facets for chevrons: the distal facet on a given vertebra is much larger than the proximal facet (0); facets are subequal (1).
184. Caudal vertebrae, form of chevron articular facets: fairly flat surface (0); deep fossa surrounded by a rim (1).
185. Caudal vertebrae, length of prezygopophyses on distal caudals: extend slightly over the preceding vertebra (0); elongate, extend nearly to the midpoint of the preceding vertebra (1).
186. o Chevrons, position of most proximal chevron: distal end of first caudal vertebra (0); distal end of second caudal vertebra (1); distal end of third caudal vertebra or more distal (2).

187. Chevrons, length relative to the length of the neural spines in the proximal caudal vertebrae: chevrons shorter than or equal in length to the neural spines, (0); chevrons longer than neural spines (1). (Modified from Prieto-Márquez and Salinas., 2010)

188. Chevrons, shape: edges are near parallel in lateral view, often with slight distal expansion (0); strongly asymmetrically expanded distally, width greater than length in mid caudals, (1). (Modified from Butler et al., 2008)

189. Sternal plates, rod-like caudolateral process: absent (0); present (1). (Modified from Butler et al., 2008, Norman, 2002)

190. Sternals, caudolateral process, shape of cross-section: round (0); flattened (1).

191. Sternal, caudolateral process, length relative to that of the craniomedial plate: caudolateral process slightly shorter or as long as the craniomedial plate (0); caudolateral process longer than the craniomedial plate (1). (Prieto-Márquez and Salinas., 2010)

192. Sternal, pronounced caudomedial process ("posterior apron" of Norman, 2015) projects from plate of sternal in addition to caudolateral process: absent (0); present (1).

193. Sternals, midline fusion: absent (0); present (1).

194. *Forelimb, proportions of humerus and scapula: scapula longer or subequal to the humerus (0); humerus substantially longer than the scapula (1). (Weishampel et al., 2003; Butler et al., 2008)

195. Scapula, acromion process size: weakly developed (0); projects prominently from the cranio-dorsal edge of the proximal scapula (1). (Modified from Butler et al., 2008)

196. Scapula, acromion process, length: does not extend beyond the edge of the coracoid (0); extends past the coracoid (1).

197. Scapula, deltoid ridge shape: wide and rounded (0); sharp, narrow (1).

198. *Scapula, deltoid ridge, orientation relative to long axis of scapula: close to parallel (0); more than 20 degrees from axis (1).

199. Scapula, supraglenoid fossa: absent (0); present (1).

200. o*Scapula, length of blade relative to minimum width: short and broad, ratio of length to width 5.7 or less (0); ratio of length to width 6 to 7.3 (1); elongate, ratio of 7.5 or greater (2). (modified from Butler et al., 2008)

201. Scapula blade, shape: expanded distally (0); parallel-sided (1). (Modified from Butler et al., 2008)

202. Scapula, expanded distal blade shape: caudoventral edge curves away from a fairly straight craniodorsal edge, creating a deep asymmetric expansion (0); edges gradually diverge from each other, forming a symmetrically expanded end (1).

203. Scapula blade, shape of dorsal edge in lateral view: straight (0); curved (1). (Norman, 2002)

204. o Scapula and coracoid, relative contributions to the glenoid fossa in transverse width: scapula wider (0); subequal (1); coracoid wider (2).

205. o Scapula and coracoid, relative contributions to the glenoid fossa in craniocaudal length: scapular portion longer (0); subequal (1); coracoid portion longer (2).
206. Coracoid, depth of preglenoid embayment: wide and shallow, depth of embayment less than 40% of its width (0); deep, depth 45% of its width or greater (1).
207. Coracoid, ratio between the length of the scapular articulation and the length of the lateral margin of the glenoid in lateral view: greater than 1.30 (0); less than 1.25 (1).
208. Coracoid, position of lateral opening of coracoid foramen: within coracoid (0); on suture between the coracoid and scapula (1).
209. Coracoid, position of medial opening of coracoid foramen: within coracoid (0); on suture between the coracoid and scapula (1).
210. Coracoid, lateral protrusion on dorsal border for origin of M. biceps: absent (0); present (1).
211. Humerus, length relative to femur: less than 62% of femoral length; (0); greater than 65% of femoral length (1). (Modified from Butler et al., 2008)
212. *Humerus, deltopectoral crest form: a well-developed projection (0); slight projection (1). (Modified from Butler et al., 2008; Norman, 2002)
213. Humerus, deltopectoral crest orientation: projects laterally (0); curves cranially (1).
214. *Humerus, deltopectoral crest length: 40% of total humeral length or less (0); 43% or more (1).
215. Humerus, humeral head position: centered within the proximal end (0); offset towards the medial edge (1).
216. o Humerus, relative width of medial and lateral distal condyles: lateral condyle wider (0); subequal (1); medial condyle wider (2).
217. Ulna, length relative to dorsoventral thickness at mid-shaft: less than 9 (0); greater than 9.5 (1). (Modified from Prieto-Márquez and Salinas., 2010)
218. o Ulna, olecranon process length as a percentage of total ulnar length: 9% or less (0); 9.5 to 15% (1); 17% or greater (2).
219. Ulna, flange on proximal end that wraps around the lateral edge of the radius: absent (0); present (1).
220. Radius, length: less than 67% of the length of the humerus (0); greater than 70% of humeral length (1). (Modified from Norman, 2002)
221. Radius, proportions: relatively gracile, minimal radial width 11% of radial length or less (0); relatively robust, the minimal radial width is equal to or greater than 12% radial length (1). (modified from Weishampel et al., 2003)
222. Radius, notch in proximal view, rostralateral to articulation with the ulna: absent (0); present (1).
223. Radius, tubercle near proximal end of radius for insertion of M. biceps: absent (0); present (1).
224. Radius, shape in distal view: round to oblong (0); triangular (1).

225. Carpals, full ossification of all elements: present (0); absent (1). (Norman, 2002)
226. Carpals, relative sizes of proximal carpals: radiale is the largest element (0); ulnare is the largest element (1).
227. Carpals, fusion: absent (0); present (1). Modified from (Serenio, 1986; Norman, 1986, 1990, Weishampel et al., 2003)
228. o Carpals, degree of fusion: metacarpal I fused to radiale (0); radiale is further fused to intermedium (1); all carpals and the first metacarpal are fused (2). Modified from (Serenio 1986; Norman 1986, 1990, Weishampel et al., 2003)
229. Carpals, ossified ligaments around carpals: absent (0); present (1).
230. Metacarpal III, ratio between length and width at mid-shaft: short, ratio less than 5 (0); long and slender, ratio greater than 5.5 (1). (modified from Horner et al., 2004; Prieto-Márquez and Salinas., 2010)
231. Manus digit I: present (0); absent (1). (Norman, 2002)
232. Manus digit I, orientation: nearly parallel to the long axis of the antebrachium (0); diverges at least 45 degrees from the antebrachial axis (1). (Modified from Weishampel et al., 2002)
233. Metacarpal I, shape: regular, elongate metacarpal (0); short, block-like (1). (Modified from Norman, 2002)
234. Metacarpals II-IV arrangement: distally divergent (0); nearly parallel (1). (Modified from Norman, 2002)
235. Metacarpals II and IV, relative length: subequal (0); metacarpal II is much shorter than metacarpal IV (1); metacarpal IV is much shorter than metacarpal II (2).
236. Manus digit III, number of phalanges: four (0); three or fewer (1). (Butler et al., 2008)
237. Manus, digit V: present (0); absent (1).
238. Manus, digit V, number of phalanges: one or two phalanges (0); three or four phalanges (1). (Modified from Wu and Godefroit, 2012)
239. Phalanges of manual digits II-IV, length: first phalanx less than twice the length of the second phalanx (0); first phalanx more than twice the length of the second phalanx (1). (Modified from Butler et al., 2008 and Weishampel et al., 2002)
240. Phalanges, extensor fossae on the dorsal surface of the distal end of metacarpals and manual phalanges: absent or poorly developed (0); deep, well-developed (1). (Butler et al., 2008)
241. Manus ungual I, shape: curved and transversely compressed (0); subconical (1). (Serenio, 1984, 1986; Norman, 1986, 1990, 2002, Weishampel et al., 2003)
242. Manus ungual I, length: less than 25% the length of the radius (0); greater than 30% the length of the radius (1).
243. Manus unguals II and III, shape: transversely compressed and pointed (0); dorsoventrally compressed, with a rounded tip (1). (Modified from Norman, 2002; Weishampel et al., 2003)

244. Ilium, medial flange partly closes acetabulum: present (0); absent (1).
245. Ilium, acetabulum size; large and concave, extends deeply into body of ilium (0); very narrow (1). (Modified from Weishampel et al., 2003)
246. Ilium, relative lengths of pubic and ischial peduncles: extends ventrally to the same level (0); ischial peduncle extends beyond the pubic peduncle (1).
247. Ilium, Ischial peduncle extends distinctly laterally from the body of the ilium: absent (0); present (1).
248. o Ilium, ischial peduncle morphology: formed by a single large ventral protrusion (0); composed of a large oval ventral protrusion and by a smaller, caudodorsally located prominence (1); formed by two protrusions of similar size (2). (Modified from Prieto-Márquez and Salinas, 2010)
249. Ilium, preacetabular process, orientation; external surface faces laterally, in approximately the same plane as the iliac body (0); process is distinctly twisted about its long axis (1). (Weishampel et al., 2003)
250. Ilium, preacetabular process, lateral deflection relative to midline: 10-20 degrees (0); more than 30 degrees (1). (Butler et al., 2008)
251. Ilium, preacetabular process, morphology of distal end: parallel-sided or slightly tapering (0); small ventral flange (1).
252. Ilium, cranial sacral facets transversely widened so that the base of the preacetabular process is thicker ventrally than dorsally: absent (0); present (1).
253. Ilium, preacetabular process, ridge on medial side originating from medial sacral ridge: absent (0); present (1).
254. Ilium, preacetabular process, second medial ridge starting from the ventral edge of the process, along the notch above the pubic peduncle: absent, (0); present (1).
255. Ilium, dorsal margin of iliac body, shape in lateral view: straight or convex (0); concave (1).
256. Ilium, dorsal margin of the iliac body, shape in dorsal view: narrow, not transversely expanded (0); transversely expanded laterally to form a narrow shelf (1). (Modified from Butler et al., 2008)
257. Ilium, pendant process ("pendule" sensu Norman, 2015) extending from lateral ilial shelf dorsal to the ischial peduncle: absent (0); present (1).
258. Ilium, brevis shelf: present (0); absent (1).
259. Ilium, brevis fossa, well defined by a lateral lip: absent (0); present (1).
260. Ilium, brevis shelf and fossa, orientation: fossa faces ventrolaterally and shelf is near vertical, creating a deep postacetabular portion (0); fossa faces ventrally and shelf is horizontal (1). (Modified from Butler et al., 2008)
261. Ilium, ridge originating from the ischial peduncle and continuing caudally along the brevis shelf, often disappearing around the middle of the postacetabular process (this is distinct from the medial boundary of the brevis shelf): absent (0); present (1).
262. o Ilium, postacetabular process, width as a percentage of its length: less than 30% (0); between 35 and

55% (1); over 60% (2).

263. o Ilium, postacetabular process, length as a percentage of the total length of the ilium: 20% or less (0); 23-30% (1); 34% or more (2). (Modified from Butler et al., 2008)

264. Ilium, postacetabular process, shape: dorsal and ventral margins are parallel and roughly the same length, so the process has a square or rounded caudal end (0); the dorsal margin is shorter than the ventral, so that the caudal margin slopes caudoventrally (1); the dorsal and ventral edges slope smoothly towards each other, forming a pointed caudal end (2).

265. Ilium, postacetabular process, orientation: extends subhorizontally, does not extend above the body of the ilium (0); extends caudodorsally, so the postacetabular process reaches further dorsally than the body of the ilium (1).

266. Ilium, orientation of the medial sacral ridge: craniocaudally directed, parallel to the dorsal margin of the ilium, and ending caudal to the level of the ischial peduncle, well into the proximal region of the postacetabular process (0); diagonal, cranioventrally to caudodorsally oriented, concave ventrally and converging with the dorsal margin at the level of the ischial peduncle (1). (Prieto-Márquez and Salinas, 2010)

267. Pubis, prepubic process: absent (0); present (1). (Butler et al., 2008)

268. Pubis, prepubic process, width: compressed mediolaterally, dorsoventral height exceeds mediolateral width (0); mediolateral width exceeds dorsoventral height (1). (Butler et al., 2008)

269. Pubis, prepubic process, shape in lateral view: unexpanded distally (0); constricted proximal portion followed by a distal expansion (1). (Modified from Norman, 2002)

270. Pubis, prepubic process, depth of the dorsoventral expansion of the distal region greater than the width of the acetabular margin; absent (0); present (1). (Modified from Prieto-Márquez and Salinas, 2010)

271. o Pubis, prepubic process, craniocaudal length of the proximal constriction relative to the length of the dorsoventral expansion: constriction longer than the dorsoventral expansion (0); constriction and distal expansion subequal (1); constriction shorter than the dorsoventral expansion (2). (Modified from Horner et al., 2004; Prieto-Márquez and Salinas, 2010)

272. Pubis, prepubic process shape, if unexpanded distally: straight (0); concave dorsally (1).

273. Pubis, prepubic process, horizontal ridge on medial side: absent (0); present (1).

274. Pubis, prepubic process, extends beyond distal end of preacetabular process of ilium: absent (0); present (1). (Butler et al., 2008)

275. Pubis, obturator foramen completely enclosed: present (0); absent (1).

276. Pubis, obturator foramen shape: elliptical (0); circular (1).

277. Pubis, obturator foramen, orientation when the prepubis is oriented in a parasagittal plane: the obturator foramen faces laterally (0); the obturator foramen faces somewhat dorsally (1).

278. o Pubis, shaft (postpubis), length: approximately equal in length to the ischium (0); reduced, extends for about half the length of the ischium (1); very short, extends less than 20% the length of the ischium (2). (Modified from Butler et al., 2008)

279. Ischium, iliac peduncle, orientation of the acetabular and caudodorsal margins: divergent approaching the articulation with the ilium (0); either parallel or slightly convergent (1). (Prieto-Márquez and Salinas, 2010)
280. Ischium, pubic peduncle, shape: transversely compressed (0); dorsoventrally compressed (1). (Butler et al., 2008)
281. Ischium, shaft, shape in lateral view: straight (0); downwardly curved (1). (Butler et al., 2008; Weishampel et al., 2003; Norman, 2002)
282. Ischium, shaft, orientation: axis of shaft is caudoventral (0); axis of shaft is caudal (1).
283. Ischium, shaft, twisted along its length so that the lateral side faces ventrally on the distal part of the shaft: present (0); absent (1).
284. Ischium, cross-section at mid-shaft: compressed mediolaterally (0); ovoid or subcircular (1). (Modified from Weishampel et al., 2002, and Butler et al., 2008)
285. Ischium, obturator process: absent (0); present (1). (Modified from Weishampel et al., 2003 and Butler et al., 2008)
286. Ischium, obturator process, shape: discrete tab (0); elongate ridge extending distally down ischial shaft (1).
287. Ischium, obturator process, position of proximal edge: beyond the proximal 29% of the length of the ischium (measured from the acetabular rim to the distal end) (0); within the proximal 25% (1). (Modified from Weishampel et al., 2003)
288. Ischium, distal end expanded to 50% or more the depth of the adjacent ischial shaft; absent (0); present (1). (Modified from Weishampel et al., 2003, Norman, 2002)
289. *Femur, length relative to tibia: shorter than or equal to (0); longer than the tibia (1). (Milner and Norman, 1984; Norman, 1984b, modified from Weishampel et al., 2003)
290. *Femur, shape in lateral view: straight (0); bowed cranially (1). (Butler et al., 2008)
291. Femur, shape in cranial view: straight (0); bowed laterally (1). (Weishampel et al., 2003)
292. Femur, head: confluent with greater trochanter (0); distinct constriction separates head and greater trochanter (1). (Butler et al., 2008)
293. Femur, head, ventromedially oriented sulcus on caudal side: absent (0); present (1).
294. Femur, 'anterior' or 'lesser' trochanter, craniocaudal width: subequal to that of the greater trochanter (0); substantially less than that of the greater trochanter (1). (Modified from Butler et al., 2008)
295. Femur, anterior trochanter, level of most proximal point relative to level of proximal femoral head: positioned distally on the shaft (0); positioned proximally, approaches level of proximal surface of femoral head (1). (Modified from Butler et al., 2008)
296. Femur, fourth trochanter, shape: pendant (0); prominent ridge (1). (Butler et al., 2008; Weishampel et al., 2003; Norman, 2002)

297. Femur, fourth trochanter, if ridge-shaped, lateral profile of the caudoventral margin: triangular and ending in a caudally, and slightly ventrally, directed point (0); smooth and arcuate (1). (Modified from Prieto-Márquez and Salinas, 2010)
298. *Femur, fourth trochanter, position: located entirely on proximal half of femur (0); positioned at mid-length or distal to midlength (1). (Weishampel et al., 2003; Butler et al., 2008)
299. Femur, muscle scar for *M. caudofemoralis longus* on medial side of fourth trochanter, position and size: a small, distinct fossa on the shaft of the femur (0); a large oblong depression mainly on the medial side of the fourth trochanter (1).
300. Femur, cranial (extensor) intercondylar sulcus on distal end: absent (0); present (1). (Norman, 2002; Weishampel et al., 2003; Butler et al., 2008)
301. o Femur, cranial intercondylar sulcus, shape: open, U-shaped (0); partially enclosed by cranial expansion of condyles (1); fully enclosed by cranial condyles (2). (Norman, 2002)
302. *Femur, caudal (flexor) intercondylar sulcus of the femur: fully open (0); medial condyle inflated laterally, partially covers opening of flexor sulcus (1). (Weishampel et al., 2003; Butler et al., 2008).
303. Femur, lateral (fibular) condyle, position and size: not inset from the lateral edge, and only slightly narrower in width than the medial condyle (0); strongly inset medially, reduced in width relative to medial condyle (1). (Modified from Butler, 2008)
304. Femur, distal condyles, shape in lateral view: moderately expanded craniocaudally (0); strongly expanded (condyle extends cranially as well as caudally) (1). (Modified from Norman, 2002)
305. Femur, distal condyles, shape of articular surface: flat articular surface (0); rounded articular surface (1); flat to concave lateral condyle and convex medial condyle (2).
306. Tibia, fibular process shape: single (0); double (1).
307. Tibia, expansion of proximal end in lateral view: width of proximal tibia is less than 2.3 times the diameter at midshaft (0); proximal tibia is more than 2.5 times the diameter at midshaft (1).
308. Fibula, expansion of proximal end, shape: flared, with concave cranial and caudal margins (0); nearly straight cranial and caudal margins (1).
309. Astragalus, astragular notch on lateral margin of ascending process: absent (0); present (1).
310. Astragalus, small fossa on cranial side of astragalus (this is directly ventral to astragular notch when both are present): absent (0); present (1).
311. Astragalus, joint with calcaneum, morphology: peg-in-socket (0); straight butt joint (1).
312. Astragalus, width relative to calcaneum width: less than 2.25 times calcaneum width (0); greater than 2.5 times calcaneum width (1).
313. Distal tarsals II and III: present (0); absent (1). (Horner et al., 2004, character 102; Prieto-Márquez and Salinas, 2010)
314. Medial distal tarsal: articulates distally with metatarsal III only (0); articulates distally with metatarsals II and III (1). (Butler et al., 2008)

315. Metatarsal I: absent (0); present (1).
316. Metatarsal I, bears digits: present (0); absent (1). (Norman, 2002; Weishampel et al., 2003; Butler et al., 2008)
317. Digit I, length: metatarsal I robust and well-developed, distal end of phalanx I-1 projects beyond the distal end of metatarsal II (0); metatarsal I reduced and proximally splint-like, end of phalanx I-1 does not extend beyond the end of metatarsal II (1). (Modified from Butler 2008)
318. Metatarsal II, tab-like process on craniolateral edge that articulates with metatarsal III: absent (0); present (1).
319. Metatarsal III, ratio of length to mediolateral width at midshaft: less than 6.5 (0); greater than 7.5 (1). (Modified from Prieto-Márquez and Salinas, 2010)
320. Metatarsal V: present (0); absent (1). (Modified from Weishampel et al., 2003; Milner and Norman, 1984; Sereno, 1984; Norman, 1986; Coria and Salgado, 1996)
321. o Pedal unguals, shape: mediolaterally compressed, tapering, and pointed (0); dorsoventrally compressed, proximally wider, tapering to a bluntly truncated tip (1); dorsoventrally compressed, mediolaterally broad and proximodistally shortened, rounded distal end ("hoof-shaped") (2). (Modified from Prieto-Márquez and Salinas, 2010; Butler et al., 2008; Weishampel et al., 2003; Norman, 2002)
322. Tendons, ossified hypaxial tendons on caudal vertebrae: absent (0); present (1). (Butler et al., 2008)
323. Tendons, ossified epaxial and hypaxial tendon arrangement: longitudinal (0); double-layered lattice (1). (Butler et al., 2008)

APPENDIX 2.

Character matrix (also available as TNT and Nexus files in supplementary documents) for download at <https://palaeo-electronica.org/content/2022/3707-iguanodontian-phylogeny>.

APPENDIX 3

List of taxa used in analysis and sources from which characters were scored.

Institutional Abbreviations: **AM**, Albany Museum, Grahamstown, South Africa; **AMNH**, American Museum of Natural History, New York City, New York, USA; **BYU**, Earth Sciences Museum, Brigham Young University, Provo, Utah, USA; **CEUM**, College of Eastern Utah Prehistoric Museum, Price, Utah, USA; **CM**, Carnegie Museum of Natural History, Pittsburgh, Pennsylvania, USA; **DMNS**, Denver Museum of Nature and Science, Denver, Colorado, USA; **GPIT**, Institut und Museum für Geologie und Paläontologie der Universität Tübingen, Tübingen, Germany; **IVPP**, Institute of Vertebrate Paleontology and Paleoanthropology, Beijing, China; **MB**, Museum für Naturkunde Berlin, Berlin, Germany; **MC**, Museum Crúzy, Crúzy, France; **MCF**, Museo Carmen Funes, Plaza Huincul, Neuquén, Argentina; **MCS**, Museo de Cinco Saltos, Rio Negro Province, Argentina; **MHN-AIX-PV**, Museum d'Histoire Naturelle d'Aix-en-Provence, Aix-en-Provence, France; **MHNM**, Museum d'Histoire Naturelle de Marseille, Marseille, France; **MNHN**, Museum National d'Histoire Naturelle, Paris, France; **MOR**, Museum of the Rockies, Bozeman, Montana, USA; **MUCPv**, Museo de Geología y Paleontología de la Universidad Nacional del Comahue, Neuquén, Argentina; **NHMUK**, Natural History Museum, London, United Kingdom; **NMV**, National Museum of Victoria, Melbourne, Australia; **OUMNH**, Oxford University Museum of Natural History, Oxford, UK; **QM**, Queensland Museum, Geoscience Collection, Brisbane, Queensland, Australia; **RBINS** (formerly IRSNB), Royal Belgian Institute of Natural Sciences, Brussels, Belgium; **ROM**, Royal Ontario Museum, Toronto, Canada; **SAM**, South African Museum (Iziko Museums of Cape Town), Cape Town, South Africa; **SDSM**, Museum of Geology, South Dakota School of Mines and Technology, Rapid City, South Dakota, USA; **UMNH**, Natural History Museum of Utah, Salt Lake City, Utah, USA; **USNM**, United States National Museum of Natural History, Washington, DC, USA; **YPM**, Yale Peabody Museum, New Haven, Connecticut, USA; **ZDM**, Zigong Dinosaur Museum, Dashanpu, China.

Taxon	Specimen Numbers	Literature Sources
<i>Agilisaurus</i>	Photographs of holotype specimens ZDM T6011 kindly provided by Han Fenglu.	Barrett et al., 2005
<i>Altirhinus kurzanovi</i>		Norman, 2002
<i>Anabisetia saldiviai</i>	MCF-PVPH-74-6.	Coria and Calvo, 2002
<i>Atlascopecosaurus</i>	NMV P166409 (holotype), 182967.	
<i>Bactrosaurus</i>		Weishampel and Horner, 1986; Godefroit et al., 1998
<i>Barilium</i>	NHMUK R798a R798b, R799-806, R4742, 4771: All holotype specimen.	Norman, 2010
<i>Batyrosaurus</i>		Godefroit et al., 2012
<i>Bolong</i>		Wu and Godefroit, 2012
<i>Camptosaurus</i>	YPM 1877 (holotype), 1878, USNM V4277, 5473, UMNH.VP.5322, 16422, 16452, 16454, 16455, 16458, 16572, 16592-3.	Gilmore, 1909; Brill and Carpenter, 2006
<i>Cedrorestes</i>	DMNS 47994 (holotype).	
<i>Cumnoria</i>	OUMNH Geol J3303 (holotype).	
<i>Dakotadon</i>	SDSM 8651 (holotype).	
<i>Dryosaurus</i>	CM 3392, 1949, 87688, DMNS 9001 (juvenile).	Galton, 1981, 1983

Taxon	Specimen Numbers	Literature Sources
<i>Dysalotosaurus</i>	MB R1316, 1318, 1320, 1322, 1329, 1333, 1335, 1338, 1351, 1358, 1370, 1372-8, 1383, 1394, 1396-8, 1408-9, 1474, 1476, 1478, 1480-1, 1485-7, 1502, 1540, 1565-6, 1585-1604, 1707, 1709, 1711, 1717-8, 2144, 2503, 2508, 2511, 2516-7, 3293, 3297, 3468, 3474. GPIT/RE/3608, 3612, 3614, 3826, 3829, 3830, 4156, 4181, 4189, 4545, 4710, 4925, 5192, 5302, 5355, 5460-3, 5636, 6067, 6161, 6169, 6189, 6269, 6399, 6544, 6549, 6803, 6987, 8425.	Janensch, 1955
<i>Edmontosaurus</i>		Lambe, 1920; Campione and Evans, 2011
<i>Eocursor</i>	SAM PK K8025 (holotype).	Butler et al., 2007
<i>Eolambia</i>	CEUM 9758 (holotype), 1233, 1251-1256, 3207, 3186, 13383, 14419, 14464, 14466, 14495, 14534, 14576, 14601, 14602, 34247, 34252, 34329, 4337, 34382, 34397, 34412, 34430, 34441, 35323, 35384, 35412, 35413, 35492, 35524, 35525, 35539, 35592, 35637, 35638, 35673, 35679, 35733, 35742, 36190, 52097, 52865, 52884, 52924, 52936, 52988, 73585, 74566, 74572, 74611, 74653, 78380.	McDonald et al., 2012
<i>Equijubus</i>	IVPP V 12534	You et al., 2003
<i>Fukuisaurus</i>		Kobayashi and Azuma, 2003
<i>Gasparinisaura</i>	MCS 1-3; MUCPv 111-2, 208 (holotype), 210, 212-3	Coria and Salgado, 1996
<i>Gilmoreosaurus</i>		Weishampel and Horner, 1986; Prieto-Márquez and Norrell, 2010
<i>Shishugou taxon</i>	IVPP 14559, field number field number WCW-02-29	
<i>Haya</i>		Makovicky et al., 2011
<i>Hexinlusaurus</i> (= <i>Yandusaurus</i>) <i>multidens</i>	Photos of holotype ZDM T6001 kindly provided by Han Fenglu.	Barrett et al., 2005
<i>Hippodraco</i>	UMNH VP 20208 (holotype)	McDonald et al., 2010b
<i>Hypacrosaurus</i>	MOR 549 (holotype <i>H. stebingeri</i>), MOR 355, MOR 548.	
<i>Hypselospinus</i>	NHMUK R1650 (holotype), 33, 1627, 1636, 1831, 1834. <i>Iguanodon hollingtoniensis</i> holotype: NHMUK R604, 811, 811b, 1148, 1629, 1632.	Norman, 2010, 2014
<i>Hypsilophodon</i>	NHMUK R146, 192-4, 197 (holotype), 2466, 2477, 2488.	Galton, 1974
<i>Iguanacolossus</i>	UMNH VP 20205 (holotype)	McDonald et al., 2010b
<i>Iguanodon</i>	RBINS R51 (lectotype)	Norman, 1980
<i>Jeholosaurus</i>		Barrett and Han, 2009; Han et al., 2012
<i>Jeyawati</i>		McDonald et al., 2010a
<i>Jinzhousaurus</i>	IVPP V12691 (holotype)	Barrett et al., 2009; Wang et al., 2010
<i>Kangnasaurus</i>	SAM 2732 (holotype), 2731a-j	Cooper, 1985
<i>Kirkwood taxon</i>	AM 6150 (holotype), 6004, 6005, 6021, 6022, 6030, 6053, 6055, 6056, 6063, 6066, 6067, 6077, 6093, 6101, 6102, 6103, 6104, 6107, 6108, 6109, 6110, 6111, 6119, 6122, 6151, 6154, 6155, 6175, 6176, 6190	
<i>Kukufeldia</i>	NHMUK R28660	
<i>Lanzhousaurus</i>		You et al., 2005
<i>Leaellynasaura</i>	NMV P185990-1 (holotype), 185992-3, 186047, 221080, 229196	
<i>Lesothosaurus</i>	NHMUK R8501, NHMUK RUB23, SAM PK K 400, 401, 1106	Sereno, 1991; Butler, 2005
<i>Levnesovia</i>		Sues and Averianov, 2009

Taxon	Specimen Numbers	Literature Sources
<i>Lurdusaurus</i>	MNHN.F.GDF 1700 (holotype)	
<i>Macrogyphosaurus</i>	MUCPv 321 (holotype)	Calvo et al., 2007
<i>Maiasaura</i>		Horner 1983; Dilkes, 2000
<i>Mantellisaurus</i>	NHMUK R5764 (holotype); RBINS R57 (this specimen was scored as a separate OTU).	Norman, 1986
<i>Muttaborrasaurus</i>	QM F6140 (holotype), 14921	
<i>Orodromeus</i>	MOR 294 (holotype); MOR 1141; MOR 473	
<i>Oryctodromeus</i>	MOR 1636	Varricchio et al., 2007
<i>Othnielosaurus</i>	BYU-ESM-163	
<i>Ouranosaurus</i>	MNHN.F.GDF 300 (casts)	
<i>Owenodon</i>	NHMUK R2998	
<i>Parksosaurus</i>	Photographs of ROM 804 (holotype) provided by Ali Nabavizadeh	Parks, 1926
<i>Planicoxa</i>	DMNS 42504 (holotype), 40909, 40914, 40917, 40918, 42477, 42505, 42506, 42507, 42508, 42511, 42513, 42521, 42525, 42599.	
<i>Proa</i>		McDonald et al., 2012
<i>Probactrosaurus</i>		Norman, 2002
<i>Protohadros</i>		Head, 1998; Main, 2013
<i>Rhabdodon</i>	MHNM.6034.11998 (holotype), MHNAIX-PV.1995, MHN-AIX-PV.2007, MCM30, 1252, 1575, 2111 3036, 3583, 4058, MC-MN30, 32, 36, 365, MC-MOB6, 7013, MC-PSP3, MC-CY.QR.1-6, 8, 11, 15, 18, 21, 24	Chanthasit, 2010
<i>Shuangmiaosaurus</i>		You et al., 2003
<i>Stormbergia</i>	SAM PK K1105 (holotype), 1107	Butler, 2005
<i>Tenontosaurus dossi</i>		Winkler et al., 1997
<i>Tenontosaurus tilletti</i>	YPM 5456, 5459, AMNH 3031, 3034, 3040	
<i>Talenkauen</i>		Novas et al., 2004; Cambiaso, 2007
<i>Telmatosaurus</i>	NHMUK R3386, 3388, 4911	Weishampel et al., 1993
<i>Tethyshadros</i>		Dalla Vecchia, 2010
<i>Theiophytalia</i>	YPM 1887	Brill and Carpenter, 2006
<i>Thescelosaurus infernalis</i>	SDSM 7210 (holotype): MOR 979	
<i>Thescelosaurus neglectus</i>	AMNH 117, 5030-1, 5034	Boyd et al., 2009; Boyd 2012
<i>Trinisaura</i>		Coria et al., 2013
<i>Uteodon</i>	CM 11337 (holotype), 15780 (paratype), 21723, 79050 (paratype)	Carpenter and Wilson, 2008; McDonald, 2011
<i>Valdosaurus</i>		Barrett et al., 2011
<i>Xuwulong</i>		You et al., 2011
<i>Zalmoxes robustus</i>	NHMUK R3809-10, 3812-4, 3390, 3392 (holotype), 3393, 3836, 4912	Weishampel et al., 2003
<i>Zalmoxes shqiperorum</i>	NHMUK R4900 (holotype)	Weishampel et al., 2003
<i>Zephyrosaurus</i>		Sues, 1980

APPENDIX 4

The following taxa are excluded from the analysis. In some cases, these are junior synonyms of taxa that are included, while other taxa lack apomorphies or a distinct combination of synapomorphies.

Darwinsaurus evolutionis Paul, 2012

=*Hypselospinus fittoni* Norman, 2010

=*Iguanodon fittoni* Lydekker, 1889

Type horizon, locality, and age: Wadhurst Clay Formation, England, Valanginian

Holotype: NHMUK R1831, 1833, 1835, 1836

This study follows Norman (2013, 2015) in considering this species a *nomen dubium*, based on the incorrect anatomical details (e.g., a long diastema) described in the dentary of NHMUK R1831, and the disparate localities of the designated holotype. Specimens NHMUK R1831, 1833, and 1835 from the Valanginian Wadhurst Clay Formation are referred to *Hypselospinus fittoni*, while NHMUK R1836 from the Barremian of the Isle of Wight is referred to *Mantellisaurus atherfieldensis* (Norman, 2014b). There has been much dispute about the presence of a diastema in this specimen (Norman, 2010; Paul, 2012; Norman, 2014b); first-hand examination by the author finds that the area rostral to the preserved teeth is weathered, but alveoli are clearly present. This highlights the importance of examining specimens directly. No matter how detailed a drawing or photograph may appear to be, they do not always reproduce the necessary details of a specimen.

Dollodon bampingi Paul, 2008

=*Mantellisaurus atherfieldensis* (Hooley, 1925)

Type horizon, locality, and age: Upper Hainaut Group, Belgium, late Barremian to early Aptian

Holotype: RBINS R57

The holotype of this species had previously been referred to *Mantellisaurus (=Iguanodon) atherfieldensis*. McDonald (2012b) and Norman (2013, 2015), both consider it to be a *nomen dubium*, though if the taxon is not valid it should be considered a junior subjective synonym of *M. atherfieldensis*. In order to further test whether this specimen and the holotype of *M. atherfieldensis* form a monophyletic group, they were coded as separate OTUs in this analysis.

Delapparentia turolensis Ruiz-Omenaca, 2011

=*Iguanodon bernissartensis* Boulanger, 1881

Type horizon, locality, and age: Camarillas Formation, Teruel, Spain, early Barremian

Holotype: MPT/I.G.

Norman (2014b) considered this taxon a *nomen dubium*, however Gasca et al. (2015) offered an emended diagnosis based on new material. These new characters, however, fail to distinguish *Delapparentia* from *Barilium*. Gasca et al. (2015) cite a single autapomorphy, a neural spine of the axis with a height from the base of the postzygapophysis that is greater than half the length of the neural spine. However, the neural spine is clearly broken cranially, so the length in this specimen cannot be determined. The unique combination of characters listed by Gasca et al. (2015) are all present in *Barilium*: the preacetabular process twists along its length so the lateral surface faces dorsally at the distal end, a large process is present and visible in the preacetabular notch of the ilium for articulation with the sacral rib, a straight dorsal margin of the ilium, a distally expanded prepubic process, and proximal caudal vertebral centra dorsoventrally expanded. While it is clear that an iguanodontian similar to or synonymous with *Barilium dawsoni* was present in the Barremian of Spain, the species *D. turolensis* remains inadequately diagnosed, and is not included in this analysis.

Elrhazosaurus (=Valdosaurus) nigerensis (Galton and Taquet, 1982)

Type horizon, locality, and age: Elrhaz Formation, Niger, late Aptian

Holotype: MNHN GDF 332

This species, assigned to its own genus by Galton (2009), is erected on a single femur. Galton (2009)

assigns it to Dryosauridae based on the deep pit on the medial side of the femur, just cranial to the fourth trochanter. However, this character state is found widely among basal neornithischians, in genera such as *Anabisetia*, *Hexinlusaurus*, and *Orodromeus*. The other features cited by Galton (2009) in the diagnosis of the new genus are plesiomorphic within Ornithopoda (greater trochanter extends further dorsally than lesser trochanter) or vague (“transversely wide raised area separating deep pit from base of fourth trochanter”), except for the deep and obliquely inclined extensor groove. This feature is similar to the extensor grooves in *Valdosaurus* and *Dysalotosaurus*, and therefore not sufficient to diagnose the species. *Elrhazosaurus nigerensis* is here considered a *nomen dubium*.

Huxleysaurus (= *Iguanodon*) *hollingtoniensis* (Lydekker, 1889)

= *Hypselospinus fittoni*, Norman, 2010

Type horizon, locality, and age: Wadhurst Clay Formation, England, Valanginian

Holotype: NHUMK R1148, 1629, 1632, 811, 811b, 604.

The genus *Huxleysaurus* was named by Paul (2012) based on the holotype specimen of *Iguanodon hollingtoniensis*, which was previously referred to *Hypselospinus fittoni* (Norman, 2010). While there is fairly little overlapping material between this specimen and that of the holotype of *Hypselospinus fittoni*, the areas of overlap are consistent with one another, including a longitudinal ridge along the brevis shelf (Character 261). Furthermore, the diagnosis of *Hu. hollingtoniensis* is inaccurate and entirely inadequate. In full, it reads “Femur robust, moderately curved, 4th trochanter pendent.” While the fourth trochanter of this specimen does come to a sharp point at its caudoventral margin, it is not pendant. While Norman (2014b) considers *Hu. hollingtoniensis* a *nomen dubium*, it is here considered a junior subjective synonym of *Hu. fittoni*.

Mantellodon carpenteri Paul, 2012

= *Mantellisaurus atherfieldensis* (Hooley, 1925)

Type horizon, locality, and age: Lower Greensand Formation, England, early Aptian

Holotype: NHMUK R3791

This new genus and species was described based on the so-called Maidstone specimen, now on display at the Natural History Museum in London. The diagnosis of this taxon, in full, states: “Limb elements slender. Ilium deep, anterior process robust, posterior acetabular body short and very triangular, dorsal margin strongly arched.” This diagnosis is vague and does not differentiate this specimen from others assigned to *Mantellisaurus atherfieldensis*, or even from other genera such as *Ouranosaurus*. It is here considered a junior subjective synonym of *M. atherfieldensis*.

Kukufeldia tilgatis McDonald, Barrett, and Chapman, 2010

Type horizon, locality, and age: Tunbridge Wells Sand Formation, Wealden Group, England, middle to late Valanginian

Holotype: NHMUK R28660

This taxon, based on the single dentary NHMUK R28860, was diagnosed based on the autapomorphy of a distinct row of foramina. While it is recognized as a *nomen dubium* by Norman (2014b), who also cites that McDonald now agrees with this, it remains unclear whether this specimen can be assigned to *Barilium* or to *Iguanodon*. As such, it was coded as a distinct OTU in this analysis.

Osmakasaurus depressus (Gilmore, 1909)

= *Camptosaurus depressus* Gilmore, 1909

= *Planicoxa depressa* Carpenter and Wilson, 2008

Type horizon, locality, and age: Lakota Formation, South Dakota, Barremian-Aptian

Holotype: USNM 4753

This genus was erected by McDonald (2011). The specific diagnosis for this taxon is by a unique combination of characters: distal end of preacetabular process of the ilium with a ventral flange (“horizontal boot” of McDonald, 2011), straight dorsal margin of the ilium, and the dorsal margin of the ilium transversely expanded. However, these character states appear widely in Iguanodontia, and are found together in several genera, including *Mantellisaurus* and *Iguanacolossus*. Thus, *Osmakasaurus depressus* is considered a

nomen dubium.

Penelopognathus weishampeli Godefroit, Li and Shang, 2005

Type horizon, locality, and age: Bayan Gobi Formation, Inner Mongolia, China, Albian

Holotype: IMM 2002-BYGB-1

This species is erected on a single dentary. As it displays only characters that are widespread among styra-costernans, it is here considered a *nomen dubium*, and not used in the analysis. This is supported by Norman (2014b), who noted that the diagnosis contains no unique characters.

Proplanicoxa galtoni Carpenter and Ishida, 2010

Type horizon, locality, and age: Upper Wessex Formation, England, late Barremian

Holotype: NHMUK R8649

This species is diagnosed by a postacetabular process of the ilium that is directed about 50° dorsolaterally. It is clear based on the wide variety of shapes present among the ilia in the specimens of *Iguanodon bernisartensis* that these elements are prone to post-mortem distortion, and this single character state is insufficient to diagnose a species. It is here considered a *nomen dubium*.

Qantassaurus intrepidus Rich and Rich, 1999

Type horizon, locality, and age: Wonthaggi Formation, Victoria, Australia, early Aptian

Holotype: NMV P199075

This taxon is diagnosed based on the deep, foreshortened dentary with only 10 alveoli. However, a low tooth count is found in juvenile individuals among many neornithischians (Horner and Currie, 1994; Scheetz, 1999; Hübner and Rauhut, 2010), and the dorsoventrally deep dentary appears to be a taphonomic feature caused by mediolateral crushing of a transversely wide dentary. The individuals referred to this taxon most likely pertain to the coeval *Atlascopcosaurus loadsi*, though the fragmentary nature of the specimens makes this difficult to determine.

Sellacoxa pauli Carpenter and Ishida, 2010

Type horizon, locality, and age: Lower Wadhurst Clay, England, early Valanginian

Holotype: NHMUK R3788

The holotype of this species has previously been referred to *Iguanodon dawsoni*, and later to *Barilium dawsoni* (Norman 2010, 2015). While this specimen lacks some features used to diagnose *B. dawsoni*, such as the transversely wide articular facet for the sacrum visible laterally through the preacetabular notch, it is also not clear that it is a distinct taxon. The diagnosis of Carpenter and Ishida includes one character state that cannot be properly determined: the sharply cranioventrally sloped preacetabular process. This region is reconstructed with plaster near its base, so the actual angle is unclear. The other characters cited are all found widely within ankylopollexians (dorsal margin of ilium concave, body of ilium deep, ischial peduncle extends laterally onto body of ilium, prepubic process mediolaterally compressed and expanded only at the distal end, ischium "T-shaped" with a straight shaft). While the proper taxonomic position of NHMUK R3788 remains unclear, the name *Sellacoxa pauli* is here considered a *nomen dubium*.

Ratchasimasaurus suranareae Shibata, Jintaskul and Azuma, 2011

Type horizon, locality, and age: Khok Kraut Formation, Thailand, Aptian

Holotype: NRRU-A2064

Siamodon nimngami Buffetaut and Suteethorn, 2011

Type horizon, locality, and age: Khok Kraut Formation, Thailand, Aptian

Holotype: PRC-4

Both of these species were named based on non-overlapping material from the Aptian-aged Khok Kraut Formation of Thailand. While they could offer intriguing biogeographic information, the fragmentary specimens reveal only characters that are widespread within Styra-costerna, and are not included in the current analysis.

APPENDIX 5

Unambiguous synapomorphies of major clades. Where topology differs between parsimony and Bayesian analyses, these are listed separately.

Taxon	Unambiguous synapomorphies (Character numbers and states correspond to those given in Appendix 1.)
Thescelosauridae (Parsimony)	<p>98.0 Dentary, shape of tooth row in dorsal view: straight.</p> <p>136.3 Maxillary teeth, maximum number of ridges extending from the base to the tip of the crown on labial side of teeth: ten to twelve ridges.</p> <p>196.0 Scapula, acromion process length: does not extend beyond the edge of the coracoid.</p>
Thescelosauridae (Bayesian)	<p>136.3 Maxillary teeth, maximum number of ridges extending from the base to the tip of the crown on labial side of teeth: ten to twelve.</p> <p>137.3 Dentary teeth, maximum number of ridges extending from the base to the tip of the crown on lingual side of teeth: nine to eleven.</p>
Clypeodonta (Parsimony)	<p>63.1 Quadrate buttress ("hamular process"): present.</p> <p>69.2 Quadrate, mandibular condyle proportions: lateral condyle is larger than medial.</p> <p>70.0/1 Quadrate, mandibular condyles, orientation of distal margin relative to long axis of quadrate: dorsomedially sloped or horizontal.</p> <p>127.1 Maxillary teeth, morphology of roots: crown tapers to root.</p> <p>128.1 Dentary teeth, morphology of roots: crown tapers to root.</p> <p>139.1 Maxillary teeth, primary ridge on labial side of crown: present.</p> <p>146.1 Maxillary teeth, base of crown defined by an everted lip which makes the crown slightly inset from the root: present.</p> <p>147.1 Dentary teeth, base of crown defined by an everted lip which makes the crown slightly inset from the root: present.</p> <p>159.1 Postaxial cervical vertebrae, proportions of centra: elongate, with craniocaudal length more than twice the dorsoventral height.</p>
Clypeodonta (Bayesian)	<p>16.1 Maxilla, diastema: present, first maxillary tooth is at least one crown width from the premaxilla.</p> <p>84.1 Prementary, length of oral margin: subequal in length to the oral margin of the premaxilla.</p> <p>101.1 Dentary, coronoid process, height: extends more than one crown height above tooth row.</p> <p>111.1 Surangular, small fenestra positioned dorsally on or near the dentary joint: present.</p> <p>114.1 Surangular foramen, position relative to the lateral lip of the glenoid: rostral.</p> <p>134.1 Cheek teeth, enamel distribution: asymmetrical: thicker on the labial side of maxillary teeth and on the lingual side of dentary teeth.</p> <p>135.1 Cheek teeth, apicobasally extending ridges on labial side of maxillary teeth and lingual side of dentary teeth: present.</p> <p>292.1 Femur, head: distinct constriction separates head and greater trochanter.</p>
Iguanodontia (Parsimony)	<p>21.1 Maxilla, dorsal process, shape in lateral view: broad and triangular.</p> <p>60.1 Quadratojugal, position of ventral margin relative to mandibular condyle of the quadrate: well-removed from the mandibular condyle.</p> <p>*131.1 Cheek teeth: number of wear facets on each tooth: one.</p> <p>157.1 Postaxial cervical vertebrae, form of central surfaces: at least slightly opisthocoelous.</p> <p>185.1 Caudal vertebrae, length of prezygopophyses on distal caudals: elongate, extending nearly to the midpoint of the preceding vertebra.</p> <p>188.1 Chevrons, shape: strongly asymmetrically expanded distally, width greater than length in mid caudals.</p> <p>199.1 Scapula, supraglenoid fossa: present.</p> <p>*236.1 Manus digit III, number of phalanges: three or fewer.</p> <p>263.1 Ilium, postacetabular process, length as a percentage of the total length of the ilium: 23-30%.</p>

Taxon	Unambiguous synapomorphies (Character numbers and states correspond to those given in Appendix 1.)
Iguanodontia (Bayesian)	<p>3.1 Premaxilla, shape of subnarial region: ventral premaxilla flares laterally to form a partial floor of the narial fossa.</p> <p>31.1 Antorbital fenestra, size: relatively small (10% basal skull length or less).</p> <p>75.1 Posttemporal foramen/fossa, position: forms a notch in the dorsal margin of the paroccipital process, enclosed dorsally by the squamosal.</p> <p>87.1 Prementary, denticulate oral margin: present.</p> <p>89.1 Prementary, ventral process, depth of bifurcation: deep bifurcation.</p> <p>125.0 Cheek teeth; dentary teeth extend farther rostrally than maxillary teeth: absent.</p> <p>126.1 Cheek teeth, spaces between the roots: absent, teeth are closely packed.</p> <p>127.1 Maxillary teeth, morphology of roots: crown tapers to root.</p> <p>128.1 Dentary teeth, morphology of roots: crown tapers to root.</p> <p>129.1 Maxillary teeth, ratio of crown height to width (for unworn teeth): 1.25 to 1.9.</p> <p>*131.1 Cheek teeth: number of wear facets on each tooth: one.</p> <p>148.1 Cheek teeth, at least moderately developed labiolingual expansion at the base of the crown ("cingulum"): absent.</p> <p>177.0 Caudal vertebrae, position of the most distal caudal rib (transverse process): 12th caudal vertebrae or more proximal.</p> <p>183.0 Caudal vertebrae, proportions of articular facets for chevrons: the distal facet on a given vertebra is much larger than the proximal facet.</p> <p>214.1 Humerus, deltopectoral crest length: 43% of total humeral length or more.</p> <p>*236.1 Manus digit III, number of phalanges: three or fewer.</p> <p>239.1 Phalanges of manual digits II-IV, length: first phalanx more than twice the length of the second phalanx.</p> <p>283.1 Ischium, shaft, twisted along its length so that the lateral side faces ventrally on the distal part of the shaft: absent.</p> <p>288.1 Ischium, distal end expanded to 50% or more the depth of the adjacent ischial shaft: present.</p> <p>300.1 Femur, cranial (extensor) intercondylar sulcus on distal end: present.</p> <p>302.1 Femur, caudal (flexor) intercondylar sulcus of the femur: medial condyle inflated laterally, partially covers opening of flexor sulcus (1).</p>
Rhabdodontoidea (Parsimony)	<p>34.1 Orbit shape: subrectangular at least in its lower margin.</p> <p>56.1 Jugal, shape of ventral edge: sinuous.</p> <p>265.1 Ilium, postacetabular process orientation: extends caudodorsally, so the postacetabular process reaches further dorsally than the body of the ilium.</p> <p>290.0 Femur, shape in lateral view: straight.</p>
Rhabdodontoidea (Bayesian)	<p>21.1 Maxilla, dorsal process, shape in lateral view: broad and triangular.</p> <p>26.2 Maxilla, shape of tooth row in ventral view: straight.</p>
Tenontosaurus+ Rhabdodontidae (Parsimony)	<p>49.1 Jugal, type of suture with maxilla: 'finger-in-recess' joint.</p> <p>55.1 Jugal, form of articulation with quadratojugal: tongue and-groove contact whereby the jugal lies lateral to the quadratojugal dorsally while ventrally the jugal lies medial to the quadratojugal.</p> <p>65.0 Quadrate (paraquadratic) foramen or notch on boundary between quadrate and quadratojugal: absent.</p> <p>123.0 Maxillary teeth, number; 13 or fewer tooth positions.</p> <p>212.0 Humerus, deltopectoral crest form: a well-developed projection.</p> <p>275.0 Pubis, obturator foramen completely enclosed: present.</p>
Rhabdodontidae	<p>138.1 Cheek teeth: apicobasally extending ridges on cutting surface of unworn teeth (lingual surface of maxillary teeth, labial surface of dentary teeth): present.</p> <p>196.0 Scapula, acromion process, length: does not extend beyond the edge of the coracoid.</p> <p>216.2 Humerus, relative width of medial and lateral distal condyles: medial condyle wider.</p> <p>219.1 Ulna, flange on proximal end that wraps around the lateral edge of the radius: present.</p> <p>249.1 Ilium, preacetabular process, orientation: process is distinctly twisted about its long axis.</p> <p>280.1 Ischium, pubic peduncle, shape: dorsoventrally compressed.</p> <p>304.1 Femur, distal condyles, shape in lateral view: strongly expanded (condyle extends cranially as well as caudally).</p> <p>320.1 Metatarsal V: absent.</p>

Taxon	Unambiguous synapomorphies (Character numbers and states correspond to those given in Appendix 1.)
Dryomorpha (Parsimony)	<p>6.1 Premaxilla, posterolateral process contacts lacrimal: present. 18.1 Maxilla, rostral process in addition to the premaxillary process: present. 26.0 Maxilla, shape of tooth row in ventral view: medially bowed, with rostral and caudal ends curving laterally. 27.1 Maxilla, articulation with lacrimal: lacrimal fits into slot between medial and lateral portions of the dorsal process of the maxilla. 47.0 Jugal, exclusion of the rostral process from the antorbital fenestra by lacrimal-maxilla contact: absent. 57.1 Quadratojugal, shape: no dorsal process, element is small and blocky. 58.0 Quadratojugal, foramen through center of element: absent. 109.1 Coronoid process, relative craniocaudal widths of dentary and surangular (at midpoint of coronoid process): subequal. 145.1 Cheek teeth, secondary ridges, shape in cross-section: thin, sharp ridges, formed mainly by enamel. 224.1 Radius, shape in distal view: triangular. 287.1 Ischium, obturator process, position of proximal edge: within the proximal 25%. 322.0 Tendons, ossified hypaxial tendons on caudal vertebrae: absent.</p>
Dryomorpha (Bayesian)	<p>*6.1 Premaxilla, posterolateral process contacts lacrimal: present. *18.1 Maxilla, rostral process in addition to the premaxillary process: present. *27.1 Maxilla, articulation with lacrimal: lacrimal fits into slot between medial and lateral portions of the dorsal process of the maxilla. *57.1 Quadratojugal, shape: no dorsal process, element is small and blocky. 63.1 Quadrate buttress ("hamular process"): present. 65.1 Quadrate (paraquadratic) foramen or notch on boundary between quadrate and quadratojugal: present. 90.1 Prementary, short midline process dorsal to dentary symphysis: present. *109.1 Coronoid process, relative craniocaudal widths of dentary and surangular (at midpoint of coronoid process): subequal. *145.1 Cheek teeth, secondary ridges, shape in cross-section: thin, sharp ridges, formed mainly by enamel. *224.1 Radius, shape in distal view: triangular. *287.1 Ischium, obturator process, position of proximal edge: within the proximal 25%.</p>
Dryosauridae	<p>9.1 Premaxilla, medial dorsal (nasal) process contacts the nasal: absent. 42.1 Palpebral(s), length relative to rostrocaudal width of orbit if unfused to orbital rim: traverses entire width of orbit. 97.0 Dentary, relationship of dorsal and ventral margins (under the tooth row): converge anteriorly. 143.0 Maxillary teeth, primary ridge position: centered, although some teeth within the same dental battery may display a slight offset of the primary ridge. 161.0 Dorsal vertebrae, number: 15 or fewer dorsal vertebrae. 167.1 Dorsal vertebrae, posterior dorsals, length of transverse processes: greater than centrum height. 195.0 Scapula, acromion process size: weakly developed. 273.1 Pubis, prepubic process, horizontal ridge on medial side: present. 275.0 Pubis, obturator foramen completely enclosed: present.</p>
Ankylopollexia	<p>198.0 Scapula, deltoid ridge, orientation relative to long axis of scapula: close to parallel. 212.0 Humerus, deltopectoral crest form: a well-developed projection. 219.1 Ulna, flange on proximal end that wraps around the lateral edge of the radius: present. 227.1 Carpals, fusion: present. 232.1 Manus digit I, orientation: diverges at least 45 degrees from the antebrachial axis. 233.1 Metacarpal I, shape: short, block-like. 241.1 Manus ungual I, shape: subconical. 259.0 Ilium, brevis fossa, well defined by a lateral lip: absent. 323.1 Tendons, ossified epaxial and hypaxial tendon arrangement: double-layered lattice.</p>
Styracosterna	<p>5.1 Premaxilla, oral margin denticulation: present. 123.2 Maxillary teeth, number: 18-28 positions. 137.1 Dentary teeth, maximum number of ridges extending from the base to the tip of the crown on lingual side of teeth: two to four ridges. 149.1 Maxillary and dentary crowns, relative width: maxillary crowns narrower. 164.1 Dorsal vertebrae, proportions of mid to posterior centra: length is much shorter than height.</p>

Taxon	Unambiguous synapomorphies (Character numbers and states correspond to those given in Appendix 1.)
Unnamed node	<p>180.1 Caudal vertebrae, shape of neural spines on proximal caudals: bowed caudally. 217.0 Ulna, length relative to dorsoventral thickness at mid-shaft: less than 9. 218.2 Ulna, olecranon process length as a percentage of total ulnar length: 17% or greater. 221.1 Radius, proportions: relatively robust, the minimal radial width is equal to or greater than 12% radial length. 223.1 Radius, tubercle near proximal end of radius for insertion of <i>M. biceps</i>: present. 242.1 Manus unguis I, length: greater than 30% the length of the radius. 276.1 Pubis, obturator foramen shape: circular.</p>
Iguanodontidae	<p>42.1 Palpebral(s), length relative to rostrocaudal width of orbit if unfused to orbital rim: traverses entire width of orbit. 45.1 Postorbital, shape of squamosal process: bifurcated. 112.1 Surangular, position of small rostral fenestra: lies within the surangular. (Note that this fenestra is not present in Iguanodon or Equijubus.)</p>
<i>Mantellisaurus</i> holotype + RBINS R57	<p>15.1 Premaxilla-maxilla boundary, fossa or foramen just dorsal to the oral margin: present. 17.0 Maxilla, diastema length: one to two tooth widths. 95.1 Dentary ramus, shape of rostral end: strongly downturned. 105.1 Dentary, coronoid process orientation: subvertical. 164.0 Dorsal vertebrae, proportions of mid to posterior centra: craniocaudal length is subequal to or longer than dorsoventral height. 211.0 Humerus, length relative to femur: less than 62% of femoral length. 230.1 Metacarpal III, ratio between length and width at mid-shaft: long and slender, ratio greater than 5.5.</p>
Bolong + Jinzhousaurus	<p>29.1 Antorbital fenestra: absent. 195.0 Scapula, acromion process size: weakly developed. 216.0 Humerus, relative width of medial and lateral distal condyles: lateral condyle wider. 217.0 Ulna, length relative to dorsoventral thickness at mid-shaft: less than 9. 221.1 Radius, proportions: relatively robust, the minimal radial width is equal to or greater than 12% radial length. 242.1 Manus unguis I, length: greater than 30% the length of the radius. 281.0 Ischium, shaft, shape in lateral view: straight.</p>
Hadrosauroidea	<p>29.1 Antorbital fenestra: absent. 73.1 Squamosal, relationship of right and left squamosals on skull roof: separated by only a narrow band of the parietal. 93.1 Dentary, length of diastema: long, the width of three teeth or more. 94.1 Dentary, rostral extent of Meckel's groove meets the dentary symphysis: absent, ends more caudally. 103.2 Dentary: caudal extent of tooth row: terminates directly ventral to apex of the coronoid process or more caudally. 105.1 Dentary, coronoid process orientation: subvertical. 107.1 Coronoid process, rostrocaudally expanded apex: present. 136.0 Maxillary teeth, maximum number of ridges extending from the base to the tip of the crown on labial side of teeth: primary ridge only. 150.1 Dentary teeth, maximum number of functional teeth exposed on the occlusal plane: one functional tooth rostrally and caudally, and up to two teeth at and approaching the middle of the dental battery. 151.1 Dentary teeth, maximum number of replacement teeth: two. 152.1 Dentary alveoli: parallel grooves lining a continuous dental battery. 186.2 Chevrons, position of most proximal chevron: distal end of third caudal vertebra or more distal. 207.1 Coracoid, ratio between the length of the scapular articulation and the length of the lateral margin of the glenoid in lateral view: less than 1.25. 220.1 Radius, length: greater than 70% of humeral length. 230.1 Metacarpal III, ratio between length and width at mid-shaft: long and slender, ratio greater than 5.5. 251.0 Ilium, preacetabular process, morphology of distal end: parallel-sided or slightly tapering. 252.0 Ilium, cranial sacral facets transversely widened so that the base of the preacetabular process is thicker ventrally than dorsally: absent. 281.0 Ischium, shaft, shape in lateral view: straight. 305.1 Femur, distal condyles, shape of articular surface: rounded articular surface.</p>